ROLE OF EXOSOMES IN NEURONAL DEVELOPMENT

By

Mikin Patel

Dissertation

Submitted to the Faculty of the

Graduate School of Vanderbilt University

in partial fulfillment to the requirements

for the degree of

DOCTOR OF PHILOSOPHY

in

Biological Sciences

May 31, 2021

Nashville, Tennessee

Approved:

Lauren P. Jackson, Ph.D.

Douglas G. McMahon, Ph.D.

James G. Patton, Ph.D.

Alissa M. Weaver, M.D., Ph.D.

Dedicated to my family and friends,

and

to the memories of my former Ph.D. advisor, Dr. Donna J. Webb,

my grandparents, my aunt and my father-in-law.

"Learn from yesterday, live for today, hope for tomorrow.

The important thing is to not stop questioning."

- Albert Einstein

Acknowledgements

First and foremost, I would like to express my sincere gratitude to my former Ph.D. advisor, Dr. Donna J. Webb, for her guidance and support during the first few years of this journey. She was always available to discuss research progress and provide helpful feedback. I am also very grateful to Dr. Alissa M. Weaver for agreeing to be my advisor and allowing me to complete my project after Dr. Webb passed away. Thank you for providing guidance whenever I needed it, being patient and supporting me through the past few years. I truly feel fortunate to have worked with two great mentors who believed in me and inspired me to become a better scientist.

I would like to thank my former committee chair Dr. Charles Singleton and my current committee members, Dr. Lauren P. Jackson, Dr. Douglas G. McMahon, Dr. James G. Patton for their patience, support and providing valuable feedback throughout the years. In addition, I would also like to thank the administrative staff in the Department of Biological Sciences. I am grateful for all the feedback and mentorship I have received from other faculty members, staff, postdocs and graduate students at Vanderbilt and also from other institutions. I would like to thank my funding sources, the National Institute of Health and also the Department of Biological Sciences. I would like to thank all the members of Webb lab and Weaver lab for making this journey memorable and more joyful. I have learned a lot from everyone.

Finally, I owe a debt of gratitude to my parents for their unequivocal support and to my sister for always inspiring me. Also, I could not have been where I am today without the support of my wife, Silvia. She is a great scientist, mother and best life partner. My son, Neil, and daughter, Erica, your hugs and smiles make life much easier and more joyful. Always keep smiling.

TABLE OF CONTENTS

LIST OF TABLES

LIST OF FIGURES

LIST OF ABBREVIATIONS

AD	Alzheimer's Disease
AMPA	α-amino-3-hydroxy-5-methyl-4-isoxazolepropionic acid
APC	Antigen presenting cell
ARRDC1	Arrestin domain-containing protein 1
ASD	Autism spectrum disorders
BDNF	Brain derived neurotrophic factor
DIV	Day *in vitro*
DRG	Dorsal root ganglia
ECM	Extracellular matrix
EGFR	Epidermal growth factor receptor
ESCRT	Endosomal sorting complex required for transport
EV	Extracellular vesicles
HBSS	Hanks' Balanced Salt Solution
HNSCC	Head and neck squamous cell carcinoma
Hrs	Hepatocyte growth factor regulated tyrosine kinase substrate
HUVEC	Human umbilical vein endothelial cells
ILV	Intra luminal vesicles
KD	Knockdown
LTBP	Latent TGF-β binding protein
LTD	Long-term depression
LTP	Long-term potentiation
MHC	Major histocompatibility complex

miRNA	Micro RNA
mRNA	Messenger RNA
MSC	Mesenchymal stem cells
MV	Microvesicle
MVB	Multi vesicular body
MVE	Multi vesicular endosome
NGF	Nerve growth factor
NMDA	N-methyl-D-aspartate
NMJ	Neuromuscular junction
N-WASP	Neural Wiskott-Aldrich syndrome protein
PDL	Poly-D-Lysine
PLL	Poly-L-Lysine
PLP	Proteolipid protein
PSD	Postsynaptic density
SEV	Small extracellular vesicles
siRNA	Small interfering RNA
shRNA	Short hairpin RNA
STAM	Signal transduction adapter molecule
TEM	Transmission Electron Microscopy
TGF-β	Transforming growth factor beta
TSP-1	Thrombospondin-1
THSD7A	Thrombospondin type 1 domain containing 7A
VASP	Vasodilator-stimulated phosphoprotein

CHAPTER I

INTRODUCTION

Overview and hypothesis

Extracellular vesicles (EVs) are lipid bilayer vesicles of heterogenous size secreted by most cell types. Among various EV subtypes, small EVs (SEVs)/exosomes are widely studied for their function in cellular communication. They carry functional cargos such as proteins, mRNAs and miRNAs that are actively sorted during the formation of these vesicles. The content of SEVs/exosomes is mostly cell type specific and represent physiological and pathological state of the secreting cell. EVs secreted into the extracellular space can regulate function of recipient cells by fusion, internalization or direct interaction with cell surface receptors. Increasing evidence suggests that EV mediated communication between different cell types in the nervous system is critical for various physiological processes such as neurodevelopment, neuroprotection and synaptic plasticity.

Neurons communicate with each other via transmission of chemical and electrical signals at synapses where axon terminal of presynaptic neurons connect with dendritic spines on postsynaptic sites. Dendritic spines evolve mainly from thin actin-rich filopodia that emerge from dendritic shafts during early stages of neuronal development. Activity dependent changes in spine morphology and synaptic strength are the bases of higher brain functions such as learning and memory. Therefore, there is a significant amount of interest in identifying factors and molecular mechanisms that regulate filopodia, spine and synapse formation. Many studies have identified intracellular regulators of filopodia formation. However, extracellular factors of filopodia

formation remain largely unknown. Additionally, astrocytes, a type of glia cells, secrete factors in extracellular space that regulate synapse formation. Astrocytes have also been shown to release EVs carrying functional cargo to induce neurite outgrowth and neuroprotection. However, the function of astrocyte-derived SEVs in the formation of dendritic spines and synapses is not well understood.

The goal of this study was to identify role of neuron-derived and astrocyte-derived SEVs in neuronal development, specifically in the formation of filopodia, spines and synapses. Based on previously known function of exosomes in adhesion formation, I hypothesized that neuronal exosomes regulate filopodia that are actin-rich adhesive structures. Furthermore, given the importance of astrocyte secreted factors in synapse formation, I postulated that astrocyte-derived SEVs promote spine and synapse formation.

Extracellular vesicles

Extracellular vesicles (EVs) are nanometer-sized vesicles released by most cells in extracellular space. The early evidence of extracellular vesicles dates back to year 1946 when Chargaff and West identified coagulant properties of "reddish brown translucent pellet" obtained by differential ultracentrifugation of plasma, which was later described as 'platelet dust' by Peter Wolf (Chargaff & West, 1946; Wolfe, 1967). In 1983, Harding and Stahl found that transferrin receptors are associated with small intraluminal vesicles that are released upon fusion of endosome to the plasma membrane during the process of reticulocyte maturation (Harding, Heuser, & Stahl, 1983). In the following years, Rose Johnstone further confirmed the evidence of transferrin receptor release in vesicles secreted by reticulocytes and coined the term 'exosomes' to define small vesicles of endocytic origin (Johnstone, Adam, Hammond, Orr, & Turbide, 1987; B. T. Pan

& Johnstone, 1984). For many years, EVs were still considered as a means for waste disposal from cells until late 1990s when Graca Raposo's group reported that B lymphocytes release exosomes containing major histocompatibility complex (MHC) class II molecules that are capable of activating T-cells (G. Raposo et al., 1996). In the following decade, exosomes were found to be secreted from many different cell types with limited understanding of their function. However, EV research started to gain traction after 2007 when Jan Lotvall's group reported that exosomes carry functional RNAs, especially micro RNAs (miRNA) and messenger RNAs (mRNA), that can be transferred between different cells (Valadi et al., 2007). Since then, researchers around the world have made significant progress in the understanding of EV biogenesis, secretion and functions.

EVs are released by most cell types and are found in all body fluids. There are no defined criteria to name EVs. Therefore, they are referred by many different names depending on the source of isolation or size such as matrix vesicles, prostasomes, ectosomes, exosome-like vesicles, oncosomes etc. However, EVs can be broadly classified in to three main categories based on their size and biogenesis mechanism. Small EVs (SEVs) including exosomes and exomeres, large EVs typically microvesicles (MVs)/ectosomes and apoptotic blebs (Akers, Gonda, Kim, Carter, & Chen, 2013; Maas, Breakefield, & Weaver, 2017b). Although they are recognized by the difference in their sizes, there is still some overlap in the size and cargo molecules present in these different class of vesicles. Exosomes are small EVs that are <200nm in size and are formed mainly through the endocytic pathway as intraluminal vesicles (ILVs) by inward budding of early endosomes that lead to formation of multivesicular body (MVB). MVBs can then either fuse with the plasma membrane to release ILVs into the extracellular space or directed toward the lysosome for degradation (Harding, Heuser, & Stahl, 2013; Graça Raposo & Stoorvogel, 2013) (Figure 1).
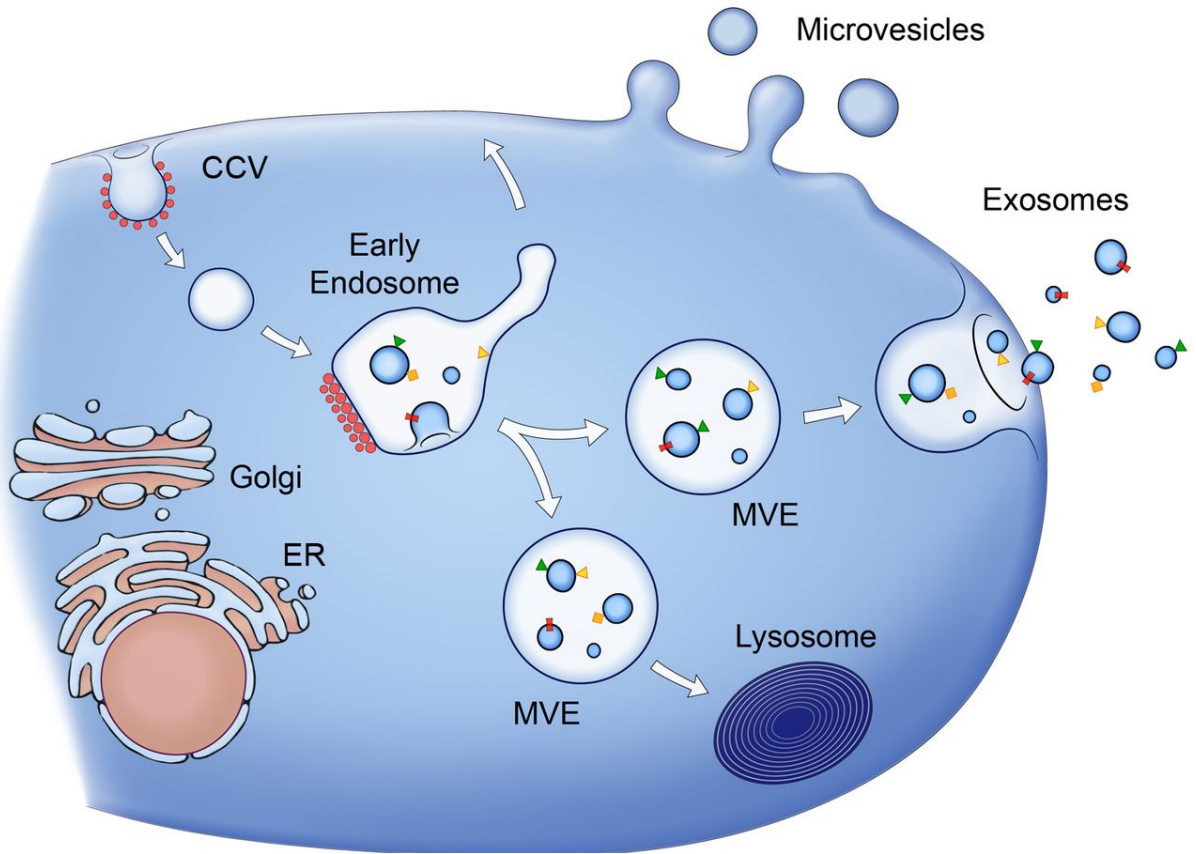
Figure 1: Release of exosomes and MVs. Exosomes are formed as ILVs by inward pulling of early endosome membrane. MVB/MVE fuses with lysosome or targeted to cell periphery for fusion and release of exosomes. MVs bud directly from the plasma membrane.
©2013 RAPOSO & STOORVOGEL. Originally published in Journal of Cell Biology
https://doi.org/10.1083/jcb.201211138

However, it is not clear what factors determine the fate of MVBs. More recently, a new class of small EVs, called exomeres, have been isolated using asymmetric-flow field-flow fractionation or by high-speed ultracentrifugation of exosome supernatant (Haiying Zhang et al., 2018; Haiying Zhang & Lyden, 2019; Q. Zhang et al., 2019). Exomeres are smaller in size and contain distinct nucleic acid and lipid content than exosomes (Q. Zhang et al., 2019). On the contrary, MVs are large EVs that range from 200-500nm in size and are released by direct budding from the plasma membrane (Colombo, Raposo, & Théry, 2014a) (Figure 1). Interchangeably, vesicles released by budding from the plasma membrane are also called ectosomes (Cocucci & Meldolesi, 2011). Apoptotic bodies range in size from few nanometers to several micrometers and are produced by membrane blebbing of dying cells (Akers et al., 2013). In the past decade, significant progress has been made to isolate and characterize different types of EVs using various methods such as differential ultracentrifugation, size exclusion chromatography and immuno-precipitation (Doyle & Wang, 2019; M. Zhou, Weber, Zhao, Chen, & Sundstrom, 2020). However, overlap in their size, buoyancy and even membrane proteins make it difficult to isolate a single EV type in its purest form.

The outer layer of EVs mimic the plasma membrane of the cell, containing a lipid bilayer with integral membrane proteins, whereas the inside of EVs mostly contains cytosolic proteins and nucleic acids such as mRNAs and miRNAs. All three EV types contain varying amounts of lipids, proteins and nucleic acids. The cargo content of EVs partially reflects their mode of biogenesis as well as the (patho)physiological state of the secreting cell. Typically, there is some overlap in proteins enriched in small EVs, such as exosomes, compared to plasma membrane derived MVs. CD63, CD81 and CD9 are tetraspanins that are commonly found in both SEVs and MVs. However, SEVs formed through via the endosomal sorting complex required for transport (ESCRT) pathway

are also enriched in the ESCRT complex protein TSG101 and the ESCRT accessory protein Alix. Apart from common protein markers, EVs also contain cell type specific adhesion molecules, cytoskeletal proteins, signal transduction molecules and transmembrane proteins. Many studies have determined the protein composition of exosomes and MVs using advanced proteomics analyses. Interestingly, protein profiles of exosomes and MVs differs widely from whole cell lysates, suggesting cargo selection mechanisms are involved during formation of these EVs. Both exosomes and MVs also contain various lipids and nucleic acids. On the contrary, apoptotic bodies contain cell organelles, large amounts of RNA, DNA, and have protein profiles similar to cell lysates (Doyle & Wang, 2019). Furthermore, it is important to note that changes in media conditions or treatment with various compounds can lead to changes in EV cargo composition. The presence of functional proteins and nucleic acids in EVs protected by the lipid-bilayer gives them a unique advantage for cellular communication at short and long distances.

Biogenesis and secretion of extracellular vesicles:

Many proteins and pathways have been identified as critical regulators of EV biogenesis and secretion. For small EVs, enrichment of the ESCRT components TSG101 and Alix strongly indicate involvement of the ESCRT pathway in ILV formation inside MVBs. The ESCRT machinery contains four ESCRT complexes, namely ESCRT-0, ESCRT-I, ESCRT-II and ESCRT-III. Hepatocyte growth factor regulated tyrosine kinase substrate (Hrs), an ESCRT-0 protein, forms a complex with the signal transduction adaptor molecule (STAM) at the limiting membrane of endosome, which initiates sequential recruitment of other ESCRT complexes for cargo sorting and ILV formation (Bache, Brech, Mehlum, & Stenmark, 2003; Urbanelli et al., 2013). Indeed, knockdown of Hrs significantly reduces exosome biogenesis in various cell types including

dendritic cells (Tamai et al., 2010), and head and neck squamous cell carcinoma (HNSCC) (D. Hoshino et al., 2013). However, ESCRT independent pathways have shown to regulate exosome biogenesis in certain cell types. In oligodendrocytes, ESCRT dependent and independent pathway simultaneously produce distinct population of ILVs containing epidermal growth factor receptor (EGFR) or proteolipid protein (PLP), respectively (Trajkovic et al., 2008). Treatment of oligodendrocytes with neutral sphingomyelinase inhibitor, GW4869, to inhibit ceramide synthesis led to significant reduction in exosome secretion and endosome localized PLP suggesting ceramide dependent biogenesis of exosomes. Apart from ESCRT and ceramide, tetraspanins are also thought to regulate ILV formation (Andreu & Yáñez-Mó, 2014; van Niel et al., 2011). These multiple mechanisms of exosome biogenesis imply distinct MVB population inside the same cell and are consistent with heterogeneity of SEVs. Similar to exosome biogenesis pathways, release of exosomes from MVBs also involves many proteins including Rab27a, Rab27b, Rab35, Rab11b and synaptotagmin-7 (D. Hoshino et al., 2013; Hsu et al., 2010; Messenger, Woo, Sun, & Martin, 2018; Ostrowski et al., 2010; Sung, Ketova, Hoshino, Zijlstra, & Weaver, 2015). Exosome release can also be stimulated by Ca^{+2} ionophores suggesting additional mechanisms involved in SEV release (Lachenal et al., 2011; Savina, Furlán, Vidal, & Colombo, 2003). In breast cancer cells, a Rab binding protein, Munc13-4, was found to control Ca^{+2} dependent increase in exosome secretion (Messenger et al., 2018). However, cargo composition in exosomes released under stimulated conditions may differ compared to constitutively secreted exosomes.

Unlike exosomes, biogenesis pathways for MVs are less defined. Initiation of MV formation can be triggered by alteration in phospholipids and recruitment of aminophospholipid translocases at the plasma membrane to induce membrane curvature. In one study, interaction of the ESCRT-I protein TSG101 with an accessory protein Arrestin Domain-Containing Protein 1

(ARRDC1) was shown to mediate MV release by relocation of TSG101 to the plasma membrane (Nabhan, Hu, Oh, Cohen, & Lu, 2012). MV shedding is also reported to be regulated by the GTP binding protein ARF6 which initiates signaling cascades leading to phosphorylation of myosin light chain (Muralidharan-Chari et al., 2009). However, more studies are required to understand detailed mechanisms of MV biogenesis and release.

Functions of extracellular vesicles:

Physiological functions of EVs:

Since their first identified role in reticulocyte maturation, EVs have been demonstrated to have important functions in many physiological processes such as development, cell migration and immune response. Precise communication between various cell types in a coordinated manner is critical for successful embryo implantation. Typically, crosstalk between maternal cells and preimplantation embryo involves secreted growth factors, proteases, cytokines and chemokines (Kurian & Modi, 2019; Machtinger, Laurent, & Baccarelli, 2016). However, many studies have identified the importance of embryonic and maternally secreted extracellular miRNAs in early embryo development and survival (Gross, Kropp, & Khatib, 2017). It remains to be seen how EV-associated miRNAs are uptaken by recipient cells to modulate signaling during embryonic development. SEVs are also enriched in ECM molecules which makes them critical regulators of cell adhesion and motility. Inhibition of exosome biogenesis and secretion, by knockdown of Rab27a and Synaptotagmin-7 respectively, reduced cell motility and directionality in chorioallantoic membranes of chick embryo (Sung et al., 2015). Furthermore, exosome associated fibronectin was found to be important for cell motility but not directionality. Exosomes also regulate directed cell migration which was visualized using pH sensitive fluorescent reporter (Sung

et al., 2020). Antigen presenting cells (APC) such as B lymphocytes and dendritic cells are known to release exosomes containing functional MHC to regulate immune response (G. Raposo et al., 1996). Furthermore, these functional peptide-MHC class II complexes can be transferred between different dendritic cell populations via exosomes (Théry et al., 2002). *In vivo*, exosomes isolated from tumor peptide loaded dendritic cells were able to inhibit tumor growth or completely eliminate tumors by inducing a strong immune response (Zitvogel et al., 1998). However, *in vitro*, peptide pulsed dendritic cells induced much stronger T-cell activation compared to exosomes. These studies have provided firm evidence for the role of exosomes in immune regulation and potential for use as cancer vaccine.

Pathological functions of EVs:

Apart from their function in normal physiology, EVs are also implicated in pathological conditions such as cancer metastasis as well as in neurodegenerative diseases. In 1989, the "seed-and-soil" hypothesis was proposed by an English surgeon Stephen Paget to understand cancer metastasis (Fidler, 2003). Based on observations from hundreds of autopsy records, he postulated that cancer metastasis occurs when certain organs (soil) favor growth of certain tumor cells (seed). Hoshino et. al. showed that exosomes derived from cancer cells colonize to specific organs and create a favorable microenvironment for future metastasis (A. Hoshino et al., 2015). Specifically, integrin β4 and β5 present on exosomes were found to be essential to form a pre-metastatic niche in lung and liver, respectively. Several other studies have also identified additional EV secreted factors in cancer metastasis (Azmi, Bao, & Sarkar, 2013).

Progression of many neurodegenerative diseases is linked to spreading of misfolded proteins. However, clear understanding of the mechanisms that contribute to this process is lacking. Recently, EVs have been found to carry misfolded proteins and exacerbate

neurodegeneration by spreading them in the brain. Many studies have shown the presence of pathological forms of Aβ-42, Tau and α-synuclein proteins in EVs that lead to neurological disorders such as Alzheimer's and Parkinson's disease (Rajendran et al., 2006; Saman et al., 2012; Yuyama & Igarashi, 2016). Whether these proteins are actively sorted during EV biogenesis or they are carried along on the EV surface for release is not well understood. In the future, the role of EVs as carriers of active cargo molecules at short and long distances will also help unravel underlying mechanisms of disease impairment in other pathological conditions.

EVs in therapeutics:

Since cargo in EVs represent physiological and pathological state of secreting cell, it is not surprising to think that EVs can provide useful information for disease diagnosis. EV biomarkers can be used for early diagnosis of disease as well as for monitoring recovery or disease progression at various stages of treatment. The abundant presence of EVs in all body fluids makes them an ideal source for clinically useful liquid biopsies compared to circulating tumor cells or circulating tumor DNA. Several studies have identified cancer associated miRNAs and mRNA biomarkers in EVs. In one study, mRNAs for a tumor specific biomarker EGFRvIII were found to be present in glioblastoma EVs (Skog et al., 2008). Another study reported that specific miRNAs that are aberrantly expressed in ovarian cancer were present at similar levels between exosomes and cancer cells (Taylor & Gercel-Taylor, 2008). Similarly, miRNA biomarkers with high specificity and sensitivity to predict Alzheimer's disease were identified by comparing miRNA profiles of serum exosomes from healthy and Alzheimer's disease (AD) patients (Cheng et al., 2015). Apart from miRNA and mRNA, exosomal proteins and DNA also serve as useful biomarkers (Allenson et al., 2017; Thakur et al., 2014; Urabe et al., 2020). In the future, the use of exosomes for biomarkers

will require refined isolation methods to reduce heterogeneity and also robust detection methods to predict disease with high specificity.

Moreover, the function of EVs in cell-cell communication can be exploited to advantage for therapeutics. Engineered EVs loaded with therapeutic cargo can be used as drug delivery vehicles. *In vivo*, dendritic cell derived exosomes with neuron specific peptides fused to exosome membrane proteins were used to deliver siRNA to neurons via intravenous injection in mice (Alvarez-Erviti et al., 2011). Exosomes loaded with siRNA were able to significantly reduce mRNA and protein levels of BACE1, a candidate therapeutic target for Alzheimer's disease. Furthermore, EVs are known to activate signaling pathways and also carry cargo molecules to contribute to the progression of disease. Therefore, the pathological functions of EVs can be blocked by therapeutic targets to inhibit EV biogenesis, secretion or uptake (Urabe et al., 2020). Intriguingly, a novel strategy using the Aethlon ADAPT™ (adaptive dialysis-like affinity platform technology) system to remove cancer exosomes, that interfere with therapeutic treatment and stimulate tumor growth, from the entire circulatory system is also proposed (Marleau, Chen, Joyce, & Tullis, 2012).

Uptake and cellular communication via extracellular vesicles:

Interest in the field of EV research increased exponentially once they were recognized to have function in cell-to-cell communication. Although significant progress has been made to understand active cargo molecules that regulate the behavior of recipient cell, how EVs deliver their content is less well understood. Several mechanisms of cargo transfer have been studied including endocytosis, fusion and also direct signaling through interaction with cell surface receptors (Urbanelli et al., 2013). At low pH conditions, exosomes from human metastatic

melanoma cells were shown to fuse with the plasma membrane of recipient cells using the lipid fluorescent dye R18 (Parolini et al., 2009). Exosome uptake by melanoma cells was reduced when cells were pretreated to inhibit proton pump activity which maintains low pH in malignant tumors. Therefore, acidic tumor microenvironment and the low pH of endosomes may play important roles in EV fusion to the plasma membrane or back fusion to MVB, respectively. The interaction of EV surface molecules with plasma membrane receptors can also induce changes in recipient cells by activation of various signaling pathways (Buzás, Tóth, Sódar, & Szabó-Taylor, 2018; French, Antonyak, & Cerione, 2017). Endocytosis-mediated uptake of EVs, including clathrin-dependent or independent endocytosis, micropinocytosis and phagocytosis, remains the most studied and widely accepted uptake mechanism (Costa Verdera, Gitz-Francois, Schiffelers, & Vader, 2017; D. Feng et al., 2010; Tian et al., 2014). Primary cortical neurons treated with oligodendroglial exosomes labelled with PKH67 dye showed co-localization of exosomes with LAMP-1 positive late endosomes (Frühbeis et al., 2013). Furthermore, neurons pretreated with Dynasore and Pitstop-2 reduced uptake of exosomes suggesting that oligodendroglial exosomes are uptaken by dynamin- and clathrin-dependent endocytosis in primary neurons (Frühbeis et al., 2013). More recently, Shelke et. al. reported endocytosis of mast cell derived exosomes by human mesenchymal stem cells (MSCs). Exosomes internalized by MSCs to endocytic compartments resulted in prolonged TGF-β signaling compared to free TGFβ1 (Shelke et al., 2019b). Although, it should be noted that multiple EV uptake mechanisms can also take place simultaneously due to EV heterogeneity.

The human brain and nervous system

The importance of the human brain in processing information to govern behavior has been recognized since the 5th century BC from the observations of Hippocrates (Breitenfeld, Jurasic, & Breitenfeld, 2014). He realized that injury to the brain leads to abnormal behaviors and affects normal body functions. For centuries the detailed structure and function of the brain remained unknown until the late 1800s when Ramon y Cajal identified neurons as the structural unit of the brain (DeFelipe, 2006). Later, the pioneering work in the 1950s by William Scoville and Brenda Milner from the case of patient H.M. established the role of the hippocampus in transforming short-term memories into long-term memories (Scoville & Milner, 1957). In the following decades, more studies on human patients and animal models identified different brain regions important for declarative or nondeclarative memories (Cohen & Squire, 1980). The medial temporal lobe, including the hippocampus, is associated with declarative (fact and event based) memory, while other brain regions including the striatum, neocortex and cerebellum are linked to nondeclarative memory (such as procedural memory) (Mayford, Siegelbaum, & Kandel, 2012). Although these previous studies identified the association of various brain regions with memory, the molecular and cellular mechanisms of memory formation and storage required further investigation.

Neurons communicate with each other via transmission of chemical and electrical signals at specialized sites called synapses. The axon terminal of the presynaptic neuron transmits signals via release of neurotransmitters that bind to receptors on dendritic spines of the postsynaptic neuron. It is now well established that dendritic spines and synapses contribute to the processes of learning and memory (Bliss, T.V.P. & Collingridge, 1993; Citri & Malenka, 2008). The molecular mechanisms of learning and memory involve structural and functional changes of synapses

mediated by long-term potentiation (LTP) or long-term depression (LTD) (Caroni, Donato, & Muller, 2012; Lamprecht & LeDoux, 2004; Mayford et al., 2012). Many studies have now established that changes in synaptic efficacy induced by LTP and LTD are linked to changes in the postsynaptic site (Manabe & Nicoll, 1994; Manabe, Wyllie, Perkel, & Nicoll, 1993; Zakharenko, Zablow, & Siegelbaum, 2001). In response to presynaptic neuronal activity, depolarization of postsynaptic neurons trigger a cascade of events leading to insertion (in case of LTP) or removal (for LTD) of AMPA receptors from the postsynaptic membrane by phosphorylation or dephosphorylation of the receptors, respectively. Such changes at the postsynaptic membrane lead to enlargement of spines due to insertion of AMPA receptors after LTP induction or shrinkage of spines following LTD (Holtmaat & Svoboda, 2009; Matsuzaki, Honkura, Ellis-Davies, & Kasai, 2004; Q. Zhou, Homma, & Poo, 2004) (Figure 3). Conversion of this short-term plasticity into long-term plasticity requires activation of PKA, MAPK and CREB signaling pathways to synthesize new proteins (Lu & Malenka, 2012; Mayford et al., 2012). An increase in the dendritic spine and synapse density has also been observed followed by LTP induction (Toni, Buchs, Nikonenko, Bron, & Muller, 1999). Therefore, alterations in spines and synapses are mediated by synaptic plasticity, ultimately regulating learning and memory.
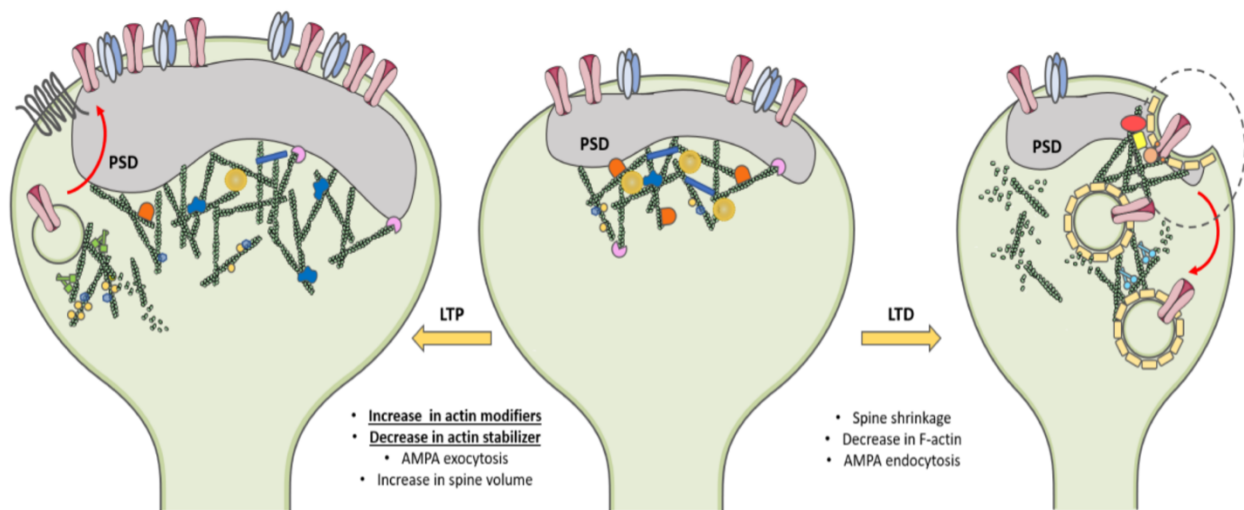
Figure 2: Remodeling of dendritic spines in response to activity-dependent synaptic plasticity. LTP induction promotes AMPA receptor insertion and spine head enlargement. LTD triggers endocytosis of AMPA and spine shrinkage.
©2020 Pelucchi et al. Originally published in International Journal of Molecular Sciences
https://doi.org/10.3390/ijms21030908
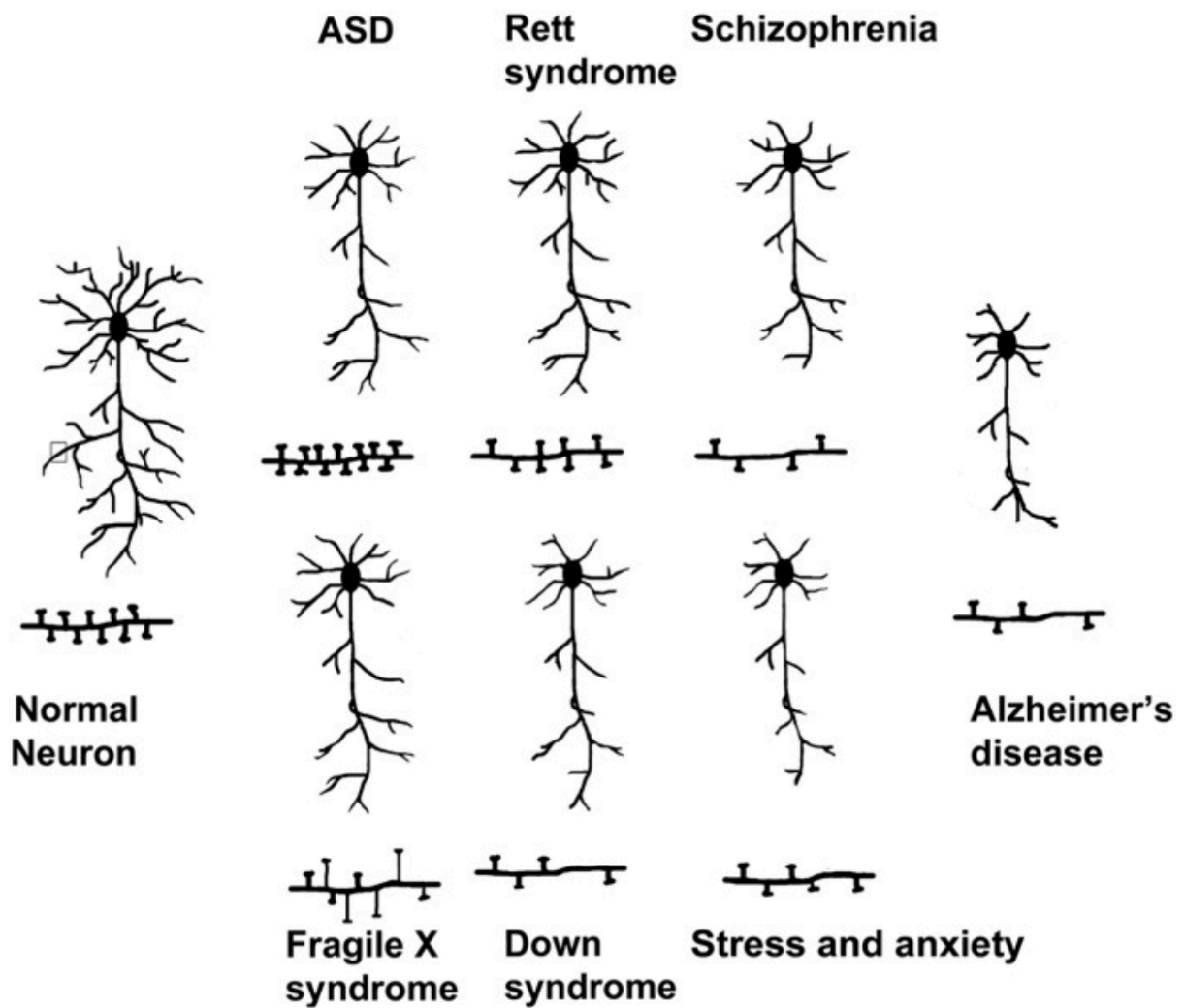
Figure 3: Schematic representation of spine density and morphology abnormalities in various neurological disorders. Spine density is decreased in AD, Schizophrenia, Rett syndrome, Down syndrome and during stress and anxiety. Spine density is increased in ASD. Abnormal thin spines are observed in Fragile-X syndrome.

Reprinted from Molecular and Cellular Neuroscience, Volume 50, Issue 1, Kulkarni & Firestein, The dendritic tree and brain disorders, P10-20, ©2012, with permission from Elsevier

Many studies have identified aberrations in spine morphology and density in neurological disorders such as AD, Schizophrenia, Autism Spectrum Disorders (ASD) and Fragile-X syndrome (Kulkarni & Firestein, 2012; S. Lee, Zhang, & Webb, 2015) (Figure 4). A decrease in spine density along with abnormal expression in Rho GTPases, Rac and Cdc42, is observed in hippocampus and cortex of AD patients (Aguilar, Zhu, & Lu, 2017; DeKosky & Scheff, 1990; S. Lee et al., 2015). Similarly, patients with Schizophrenia exhibit a reduction in spine density within the cortex, striatum and hippocampus with an accompanying reduction in Cdc42 expression (Hill, Hashimoto, & Lewis, 2006; S. Lee et al., 2015). By contrast, autism spectrum disorder patients display increased spine densities (Hutsler & Zhang, 2010). In Fragile-X syndrome, a significant increase in abnormally thin spines is observed (Irwin et al., 2001). However, closer examination of spine densities in Fragile-X syndrome mice using super-resolution microscopy revealed no significant changes in spine density but instead, development of stage-specific morphological changes in spines (Wijetunge, Angibaud, Frick, Kind, & Nägerl, 2014). Additionally, mutations in various postsynaptic adhesion proteins, actin-binding proteins and scaffold proteins are linked to ASD, AD and Schizophrenia (Penzes, Cahill, Jones, VanLeeuwen, & Woolfrey, 2011). These and many other studies suggest an undisputable association of spine and synapse function in neurological diseases.

Advancements in imaging techniques have allowed us to visualize *in vivo* spine dynamics during brain development. *In vivo*, spine density increases significantly throughout the early postnatal stage followed by selective spine elimination in adolescence. Later, in adulthood, spine density mostly remains constant when new spine formation and elimination are equalized (Chen, Lu, & Zuo, 2014) (Figure 5). The ability to culture primary neurons has enabled us to examine changes in neuronal structure and function at different developmental time points *in vitro*.
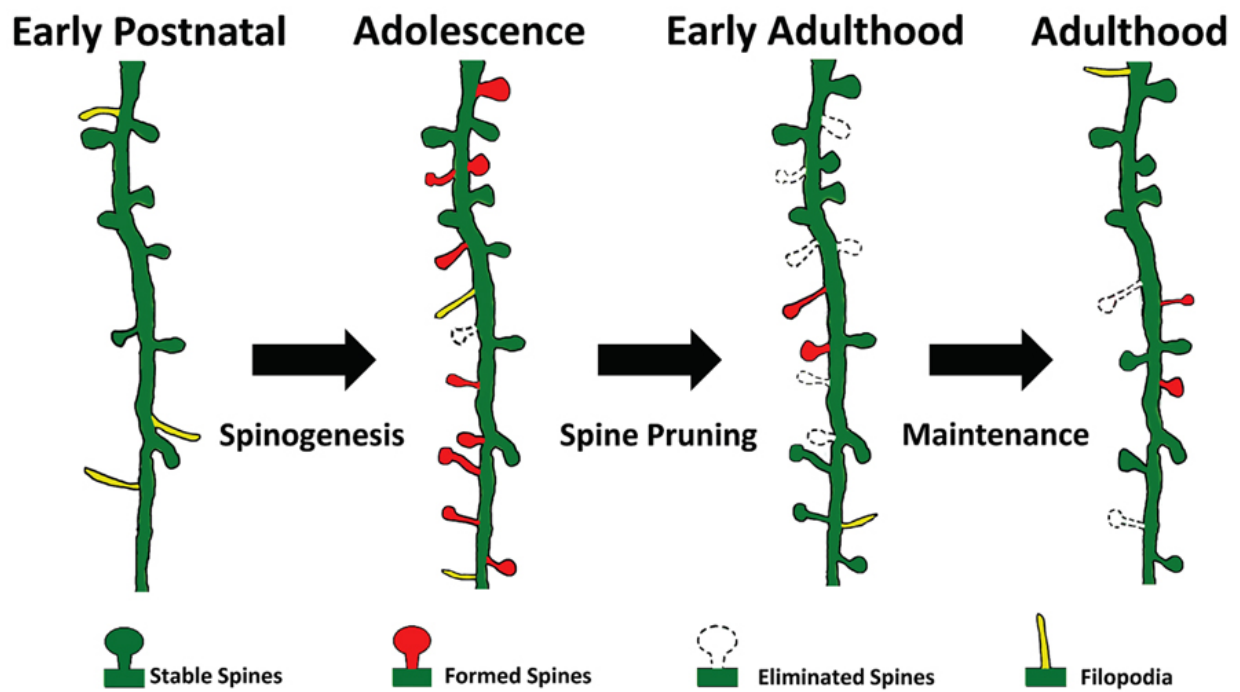
Figure 4: Dendritic spine dynamics throughout brain development. Spines are formed rapidly during early postnatal stage. Elimination of spines at adolescence is followed by equilibrium between spine formation and elimination in adulthood.
©2014 Chen et al. Originally published in Frontiers in Neuroanatomy
https://doi.org/10.3389/fnana.2014.00028

Similar to *in vivo* observations, spine density in primary hippocampal neuron cultures increases from week 1 to week 3 and then starts declining (M Papa, Bundman, Greenberger, & Segal, 1995). In multiple studies, researchers have made a common observation that neuronal dendrites possess numerous filopodia during the early stages of development that reduce in numbers as neurons mature. Also, the decrease in the number of filopodia correlates with an increase in dendritic spines and synapse formation suggesting spines evolve from filopodia (M Papa et al., 1995; Ziv & Smith, 1996; Zuo, Lin, Chang, & Gan, 2005). Further characterization of long-term neuron cultures have established their use in investigating spine and synapse formation *in vitro* (Lesuisse & Martin, 2002).

Structure and function of neurons and astrocytes:

The human brain is a remarkably complex organ that contains over 100 billion neurons and trillions of non-neuronal cells, called glia. These two main classes of cells are considered cellular building blocks of the nervous system. Neurons can be characterized into many different classes according to their size, shape, location or function. Based on structure, multipolar neurons (containing an axon and multiple dendrites) are the most common type of neurons in the mammalian nervous system. While glial cells can be classified into three main types: immune cells of the brain called microglia, myelin-producing oligodendrocytes/Schwann cells and astrocytes (Raisman, 1991). Precise communication between these various cell types is critical for brain function.

Neurons are highly polarized cells of the CNS that form intricate communication networks, locally or at long distances, with other neurons. Most neurons in the brain contain a single axon, a process extending from the neuronal cell body, to transmit signals to neighboring neurons for inter-

neuronal communication. The signal is transmitted via the release of synaptic vesicles containing neurotransmitters from axon terminals at specialized sites called synapses and is received in adjacent neurons through neuronal extensions called dendrites (Wells, 2005). The term dendrite is derived from the Greek word 'Dendron' (tree) due to its resemblance to branches of a tree. Dendritic complexity varies between different types of neurons which may dictate the degree of input received by neurons. Neuronal dendrites contain short actin-filled protrusions, called dendritic spines, that also serve as postsynaptic sites of most excitatory synapses (Jan, 2001).

Astrocytes are roughly star-shaped glial cells that provide biochemical, nutritional and structural support to neurons. They also play a critical role in the regulation of synapse formation, maintenance and elimination (Allen, 2014; Chung, Allen, & Eroglu, 2015). Primary neurons grown in co-culture with astrocytes are commonly used to study neuronal development and neuron-astrocyte interactions as they provide trophic factors for synapse formation and maturation (Banker, 1980; Jones, Cook, & Murai, 2012). Astrocytes also form tripartite synapses by enwrapping presynaptic and postsynaptic sites to modulate synaptic transmission and activity (Allen, 2014; Perea, Navarrete, & Araque, 2009). In the cortex, each astrocyte is estimated to contact over 500 neuronal dendrites which clearly indicates the importance of astrocyte communication to neurons (Halassa, Fellin, Takano, Dong, & Haydon, 2007). Contrary to the traditional view that brain function is dictated only by coordinated communication between neurons, emerging evidence suggests the involvement of astrocytes in this process. Several studies have reported that ablation of astrocytes in mice leads to neurodegeneration which could be attributed to excitotoxicity (Cui, Allen, Skynner, Gusterson, & Clark, 2001; Delaney, Brenner, & Messing, 1996). Astrocytes help protect neurons by uptaking excess potassium and neurotransmitters from the extracellular space between neurons (Larsen et al., 2014; López-

Bayghen & Ortega, 2011). Furthermore, astrocyte secreted molecules including hevin, thrombospondins, glypicans, cholesterol and tumor necrosis factor α (TNFα) have been shown to contribute to the formation of synapses (Allen, 2014; Christopherson et al., 2005; Kucukdereli et al., 2011).

Dendritic filopodia

Dendritic filopodia are thin actin-rich protrusions, up to 10µm long, arising from dendritic shafts during early stages of development (Gallo, 2013). They are highly motile structures with an average lifespan of 5-7 min in neurons (Portera-Cailliau, Pan, & Yuste, 2003). Both axons and dendrites of neurons form transient filopodia that are dependent on the regulation of actin cytoskeletal dynamics. The formation of filopodia involves small GTPases of the Rho superfamily and coordinated function of numerous actin-regulating proteins, such as Arp2/3 complex, ENA/VASP and fascin, for nucleation and elongation of actin filaments (Mattila & Lappalainen, 2008) (Figure 6). Filopodia present in the growth cone of axons probe the environment for axon guidance. However, they are not actively involved in establishing synaptic contact (Gallo, 2013). By contrast, dendritic filopodia through their dynamic movement search for presynaptic contact to form stable connections and mature into dendritic spines. A subset of dendritic filopodia that fail to make contact with an axon, retract back into the dendritic shaft (Ethell & Pasquale, 2005). Transformation of dendritic filopodia into spines upon presynaptic contact has been observed with live-imaging studies in both hippocampal and cortical neurons (Ziv & Smith, 1996; Zuo et al., 2005).
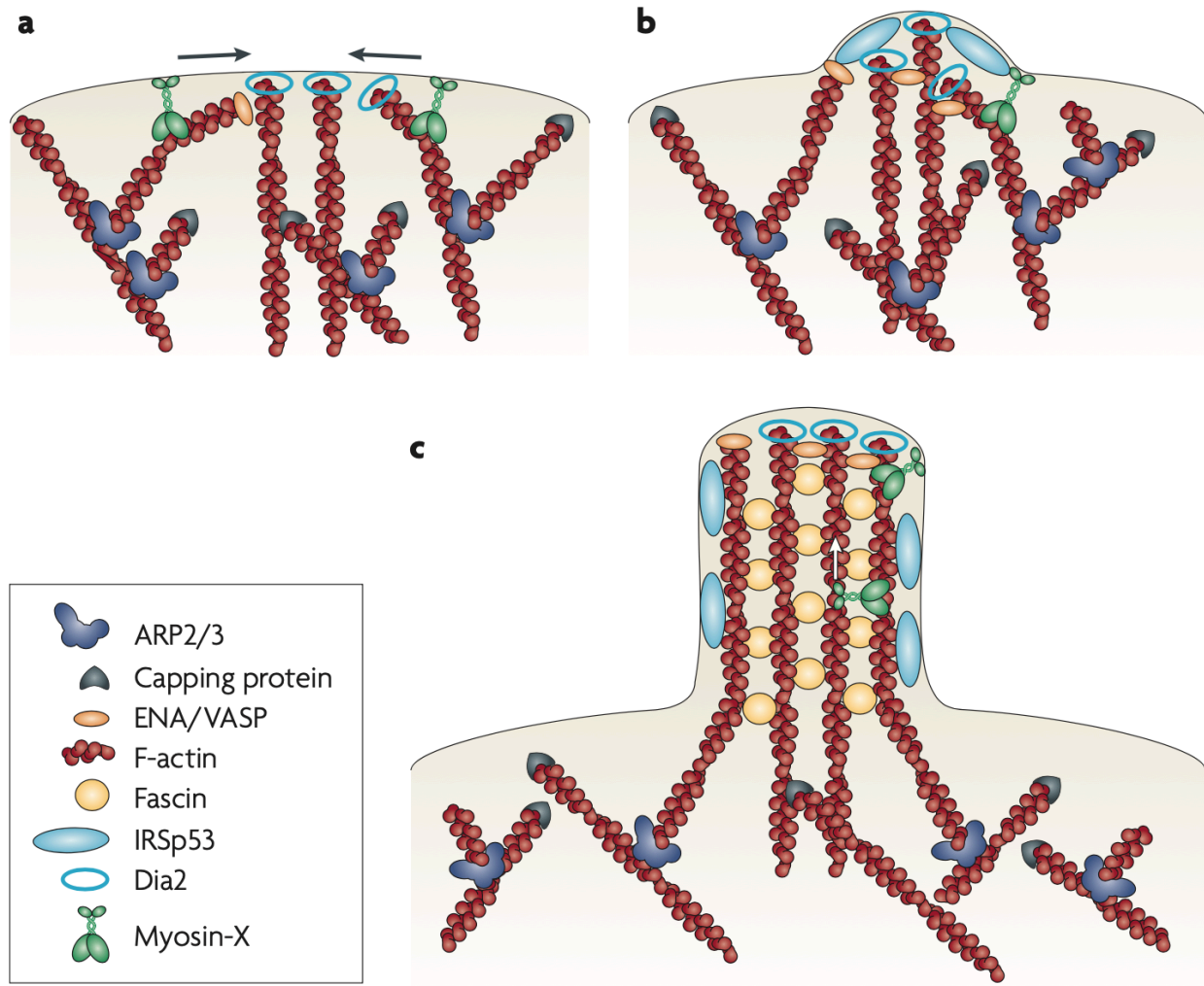
Figure 5: Model for filopodia formation. (a) Subset of actin filaments of Arp2/3 are targeted by mDia2 and/or ENA/VASP for elongation and converged by Myosin-X for initiation of filopodia formation (b) (I)-BAR domain containing proteins such as IRSp53 facilitate elongation by deforming the membrane and recruiting additional proteins (c) fascin bundles actin filaments. Reprinted by permission from Springer Nature. Nature Reviews Molecular Cell Biology. Mattila & Lappalainen. Filopodia: molecular architecture and cellular fucntions. ©2008.

Intracellular and extracellular regulators of filopodia formation:

Filopodia dynamics are regulated by many intracellular and extracellular factors. Proteins that directly control actin cytoskeletal dynamics, such as formins, Arp2/3 complex and fascin, are the most common intracellular regulators of filopodia (Mattila & Lappalainen, 2008). A study performed by Marc Kirschner's group discovered that Arp2/3 complex is required but not sufficient for Cdc42-induced filopodia formation (Ma, Rohatgi, & Kirschner, 1998). Later, they identified another Cdc42 interacting protein Neural Wiskott-Aldrich syndrome protein (N-WASP) to stimulate actin polymerization via activation of Arp2/3 complex (Rohatgi et al., 1999). However, several studies have reported no significant defects in filopodia formation in the absence of Arp2/3 suggesting the process of filopodia formation involves many different regulators and is dependent on cell type (Di Nardo et al., 2005; Steffen et al., 2006). The actin network formed by the Arp2/3 complex is highly branched, while formins are known to be involved in nucleation of linear actin filaments at the tips of filopodia. The Rho family GTPases Cdc42 and Rif1 are known to activate the formin mDia2 to induce filopodia formation (Pellegrin & Mellor, 2005; Peng, Wallar, Flanders, Swiatek, & Alberts, 2003). Although formins are mainly localized at the tips of filopodia, Jaiswal and colleagues showed that the mammalian formin Daam1 is also localized throughout the filopodial shaft by direct association with Fascin and have actin bundling function (Jaiswal et al., 2013). Additionally, the actin motor protein Myosin X has also been shown to promote filopodia formation, both *in vivo* and *in vitro*, by transporting integrins to the tips of filopodia (Heimsath, Yim, Mustapha, Hammer, & Cheney, 2017; Lin, Hurley, Raines, Cheney, & Webb, 2013).

Although, multitude studies have identified intracellular regulators of filopodia formation, only a handful of extracellular factors are known to date. In one study, nitric oxide was found to

increase the length but reduce the density of axonal growth cone filopodia in neurons containing soluble guanylyl cyclase (Van Wagenen & Rehder, 2001). In the dendritic shaft, blocking neuronal activity using a sodium channel blocker, TTX, or calcium depletion was shown to significantly increase filopodia length and density. However, application of glutamate only induced filopodia length and not the density (Portera-Cailliau et al., 2003). In another study, neuronal activity was found to have a positive effect on filopodia formation. Neurotrypsin released in response to presynaptic activity led to NMDA receptor activation and agrin cleavage on the postsynaptic site to induce filopodia formation (Matsumoto-Miyai et al., 2009). Overall, these results indicate the importance of neuronal activity in the regulation of filopodia density and dynamics through extracellular factors. Recently, filopodia length and density in various human cancer cell lines were shown to have direct correlation with extracellular level of hyaluronan, an ECM component (Kyykallio et al., 2020). Among other extracellular regulators, soluble thrombospondin type 1 domain containing 7A (THSD7A) is known to promote filopodia formation in human umbilical vein endothelial cells (HUVEC) (Kuo, Wang, Wu, Chang, & Chuang, 2011).

Dendritic spines and synapses

Dendritic spines are postsynaptic sites of most excitatory synapses that contain electron dense region across the presynaptic axon, called the postsynaptic density (PSD) (Ebrahimi & Okabe, 2014). A widely accepted view based on microscopic observation suggests that spines evolve from dendritic filopodia (Marrs, Green, & Dailey, 2001; Michele Papa, Bundman, Greenberger, & Segal, 1995; Ziv & Smith, 1996; Zuo et al., 2005). Dendritic spines can also form without precursor filopodia, directly emerging from the dendritic shaft without presynaptic contact (Ethell & Pasquale, 2005). Based on their morphology, spines are classified as mushroom, thin or

stubby spines. However, electron microscopy (EM) analysis of mature hippocampal neurons revealed that there is wide morphological variation among even a single class of spines suggesting a spectrum of spine morphologies. The spine head is filled with branched actin filaments, the base contains more linear actin filaments, while the spine neck is enriched in both branched and linear actin filaments (Korobova & Svitkina, 2010). Compartmentalization of dendritic spines due to thin necks and enlarged heads provides greater control over Ca^{+2} concentration, by hindering Ca^{+2} diffusion to dendritic shafts, to regulate the activities of Ca^{+2} dependent proteins present in dendritic spines (Nimchinsky, Sabatini, & Svoboda, 2002).

Intracellular and extracellular regulators of spine and synapse formation:

Spines are densely packed dendritic protrusions made of linear and branched actin filaments which constantly undergo changes mediated by intracellular or extracellular molecules regulating various signaling pathways. Spine formation and remodeling are heavily dependent on actin dynamics mediated by actin binding proteins and Rho family small GTPases (RhoA, Rac and Cdc42) (Calabrese, Wilson, & Halpain, 2006; Tada & Sheng, 2006; Yoshihara, De Roo, & Muller, 2009). Primary hippocampal neurons transfected with a dominant-negative version of Rac or Cdc42 show reduced dendritic spine formation (Irie & Yamaguchi, 2002; Huaye Zhang, Webb, Asmussen, & Horwitz, 2003). Additionally, transgenic mice expressing a constitutively active form of Rac in Purkinjie cells showed a drastic increase in spine density but a reduction in spine size (Luo et al., 1996). In a study conducted using hippocampal slice cultures, expression of a constitutively active RhoA shortened spine necks and reduced spine density (Tashiro, Minden, & Yuste, 2000). Moreover, Cdc42 and Rac guanine nucleotide exchange factors (GEFs) Intersectin and Asef2, respectively, also increase spine density (Evans, Robinson, Shi, & Webb, 2015; Irie &

Yamaguchi, 2002). Many actin binding proteins regulate spine dynamics in association with scaffold proteins present at PSDs. For instance, the C-terminal SH3 domain of cortactin interacts with Shank family proteins. Both, cortactin and shank have been shown to promote spine morphogenesis (Hering & Sheng, 2003; Romorini, Piccoli, & Sala, 2006). Furthermore, a headless form of the actin motor protein Myosin X induces dendritic spine and synapse formation indirectly via increased retention of vasodilator-stimulated phosphoprotein (VASP) in spines (Lin et al., 2013; Lin, Nebhan, Anderson, & Webb, 2010). Dynamic interplay between these and numerous other intracellular proteins regulate spine and synapse formation (Ethell & Pasquale, 2005; Sekino, Kojima, & Shirao, 2007).

Most extracellular molecules involved in spine formation and maturation, including neurotransmitter release from presynaptic terminals, ECM proteins, adhesion molecules and factors secreted by astrocytes, function via interaction with cell surface receptors on postsynaptic sites. Several studies have identified a function of TGF-β signaling in synaptogenesis. In particular, TGF-β1 secreted from astrocytes and Schwann cells is known to induce synaptogenesis in mouse cortical neurons and xenopus neuromuscular junctions (NMJs), respectively (Diniz, Almeida, Tortelli, Lopes, et al., 2012a; Z. Feng & Ko, 2008). In primary neurons, the synapse inducing activity of murine and human astrocyte conditioned media was partially or completely abolished in the presence of TGF-β signaling inhibitor SB431542. Furthermore, treatment of TGF-β1 alone was sufficient to induce synapse formation by increasing levels of the NMDA receptor co-agonist D-serine (Diniz, Almeida, Tortelli, Lopes, et al., 2012a). In Xenopus neuron-muscle cocultures, Schwann cell conditioned media and TGF-β1 significantly increased acetylcholine receptor clusters, a characteristic of NMJ synapse formation (Z. Feng & Ko, 2008). These studies demonstrate that synaptogenesis in both CNS and PNS is regulated by glia secreted TGF-β1. Also,

CNS specific TGF-β1 deficient mice display reduced dendritic spines and abnormal synaptic activity (Koeglsperger et al., 2013). It remains to be defined what extracellular factors regulate bioavailability of active TGF-β by releasing from its latent complex.

Moreover, glutamate released from presynaptic sites binds to postsynaptic glutamate receptors. Previous studies have shown that NMDA receptor activity is coupled with spine outgrowth. Whereas AMPA receptor activation by 100μM glutamate alone is sufficient to inhibit spine motility for stabilization (Fischer, Kaech, Wagner, Brinkhaus, & Matus, 2000). Brain derived neurotrophic factor (BDNF) also has an implied function in regulation of neuronal structures depending on the brain region and developmental stage. In mature hippocampal neurons, dendritic spine density was drastically reduced by blocking endogenous BDNF using function blocking antibodies (Kellner et al., 2014). Additionally, trans-synaptic interaction of postsynaptic EphB with axonal ephrinB leads to spine formation and eventually stabilization (Aoto et al., 2007; Sheffler-Collins & Dalva, 2012). Specifically, spine and synapse density in cortical neuron cultures transfected with EphB2 shRNA was significantly reduced compared to control (Kayser, Nolt, & Dalva, 2008). Similarly, presynaptic neurexins connect with postsynaptic neuroligins to initiate synapse formation by stabilizing pre and post synaptic contacts (Krueger, Tuffy, Papadopoulos, & Brose, 2012). Factors secreted by astrocytes also modulate spine and synapse formation, stability and maturation (Allen, 2014; Chung et al., 2015). Finally, ECM proteins present in extracellular space near synaptic cleft can also regulate synaptic plasticity (Ethell & Pasquale, 2005). EVs are known to carry ECM molecules and they also regulate various physiological processes of the nervous system. However, regulation of spine and synapse formation via astrocyte-derived EVs is not well understood.

Extracellular vesicles in nervous system:

Proper functioning of neural cells requires reciprocal communication between different cell types in the nervous system. Many studies have reported release of EVs from various cell types of the peripheral nervous system (PNS) and the central nervous system (CNS) including Schwann cells, microglia, oligodendrocytes, astrocytes and neurons (Budnik, Ruiz-Cañada, & Wendler, 2016b). Via autocrine and paracrine signaling, EVs exert a diverse set of physiological and pathological functions in the nervous system such as regulation of neurite outgrowth, neuroprotection, synaptic plasticity and spreading pathological proteins (C. P. K. Lai & Breakefield, 2012; Xiao et al., 2017) (Figure 2).

In the PNS, Schwann cells play an essential role in axonal regeneration after peripheral nerve injury. This process requires bidirectional communication between Schwann cells and neurons for Schwann cell dedifferentiation, proliferation and axonal regeneration. In a study by Lopez-Verrilli and colleagues, Schwann cell derived exosomes were found to be internalized by dorsal root ganglia (DRG) axons and increase axonal regeneration by reducing the activity of RhoA GTPase (Lopez-verrilli, Picou, & Court, 2013). Also, axonal regeneration was markedly enhanced *in vivo* by injecting exosomes following sciatic nerve injury. Recently, Schwann cell exosomes were also shown to increase DRG cell activity after electrical stimulation (Hu et al., 2019).

Emerging evidence also indicates a role for EVs in communication between different types of neurons and glia in the CNS (Figure 2). Oligodendrocytes, a type of glial cells, are mainly important for axon myelination. However, they also provide trophic factors for protecting neurons.
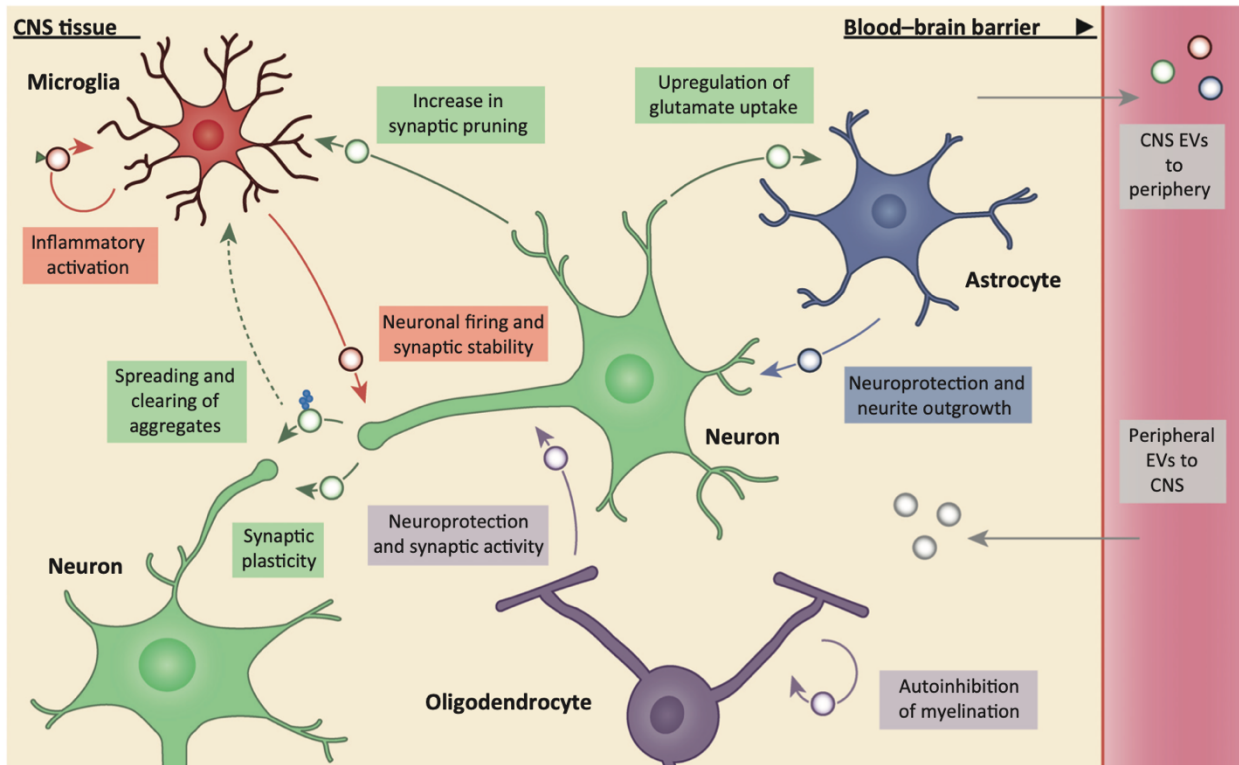
Figure 6: Role of EVs in the CNS. EVs are secreted by most cell types in the CNS. Neurons and glia communicate through EVs containing functional cargo. Neuronal EVs are secreted in response to synaptic activity. Astrocyte-derived EVs regulate neuroprotection and neurite outgrowth. Neuronal EVs also propagate toxic protein aggregates in neurodegenerative diseases. EVs can also cross blood-brain barrier.
Reprinted from Trends in Neuroscience, Volume 41, Issue 6, Holm et al., Extracellular Vesicles: Multimodal Envoys in Neural Maintenance and Repair, P360-372, ©2018, with permission from Elsevier

Oligodendrocytes provide neuronal protection against iron mediated cytotoxicity by releasing ferritin heavy chain in EVs (Mukherjee et al., 2020). Secretion of EVs from oligodendrocytes is known to be regulated by a small GTPase Rab35 (Hsu et al., 2010). Conditional knockout of Rab35 in mice showed increased oxidative DNA damage at 6 and 12 months (Mukherjee et al., 2020). Furthermore, exosome secretion from oligodendrocytes occurs in response to neuronal activity such as depolarization and neurotransmitter release (Frühbeis et al., 2013). Exosomes released by oligodendrocytes contain antioxidant enzymes such as catalase and superoxide dismutase to protect neurons from oxidative stress (Fröhlich & Kuo, 2014). Apart from their function in neuroprotection, EVs secreted by oligodendrocytes are also known to contain high levels of myelin proteins (Frühbeis et al., 2013). Whether EV associated myelin has any function in communication or if it is only a way to dispose redundant myelin protein remains unknown. However, microglia mediated clearance of oligodendroglial exosomes by constitutive macropinocytosis has been reported (Fitzner et al., 2011).

EVs released by microglia have been shown to regulate both excitatory and inhibitory transmission in neurons. MVs derived from microglia enhance excitatory neurotransmission by facilitating sphingolipid metabolism in neurons (Antonucci et al., 2012). Simultaneously, endocannabinoids present on the surface of MVs and exosomes secreted by microglia activates presynaptic type-1 cannabinoid receptors and decrease inhibitory transmission (Gabrielli et al., 2015). The most abundant type of glia, astrocytes, also secrete EVs to regulate neuronal functions. Internalization of astrocyte derived EVs carrying Apolipoprotein D by neurons can enhance neuronal survival under oxidative stress (Pascua-Maestro et al., 2019). Cargo selection in astrocyte EVs is highly dependent on environmental stimuli (Chaudhuri et al., 2018; Ibáñez, Montesinos, Ureña-Peralta, Guerri, & Pascual, 2019). EVs secreted by astrocytes in response to the trophic

stimulus ATP or anti-inflammatory stimulus IL10 contain proteins that promote neurite outgrowth, neuronal survival, and dendritic complexity. By contrast, astrocyte EVs secreted in the presence of an inflammatory stimulus IL-1β contain proteins that regulate immune cell trafficking and immune response (Chaudhuri et al., 2018).

Exosomes secreted by primary cortical neurons contain neuron specific proteins including L1 cell adhesion molecule and AMPA receptor subunits GluR2/3. Additionally, the ESCRT-I protein TSG101 and the ESCRT accessory protein Alix are also present in neuronal exosomes suggesting an endocytic origin of neuronal exosomes (Fauré et al., 2006). The spontaneous increase in glutamatergic activity by GABA$_A$ receptor inhibitors, bicucullin and picrotoxin, leads to significant increase in neuronal exosome secretion (Lachenal et al., 2011). Therefore, exosome secretion from primary neurons is regulated by synaptic activity. Furthermore, secreted exosomes display selectivity in uptake by recipient cells. For instance, stimulated neurons release exosomes that bind to and are internalized only by neurons, and not glial cells (Chivet et al., 2014). Collectively, these studies show that neuronal exosome secretion and uptake are highly regulated processes which can be utilized by neurons to transfer specific cargo molecules for interneuronal communication. However, role of neuronal exosomes during development and identification of functional cargo in neuronal exosomes remain less well studied.

The goal of my research was to identify role of neuron-derived and astrocyte-derived SEVs in filopodia, spine and synapse formation. Chapter II focuses on the role of neuronal exosomes in filopodia formation and identification of THSD7A as a unique exosome cargo responsible for filopodia formation. Chapter III includes my research on function of astrocyte-derived SEVs in synaptogenesis via fibulin-2-mediated activation of TGF-β signaling. Chapter V contains conclusions and future directions for SEV secretion and function during neuronal development.

CHAPTER II

NEURONAL EXOSOMES INDUCE FILOPODIA FORMATION VIA THSD7A

Abstract:

Dendritic filopodia are highly dynamic actin-rich protrusions emerging from the dendritic shaft during the early stages of neuronal development. Several live imaging studies have shown that dendritic filopodia are precursors of dendritic spines in hippocampal and cortical neurons. So far, many intracellular factors that regulate filopodia formation have been identified. However, extracellular mechanisms of filopodia formation are largely unknown. Exosomes have the potential to regulate filopodia, spine and synapse formation in an autocrine or paracrine manner due to their unique cargo composition. Here, we examine the role of exosomes in filopodia, spine and synapse formation. We find that the MVB docking factor GFP-Rab27b localizes to the tips and bases of actin-rich filopodia and spines in primary neurons. Genetic regulation of exosome secretion by overexpression or knockdown of Rab27b or Hrs leads to respective increases or decreases in the number of filopodia, spines and synapses. The defects of exosome-inhibited neurons in filopodia density are rescued by the add-back of neuronal exosomes. A quantitative proteomics analysis of SEVs combined with assessment of biological activity identified THSD7A in neuronal exosomes to be a key cargo molecule for filopodia formation. We propose a model in which the targeted release of neuronal exosomes carrying THSD7A induces filopodia formation.

Introduction:

Filopodia are thin actin structures extending from the cell surface that probe the environment for external cues to regulate important physiological processes such as cell migration, neurite outgrowth and spine formation (Heckman & Plummer, 2013; Mattila & Lappalainen, 2008a). In neurons, dendritic spines evolve from filopodia by active rearrangement of the actin cytoskeleton (Portera-Cailliau et al., 2003; Ziv & Smith, 1996). These precursors of spines dynamically grow and reach the presynaptic partner to form a mature spine or shrink back to the dendritic shaft (Ethell & Pasquale, 2005). Aberrations in size and density of dendritic spines are associated with many neurological disorders (Ebrahimi & Okabe, 2014). Therefore, it is critical to understand factors that regulate the formation of precursor dendritic filopodia.

The highly dynamic behavior of filopodia results from active rearrangement of the actin cytoskeleton regulated by numerous actin-binding proteins such as Arp2/3 complex, formins and fascin (Gallo, 2013). These proteins function in a highly coordinated manner at the different stages of initiation, elongation and bundling of actin filaments in filopodia. Many of the intracellular cytoskeletal regulators of filopodia function downstream of Rho family GTPases, Cdc42 and Rac1 (Mattila & Lappalainen, 2008).

In neurons (and other cells), many studies have identified intracellular regulators of filopodia formation (Barzik, McClain, Gupton, & Gertler, 2014; Gallo, 2013; Ma et al., 1998). However, few extracellular factors that regulate filopodia have been identified. Several studies have shown the importance of growth factors in the regulation of axonal filopodia. Brain derived neurotrophic factor (BDNF) has been shown to induce axonal filopodia formation via MAPK dependent phosphorylation of actin regulatory protein Eps8 (Menna et al., 2009). In another study, nerve growth factor (NGF) was shown to promote filopodia formation through activation of the

PI3K signaling pathway (Ketschek & Gallo, 2010). Furthermore, NGF also induces protein translation of Arp2/3 complex regulators, WAVE1 and Cortactin, downstream of PI3K signaling (Spillane et al., 2012). Whether neurotrophins also control dendritic filopodia formation through similar pathways is not well understood. Although neurotrophin receptors, p75^{NTR} and truncated TrkB, are implicated for dendritic filopodia formation, their function in inducing filopodia formation was found to be independent of activation by extracellular neurotrophins (Hartmann et al., 2004).

In the past decade, extracellular vesicles (EVs) are being increasingly recognized for their function in cellular communication (Maas et al., 2017b; Graça Raposo & Stoorvogel, 2013). Exosomes are small EVs of endocytic origin that carry functional cargo molecules including proteins, lipids and nucleic acids. They participate in diverse physiological and pathological functions by regulating the behavior of recipient cells in an autocrine or paracrine manner (Colombo, Raposo, & Théry, 2014; Urbanelli et al., 2013). Most studies in neuronal exosomes are centered around their function in spreading misfolded proteins in neurodegenerative diseases (Saman et al., 2012; Xiao et al., 2017; Yuyama & Igarashi, 2016). A few studies have examined exosomes released by healthy primary neurons to analyze their secretion in response to synaptic activity and specificity for uptake by neurons (Chivet et al., 2014; Lachenal et al., 2011). However, their function in normal neuronal development and synapse formation is largely unknown.

Previous studies from our lab found that exosomes released from cancer cells can induce formation of actin cytoskeletal structures used for cell migration and invasion, including invadopodia (D. Hoshino et al., 2013) and adhesion formation (Sung et al., 2015). Since filopodia are actin-rich adhesive structures that are critical for normal neuronal synapse formation, we investigated the role of exosomes in filopodia formation by neurons. To model the process of

neuronal filopodia formation during development, we used primary cultures of embryonic hippocampal and cortical neurons.

Here, we find that GFP-Rab27b is localized to the tips and bases of filopodia and spines in primary cultures of hippocampal and cortical neurons. Also, the expression of Rab27b increased filopodia density while knockdown of Hrs or Rab27b significantly reduced the number of filopodia. Consequently, the increases or decreases in filopodia density followed respective increases or decreases in the dendritic spine and synapse density. These defects in filopodia density were rescued by the addition of purified neuronal exosomes. Furthermore, we identified THSD7A as a key cargo molecule responsible for filopodia formation through an iTRAQ proteomics analysis. Recombinant THSD7A was able to rescue filopodia defects in Hrs KD neurons in a dose-dependent manner. Additionally, exogenous expression of THSD7A revealed its localization to the tips of filopodia and also enhanced filopodia density. In summary, this work demonstrates the function of neuronal exosomes in inducing filopodia formation mediated by THSD7A.

Materials and methods:

Reagents and constructs:

mCherry cDNA was a generous gift from Dr. Roger Tsien (University of California, San Diego, CA). GFP and mCherry were cloned into pTαS2 vector, a kind gift from Dr. Freda Miller, for expression in neurons. SV2 monoclonal antibodies were obtained from Developmental studies hybridoma bank (University of Iowa, Iowa City, IA). PSD95 antibody was from Millipore Sigma (MAB1598). THSD7A antibody was from Sigma-Aldrich (HPA000923). TSG101 antibody was from Abcam (ab30871). Alix antibody was from Cell Signaling (#2171). Flotillin-1 and GM130 antibodies (#610820 and #610822) were purchased from BD Biosciences. Recombinant human

THSD7A protein was from R&D Systems (9524-TH). Alexa Fluor 488 Anti-Rabbit and Alexa Fluor 647 Anti-Mouse were from Molecular Probes. For neuronal cultures, B27 media was prepared by adding a 2% B27 supplement and L-glutamine to neurobasal media. pCMV-FLAG and pCMV-FLAG-THSD7A expression vectors were kindly provided by Dr. Yung-Jen Chuang (Kuo et al., 2011).

Primary cultures of neurons:

Rat hippocampal and cortical neurons were isolated from day 19 embryos and plated on 1 mg/ml Poly-L-Lysine (PLL) or 50ug/ml Poly-D-Lysine (PDL) coated glass coverslips. Low-density cultures were prepared as described previously (Kaech & Banker, 2006). In brief, the hippocampus and cortex were removed from dissected brains of day 19 rat embryos and incubated in 0.05% trypsin in HBSS for 10 mins at 37°C. Neurons were washed with HBSS, homogenized by gentle mixing, and plated on PLL or PDL coated coverslips. After 3-4 hours, neuron coverslips were transferred to 60mm dishes containing primary astrocytes for co-culture.

Calcium phosphate transfection:

Neurons were transfected with a modified calcium phosphate transfection method at day 3 or 5. 1 ug of mCherry-pTαS2 and 1 µg of GFP-pTαS2 or 3 µgs of GFP-Rab27b/ shRNAs or 2 µgs of pCMV-FLAG/pCMV-FLAG-THSD7A were mixed with 120µl of 250mM $CaCl_2$ in an Eppendorf tube. 120µl of 2x HBS (274 mM NaCl, 9.5 mM KCl, 15 mM glucose, 42 mM HEPES, 1.4 mM Na_2HPO_4, pH – 7.15) was added drop by drop to the DNA- $CaCl_2$ mixture with continuous aeration and incubated at room temperature for 15 min. Neuron coverslips were removed from co-cultures and transferred to another dish for dropwise addition of transfection mixture. Neuron dishes were kept in the incubator at 37° C for about 30-40 minutes and then washed three times with HBSS washing buffer (135 mM NaCl, 4mM KCl, 2mM $CaCl_2$, 1mM $MgCl_2$, 10 mM glucose, 20 mM

HEPES, pH 7.35). Neuron coverslips were then transferred back to the home dishes containing astrocytes. Transfection efficiency was obtained in the range of 5-10% using this method.

Microscopy and Image Analysis:

Neuronal imaging was performed on a Quorum Wave-FX Yokogava CSU-X1 spinning disk confocal system with a Nikon Eclipse Ti microscope. Images were acquired using MetaMorph software (Molecular Devices, Sunnyvale, CA) and a Plan Apo TIRF 60x (NA 1.49) objective. Images for GFP, mCherry and SV2 647/PSD95 647 were acquired by laser excitation at 491 nm, 561 nm and 642 nm respectively. Emission filters for these fluorophores were 525/50, 593/40 or 620/60 and 700/75 respectively (Semrock, Rochester, NY). Primary or secondary dendrites from confocal images were randomly selected for quantification of filopodia and spine density. Dendritic filopodia were defined as thin headless protrusions negative for SV2 staining. Dendritic spines were identified as dendritic protrusions that co-localize with synaptic markers SV2 or PSD95. Synapses were defined as SV2 puncta present on both dendritic shaft and protrusions.

Please refer to chapter III for following methods:

Exosome Isolation, Immunocytochemistry, Western blot, EM, Statistics.

Results:

<u>*MVB docking factor RAB27b localizes to filopodia and spines:*</u>

To determine potential sites of exosome release in neurons, we examined the localization of the MVB docking factor GFP-Rab27b to filopodia and spines. In primary neuron cultures, numerous filopodia are present on dendritic shafts at day in vitro (*DIV*) 6 and dendritic spines around *DIV*12 (Lin et al., 2013). Neurons isolated from day 19 rat embryos in co-culture with

astrocytes were transiently transfected at *DIV*5 with GFP-Rab27b, and with mCherry as a filler to visualize the neuronal structure. Neurons were then fixed and stained with the synaptic marker SV2 at *DIV*6 or *DIV*12 to analyze dendritic filopodia and spines, respectively. Notably, GFP-Rab27b localized to the bases and tips of dendritic filopodia in both hippocampal and cortical neurons (Figure 7A and 7C). In cortical neurons, ~63% of GFP-Rab27b localized to the bases of filopodia while 37% localized to the tips (Figure 7B). Similarly, hippocampal neurons displayed ~67% and ~33% localization of Rab27b in the bases and tips of filopodia, respectively (Figure 7D). Similarly, GFP-Rab27b localization was also observed in dendritic spines but not to the same extent possibly due to degradation of some GFP-Rab27b from the time of expression after transfection (*DIV*5) to immunostaining (*DIV*12) (Figure 7E and 7F).

Hrs and Rab27b expression affects filopodia, spine and synapse density:

In neurons, filopodia formation is critical for the subsequent development of synapses, as filopodia mature into postsynaptic specializations called dendritic spines (Portera-Cailliau et al., 2003; Ziv & Smith, 1996). To test whether exosomes regulate filopodia in neurons, we altered the expression of exosome regulators in primary rat hippocampal and cortical neurons. Cortical neurons overexpressing GFP-Rab27b exhibited a significant increase in the number of filopodia examined at *DIV*6, quantitated as thin protrusions that were negative for SV2 (Figure 8A and 8B). This increase in filopodia density translated into an increased number of SV2-positive dendritic spines and synapses at *DIV*12 (Figure 8C and 8D). A similar increase in filopodia, spine and synapse density was also observed in primary hippocampal neurons upon GFP-Rab27b expression (Figure 10A and 10B).
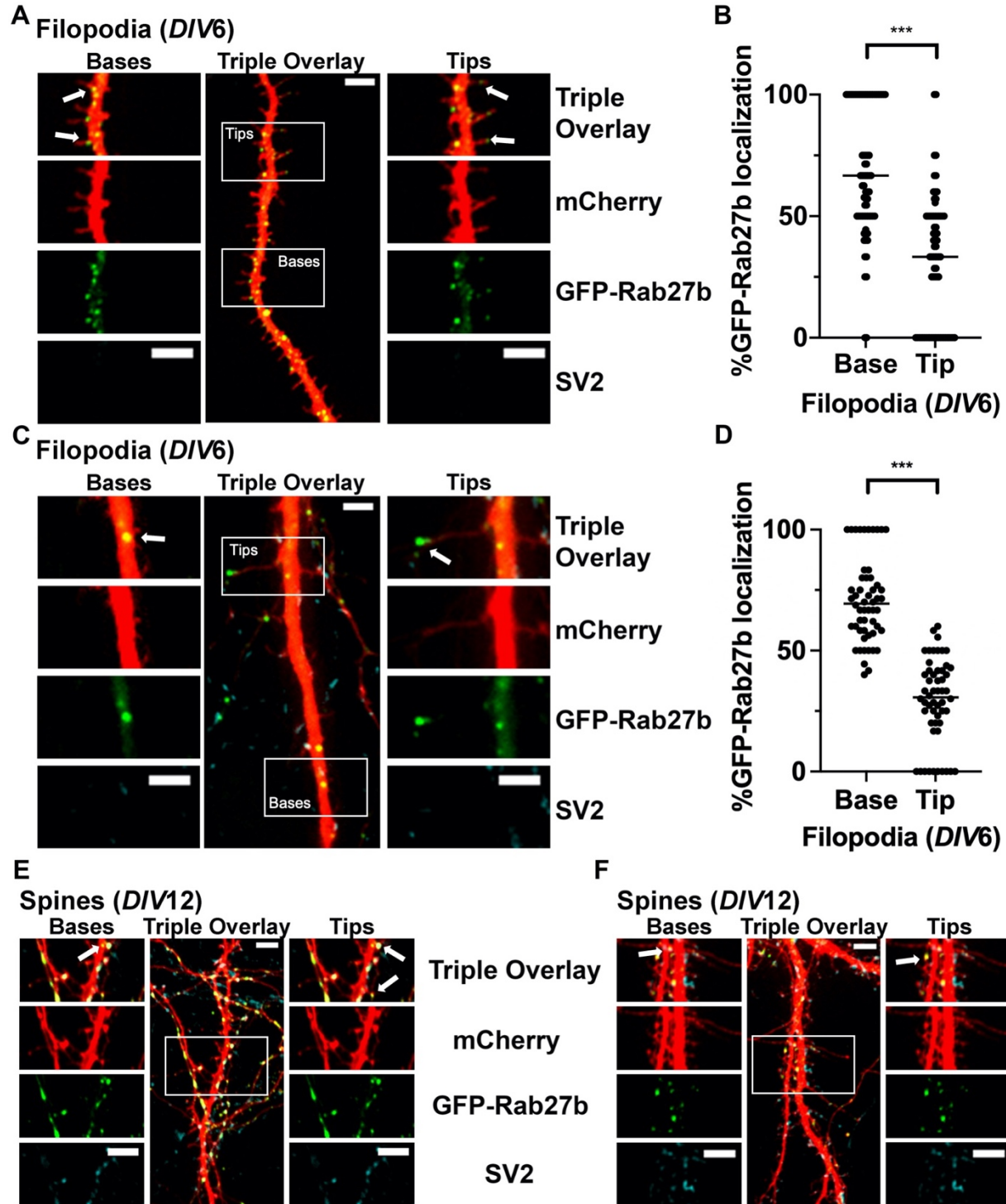
Figure 7. MVB marker GFP-Rab27b localize to the bases and tips of filopodia and spines. Primary cortical neurons (A and E) and hippocampal neurons (B and F) were co-transfected with GFP-Rab27b (green) and mCherry (red) on *DIV*5 and immunostained for SV2 on *DIV*6 (A and C) or *DIV*12 (E and F). Arrows indicate localization at tips and bases of filopodia. Scale bar, 5μm. Quantification of percentage GFP-Rab27b localization at tips vs bases in cortical neurons (B) and hippocampal neurons (D) from three independent experiments. ***p<0.001.
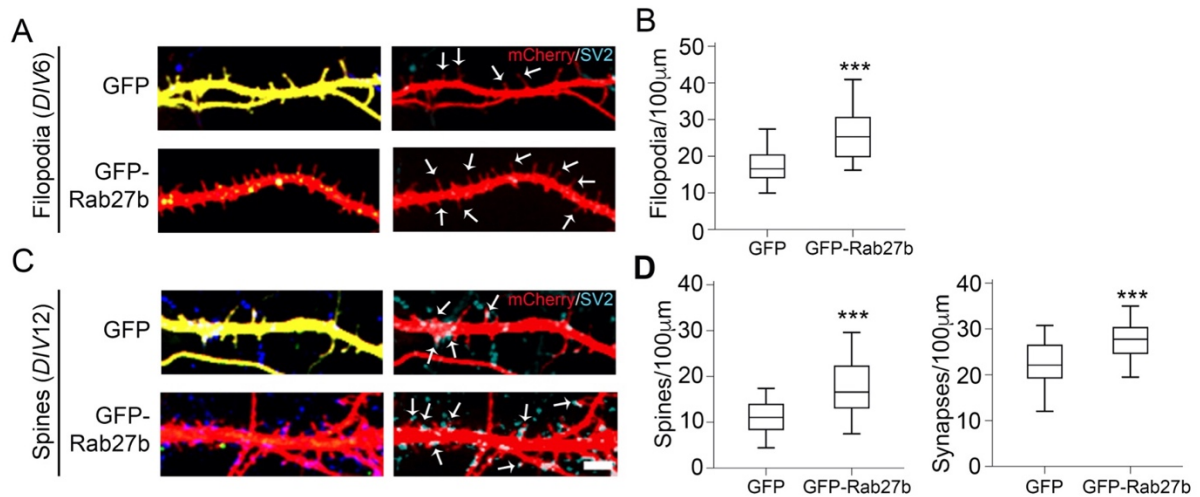
Figure 8. GFP-Rab27b expression in cortical neurons promotes filopodia, spines and synapses. Neurons co-transfected with GFP or GFP-Rab27b and mCherry on *DIV*5 and immunostained for SV2 at *DIV*6 (A) or *DIV*12 (C). Left panel: Triple overlay. Right panel: Overlay of mCherry and SV2. Arrows indicate filopodia (A) or spines (B). Quantification of filopodia density at *DIV*6 (B) or spines and synapse density at *DIV*12 (D) from three independent experiments. Data represented as box and whiskers plot, bar indicating the median, and the box showing interquartile range. Scale bar, 5 μm. ***p<0.001.

To inhibit exosome secretion, we knocked down Hrs or Rab27b in primary cortical and hippocampal neurons by transient transfection with two different shRNAs at least 48 hours prior to immunostaining. For both genes, shRNA-transfected neurons exhibited a 40-60% reduction in protein expression analyzed by fluorescence intensity (Figure 9A-D). Analysis of immunostained cells revealed that loss of either Rab27b or Hrs KD in neurons led to a significant reduction in filopodia, spines, and synapse density compared to NTshRNA controls (Figure 9E-H and 10C-F). For further validation, a postsynaptic marker, PSD95, was also used to analyze dendritic spines (Figure 11). Both hippocampal and cortical neurons exhibited a significant increase in dendritic spines upon Rab27b overexpression and a significant reduction with knockdown of Hrs or Rab27b. These results indicate that the exosome biogenesis and secretion regulators, Hrs and Rab27b, affect filopodia density in primary neurons.

The effects of Hrs- and Rab27b-KD on filopodia density are rescued by add-back of purified neuronal exosomes:

To further verify that the filopodia density defects were due to changes in exosome release, we performed rescue experiments by treating Rab27b- or Hrs-KD primary cortical neurons for 24 h with exosomes isolated from *DIV*9 primary cortical neurons. To obtain purified exosomes, neuronal conditioned media was serially centrifuged at 300xg to remove cells, 2000xg to remove cell debris and 10,000xg to remove MVs followed by ultracentrifugation at 100,000xg for 18 h to pellet exosomes. Purified exosomes were characterized for their size, common protein markers and morphology.
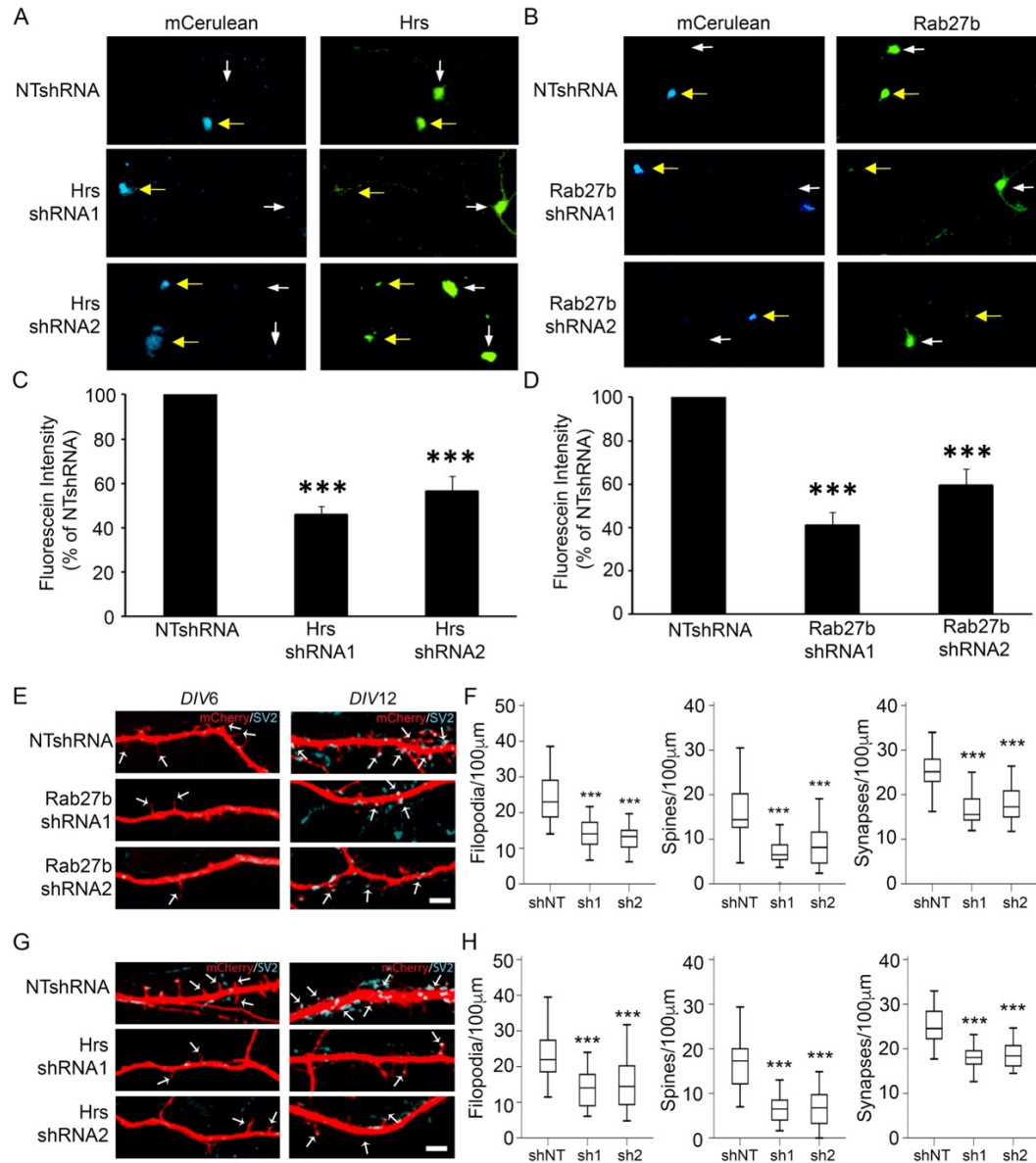
Figure 9. Rab27b and Hrs knockdown reduce filopodia, spine and synapse density in cortical neurons. Neurons co-transfected with mCerulean filler and NTshRNA or Hrs shRNA1/2 (A) or Rab27b shRNA 1/2 (B) and immunostained for Hrs (A) or Rab27b (B). Yellow arrows indicate transfected neurons expressing mCerulean (left panel) and Hrs or Rab27b staining (right panel). Quantification of fluorescence intensity of Hrs (C) or Rab27b (D) in Hrs/Rab27b shRNA transfected neurons relative to NTshRNA transfected neurons. Error bars show s.e.m. ***p<0.001 (A-D, unpublished data from Dr. Mingjian Shi). Neurons co-transfected with mCherry and NTshRNA or shRNAs against Rab27b (E) or Hrs (G) and immunostained for SV2. Left panel: Overlay of mCherry and SV2 at *DIV*6. Right panel: Overlay of mCherry and SV2 at *DIV*12. Arrows indicate filopodia (left panel) or spines (right panel). Quantification of filopodia, spine and synapse density in Rab27b KD (F) or Hrs KD (H) neurons from three independent experiments. Data represented as box and whiskers plot, bar indicating the median, and the box showing interquartile range. Scale bar, 5μm. ***p<0.001.
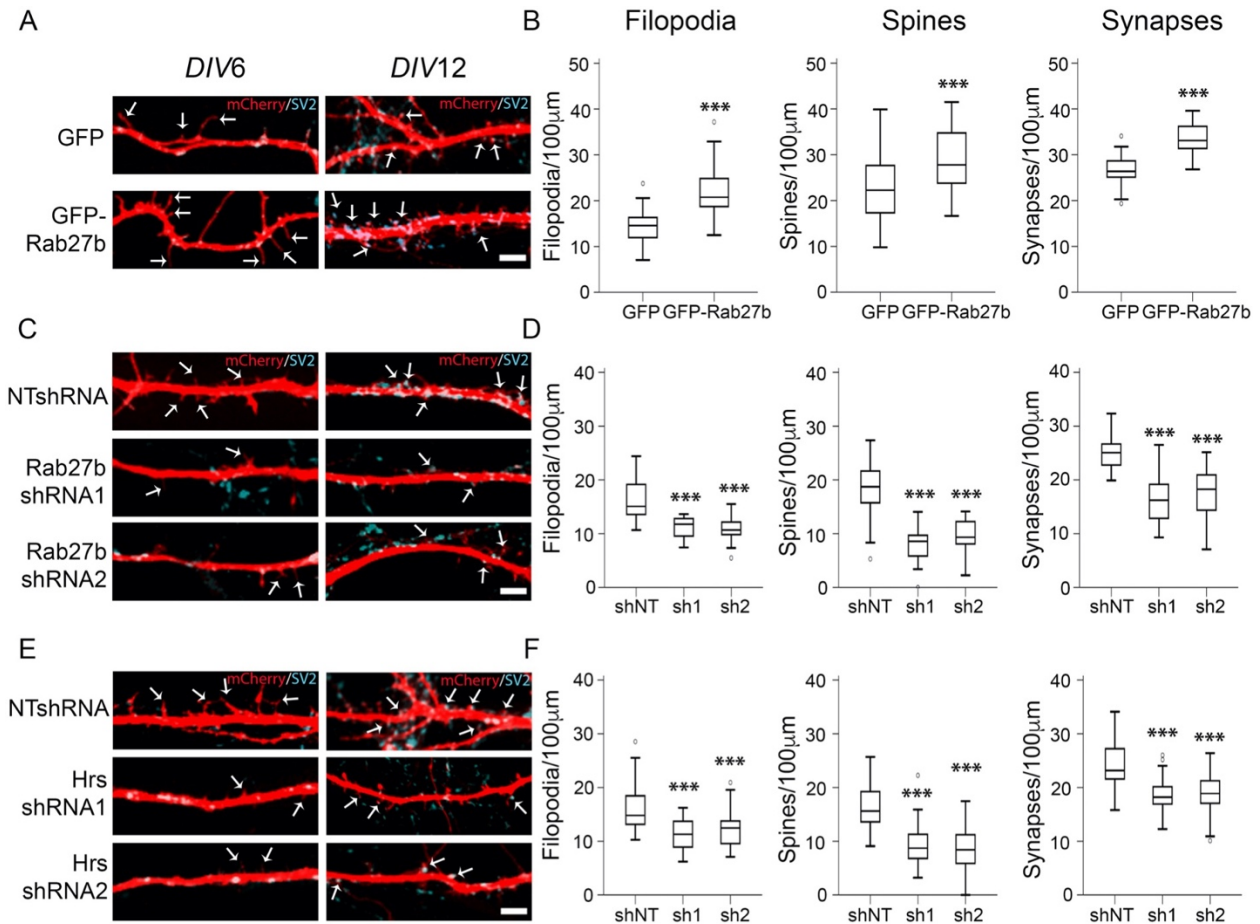
Figure 10. Rab27b and Hrs expression affect filopodia, spine and synapse density in hippocampal neurons. Neurons co-transfected with mCherry and GFP or GFP-Rab27b (A), NTshRNA or shRNAs against Rab27b (C) or Hrs (E) and immunostained for SV2 at *DIV*6 (left panel) or *DIV*12 (right panel). Images show mCherry and SV2 overlay. Arrows indicate filopodia (left) or spines (right). Quantification of filopodia, spine and synapse density in GFP-Rab27 expressing neurons (B), Rab27b KD neurons (D) or Hrs KD neurons (F) from three independent experiments. Data represented as box and whiskers plot, bar indicating the median, and the box showing interquartile range. Scale bar, 5μm. ***p<0.001.
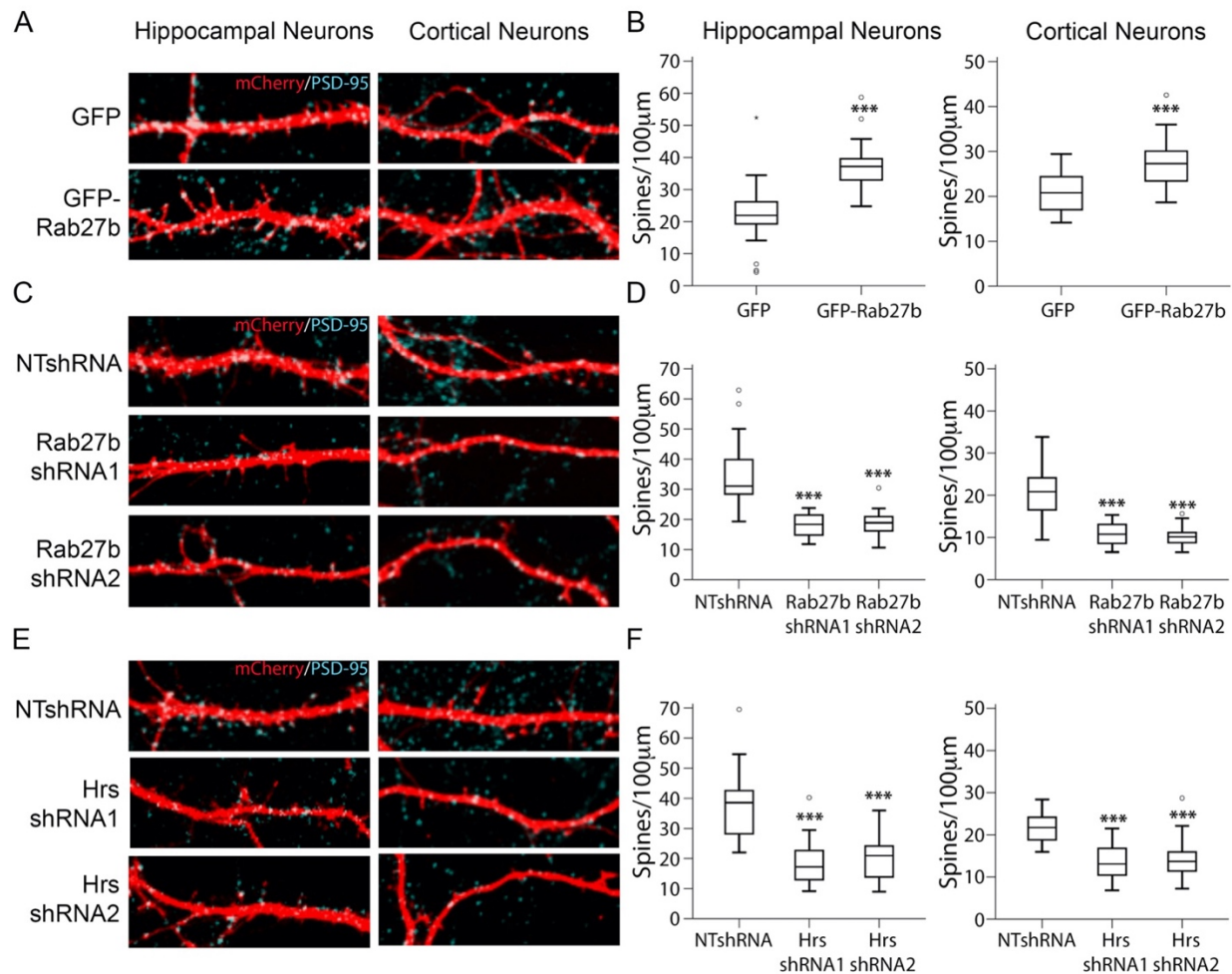
Figure 11. Dendritic spines affected by Rab27b and Hrs expression are also positive for PSD95. Hippocampal neurons (left panel) or cortical neurons (right panel) co-transfected with mCherry and GFP or GFP-Rab27b (A), NTshRNA or shRNAs against Rab27b (C) or Hrs (E) and immunostained for PSD95 at *DIV*12. Images show mCherry and PSD95 overlay. Quantification of PSD95 positive spines in GFP-Rab27 expressing neurons (B), Rab27b KD neurons (D) or Hrs KD neurons (F) from three independent experiments. Data represented as box and whiskers plot, bar indicating the median, and the box showing interquartile range. Scale bar, 5μm. ***p<0.001.
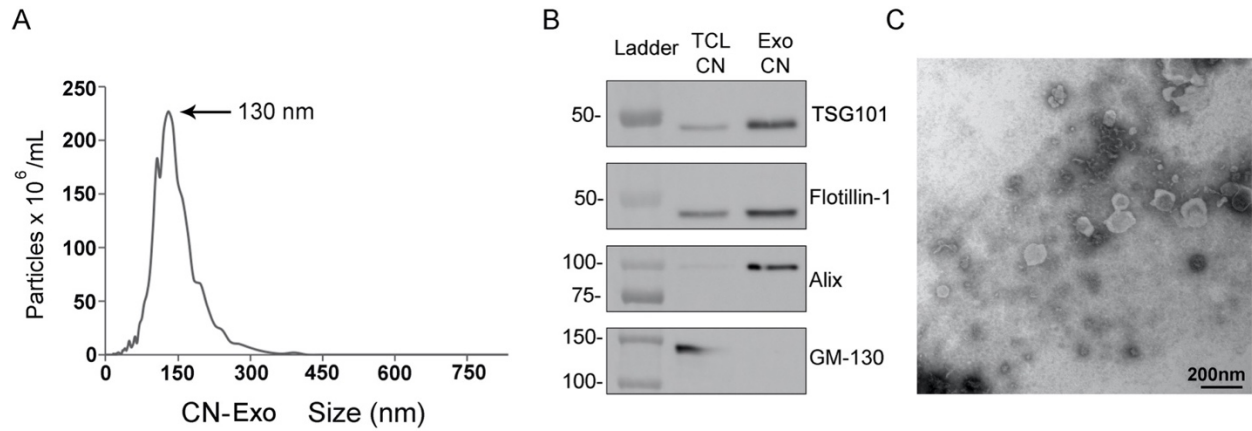
Figure 12. Neuronal exosomes display the size, protein markers and morphology of typical exosomes. (A) Representative particle size traces from nanoparticle tracking analysis of neuronal exosomes. (B) Western blot showing the presence of exosome markers TSG101, Flotillin-1, Alix and absence of the Golgi marker GM130 in neuronal exosomes. TCL and exosomes loaded at equal protein concentration. TCL, total cell lysate. (C) TEM image of negative stained neuronal exosomes.

Neuronal exosomes displayed expected size, below 150nm, and morphology, as measured by NTA and TEM (Figure 12A and 12C). Western blot analysis revealed enrichment of common protein markers TGS101, Flotillin-1 and Alix in exosomes compared to total cell lysates which had the presence of also a Golgi marker GM130 (Figure 12B). Hrs and Rab27b KD neurons were treated with 200 exosomes/cell from *DIV*5-6. The dose of 200 exosomes per neuron was determined based on the estimated exosome secretion rate from primary cortical neurons over the 24 h time period of the assay. In the Rab27b-KD condition, exosome treatment fully rescued the filopodia number defects of untreated KD controls (Figure 13A and 13C). For the Hrs-KD condition, there was a partial rescue in filopodia density upon exosome treatment (Figure 13B and 13D). However, in both cases, exosome treatment significantly increased filopodia density compared to untreated KD neurons. Additionally, neurons treated with increasing doses of neuronal exosomes for 24 h displayed a dose-dependent increase in filopodia, as assessed by phalloidin staining (Figure 13E). The effect of exosomes on filopodia was specific to neuronal exosomes and was not observed by the treatment of astrocyte-derived or C6 glioma-derived SEVs (Figure 13E and 13F). These data suggest that significant amounts of endogenous exosomes are secreted by neurons and that they are required for filopodia formation.

THSD7A is a unique exosomal cargo that promotes filopodia formation:

Similar to effects observed in neurons, cancer cell exosomes were also found to have a function in promoting filopodia formation. In cancer cells, we have identified THSD7A as a key cargo molecule associated with filopodia inducing activity of exosomes (unpublished data, Dr. Caitlin McAtee). To identify functional cargo responsible for filopodia formation in neurons, we performed comparative proteomic analysis of SEVs isolated from neurons, astrocytes and C6 cells.
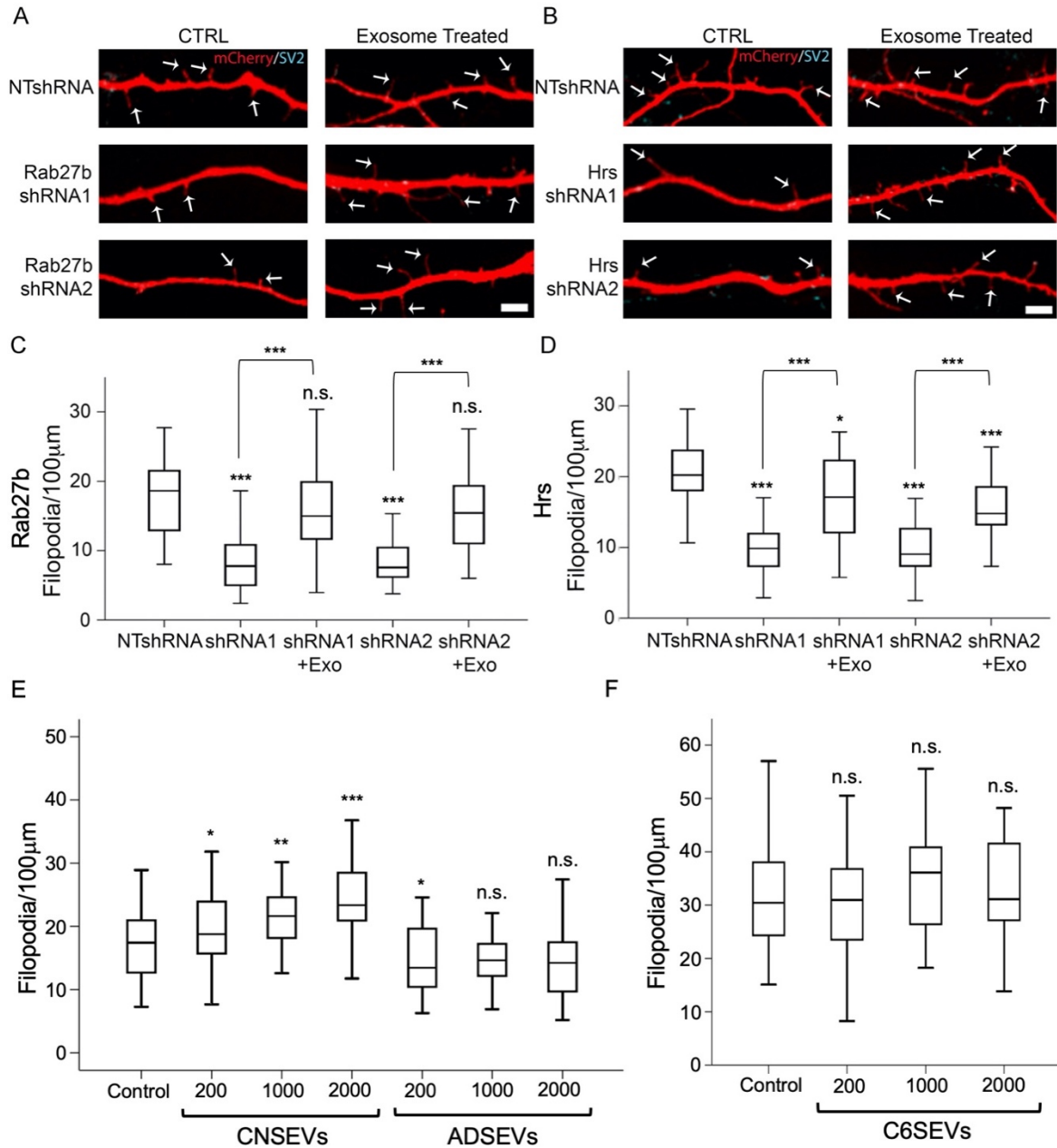
Figure 13. Purified neuronal exosomes rescue defects of filopodia density in Rab27b or Hrs KD neurons. Neurons co-transfected with mCherry and NTshRNA or shRNAs against Rab27b (A) or Hrs (B) treated for 24 h with vehicle control (left panel) or neuronal exosome (right panel) and immunostained for SV2 at *DIV*6. Images show overlay of mCherry and SV2. Arrows indicate filopodia. Quantification of filopodia density in Rab27b KD (C) or Hrs KD (D) neurons with or without exosome treatment from three independent experiments. (E) Quantification of filopodia in neurons without treatment or treatment with doses of 200, 1000 or 2000 neuron-derived or astrocyte-derived SEVs per neuron. (F) Quantification of filopodia in neurons without treatment or treatment with doses of 200, 1000 or 2000 C6 glioma-derived SEVs per neuron. Data represented as box and whiskers plot, bar indicating the median, and the box showing interquartile range. Scale bar, 5μm. *p<0.05, **p<0.01, ***p<0.001, n.s. - not significant.
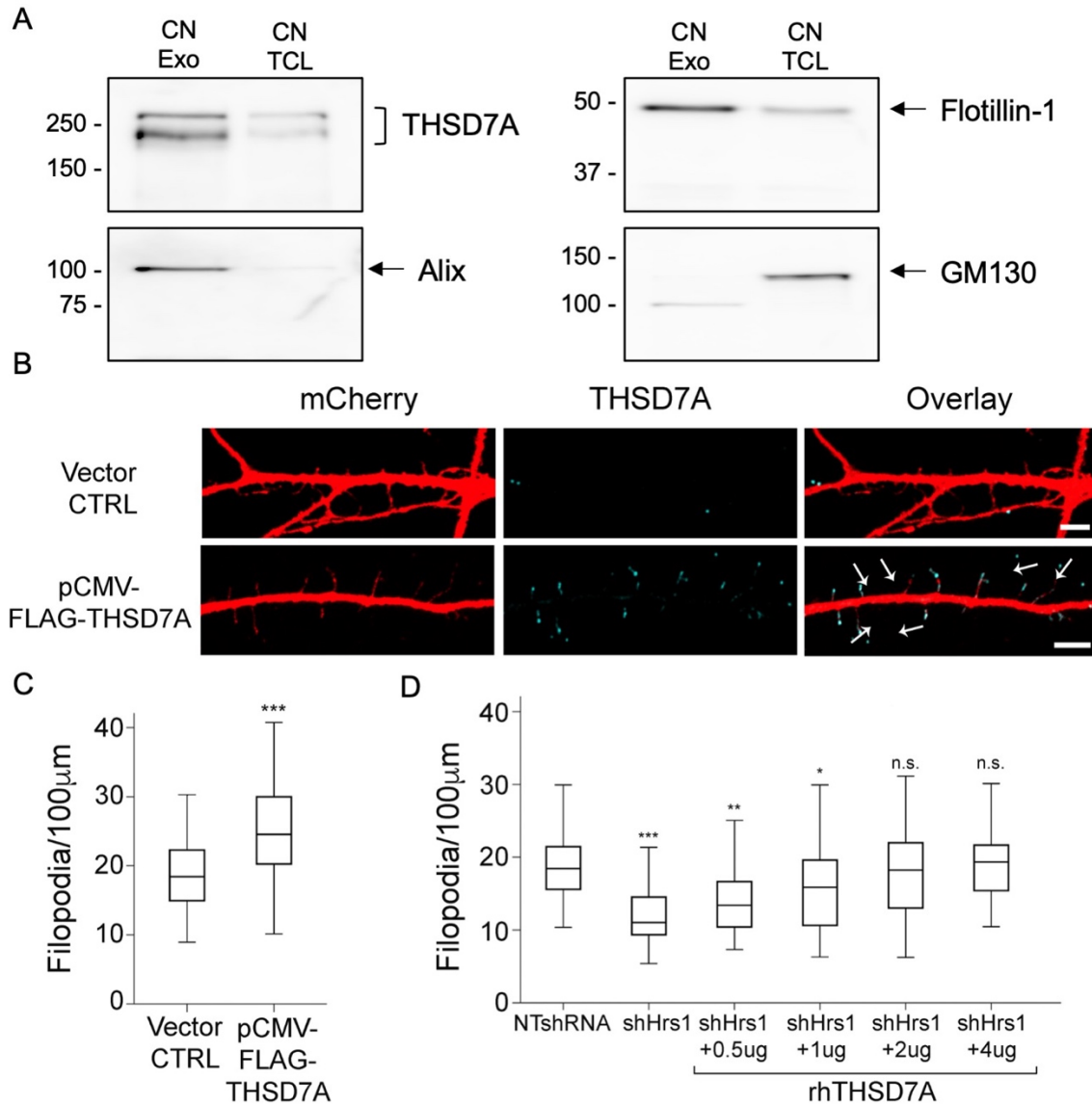
Figure 14. THSD7A is a unique cargo in neuronal exosomes that enhance filopodia formation. (A) Representative Western blot showing enrichment of THSD7A in neuronal exosomes along with common exosome protein markers Alix and Flotillin-1, but not the Golgi marker GM130, compared to total cell lysates (TCL). Exosomes and TCL loaded at equal protein concentration. (B) Neurons co-transfected with mCherry and pCMV-FLAG (vector control) or pCMV-FLAG-THSD7A at *DIV*5 and immunostained for THSD7A on *DIV*6. Left panel: Only mCherry. Middle panel: Only THSD7A immunostaining. Right panel: Overlay of mCherry and THSD7A. (C) Quantification of filopodia in THSD7A expressing neurons compared to vector control from three independent experiments. (D) Quantification of filopodia in Hrs KD neurons in the absence or presence of 0.5, 1, 2 or 4ug/ml THSD7A coating. Data represented as box and whiskers plot, bar indicating the median, and the box showing interquartile range. Scale bar, 5μm. *p<0.05, **p<0.01, ***p<0.001, n.s. - not significant.

THSD7A was found in CNSEVs at 2.1- and 3.9-fold change higher compared to ADSEVs and C6SEVs, respectively. Validation of proteomics by Western blot analysis showed that THSD7A was enriched in neuronal exosomes along with exosome protein markers Flotillin-1 and Alix (Figure 14A). To assess the effects of THSD7A expression, neurons were transiently transfected with pCMV-FLAG-THSD7A or pCMV-FLAG control vector, and co-transfected with mCherry as a filler. Neurons expressing THSD7A displayed a significant increase in filopodia density compared to control vector transfected neurons (Figure 14B and 14C). Additionally, immunostaining of THSD7A in transfected neurons revealed its localization at the tips of filopodia (Figure 14B). The biological activity of THSD7A was further analyzed using recombinant human THSD7A (rhTHSD7A). Primary neurons cultured on rhTHSD7A coated coverslips were able to rescue filopodia defects of Hrs-KD neurons in a dose-dependent manner. Complete rescue of filopodia density was observed at 2 µg/ml rhTHSD7A (Figure 14D). Collectively, these results indicate that neuronal exosomes induce filopodia formation through THSD7A.

Discussion:

Precise regulation of dendritic filopodia formation is essential for the subsequent development of spines and synapses to establish accurate neuronal connections. Our current understanding of extracellular regulators of filopodia is highly restricted. In this study, we have determined the role of neuronal exosomes in filopodia formation. We find that MVBs are primarily localized at the bases of dendritic filopodia and regulation of exosome release from neurons is critical for their function in filopodia formation (Figure 15). THSD7A is a unique cargo of neuronal exosomes that induces filopodia formation.
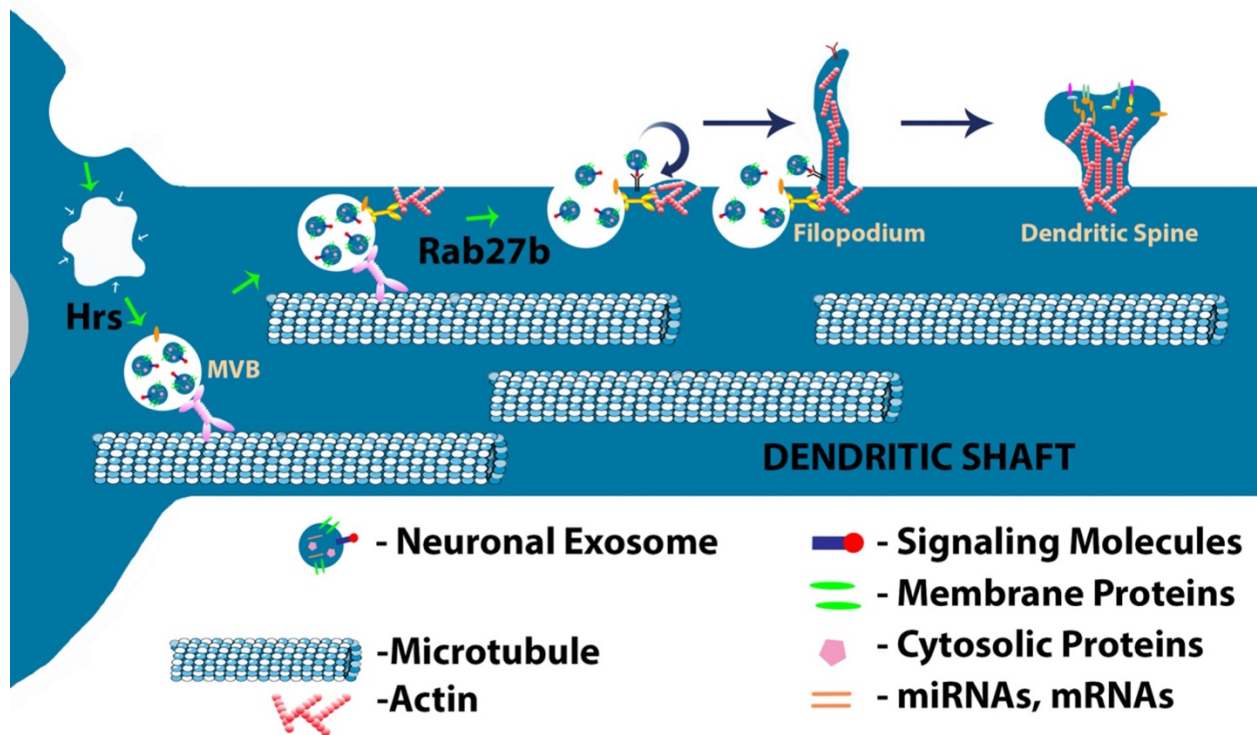
Figure 15. Model of neuronal exosomes in regulation of filopodia formation. Exosomes formed via ESCRT-dependent pathway inside MVB get targeted at actin structures in dendritic shaft. Rab27b mediated MVB docking and exosome release provide THSD7A locally for filopodia formation which further evolves into spines.

Consistent with other studies that have reported association of actin structures and exosome secretion (Beghein, Devriese, Van Hoey, & Gettemans, 2018; D. Hoshino et al., 2013; Mittelbrunn et al., 2011; Seema Sinha et al., 2016), we have demonstrated that actin structures in neuronal dendrites are potential sites of exosome release. In fixed cell imaging, we observed localization of MVB docking factor GFP-Rab27b mostly at the tips and bases of filopodia and spines. In 1961, papas and purpura observed MVB association to postsynaptic sites using EM in the adult cat neocortex (Pappas & Purpura~, 1961). More recently, primary cortical neurons were also found to have MVBs present in mostly neuronal cell body and dendritic compartments (Lachenal et al., 2011). Therefore, it is likely that postsynaptic spines and their precursor filopodia are sites of exosome secretion. However, the possibility of exosome release from the presynaptic terminal cannot be ruled out. At Drosophila NMJ, exosomes containing Wingless in association with Wntless are secreted from the presynaptic boutons, away from the active zones of synaptic vesicle fusion (Budnik, Ruiz-Cañada, & Wendler, 2016a; Koles et al., 2012). Considering similarities between CNS synapse and NMJ, it is possible that exosomes are released from the presynaptic terminal without affecting neurotransmitter release.

Here, we genetically modified the expression of two key proteins, Hrs and Rab27b, with known functions in exosome biogenesis and secretion. We found that changes in expression of Hrs or Rab27b had a strong effect on filopodia density. Hrs is an ESCRT-0 protein that has known functions in sorting ubiquitinated proteins to early endosome and MVB formation (Bache et al., 2003; Raiborg et al., 2002; Tamai et al., 2008). By contrast, Rab27b is important for synaptic vesicle docking at the presynaptic terminal and exosome release (Arias-Hervert et al., 2020; Ostrowski et al., 2010; Nathan J. Pavlos & Jahn, 2011). Although disruption of other functions of Hrs or Rab27b can theoretically also lead to changes in neuronal phenotype, our data indicate that

changes in filopodia density are largely related to changes in exosome secretion, since the addition of purified exosomes rescued filopodia density in Hrs or Rab27b KD neurons.

Our data suggest an important role of exosome-associated THSD7A in filopodia formation. However, the detailed molecular mechanism of its function remains unknown. Full-length THSD7A is a membrane-anchored large glycoprotein that may also be present in the extracellular space as a soluble form cleaved by unknown protease (Kuo et al., 2011). The presence of a membrane anchor suggests that THSD7A is likely to be specifically sorted to and tethered to EVs. In agreement to this hypothesis, the peptide identified in our iTRAQ analysis is in the transmembrane region of THSD7A. However, our Western blot analysis of neuronal exosomes and cell lysates indicates the presence of both soluble and full-length THSD7A. It is important to understand which form of THSD7A is carried by exosomes, as biological functions of THSD7A seem to be highly dependent on its form. For instance, full-length THSD7A expression leads to a decrease in cell migration in podocytes assessed by scratch assay. By contrast, in HUVECs, soluble THSD7A induces cell migration whereas THSD7A C-terminal fragment expression decreases cell migration (Herwig et al., 2019; Kuo et al., 2011; C. H. Wang et al., 2010). However, it remains to be seen how these different forms of THSD7A function at the molecular level.

In glomerular epithelial cells, also known as podocytes, THSD7A localizes to filopodia as well as to F-actin-free membrane protrusions (Herwig et al., 2019). In HUVECs, THSD7A co-localizes with paxillin and αvβ3 integrin at focal adhesions (C. H. Wang et al., 2010). Similarly, we find THSD7A localizes to the tips of dendritic filopodia. Additionally, THSD7A contains an integrin recognition RGD motif in its extracellular region. Hence, integrins may serve as receptors for THSD7A (Kuo et al., 2011; C. H. Wang et al., 2010). However, THSD7A was only slightly localized with β1 or β3 integrin at the leading edge of filopodia in podocytes suggesting an

interaction between integrins and THSD7A may be dependent on the cell type (Herwig et al., 2019). Further studies are required to better understand interactions between THSD7A and integrins.

In summary, we have identified novel function of neuronal exosomes in filopodia formation. Additionally, we show that exosome associated THSD7A is critical for exosome mediated effects of filopodia formation.

<div align="center">

CHAPTER III

ASTROCYTE-DERIVED SMALL EXTRACELLULAR VESICLES PROMOTE

SYNAPSE FORMATION VIA FIBULIN-2 MEDIATED TGF-β SIGNALING

</div>

Mikin R. Patel[1,2], Alissa M. Weaver[1,3,4]

[1]Department of Cell and Developmental Biology, Vanderbilt University School of Medicine, Nashville, TN 37232, USA

[2]Department of Biological Sciences, Vanderbilt University, Nashville, TN 37232, USA

[3]Department of Pathology, Microbiology, and Immunology, Vanderbilt University Medical Center, Nashville, TN 37232, USA

Summary

Neuronal synapse formation is critical for brain development and depends on secreted factors from astrocytes. Here, we report that small extracellular vesicles (EVs) secreted from primary astrocytes, but not from neurons or C6 glioma cells, greatly enhance spine and synapse formation by primary cortical neurons. A comparative proteomics analysis of small EVs from astrocytes, neurons, and C6 glioma cells identified fibulin-2 as a promising EV cargo to regulate synaptogenesis. Treatment of cortical neurons with recombinant fibulin-2 increased the formation of spines and synapses, similar to the effect of small EVs. In addition, treatment of neurons with fibulin-2 or astrocyte-derived small EVs led to increased phosphorylation of Smad2, an indicator of TGF-β signaling. Finally, the effects of fibulin-2 and astrocyte-derived small EVs on synapse formation were reversed by inhibiting transforming growth factor b (TGF-β) signaling. These data suggest a model in which astrocyte EVs promote synapse formation via fibulin-2-mediated activation of TGF-β signaling.

Introduction

Synapses are specialized neuronal structures that consist of presynaptic and postsynaptic apposed membranes and are critical for neuronal communication, learning, and memory. Dendritic spines are protrusive postsynaptic membrane specializations with characteristic mushroom-like morphology. Formation of proper synapses occurs during early post-natal development and is highly regulated. In the past few decades, many studies have identified the importance of astrocyte to neuron communication for guiding dendritic spine and synapse formation during development (Allen, 2014a; Chung et al., 2015; Jones et al., 2012; Shi et al., 2013; Ullian, Sapperstein, Christopherson, & Barres, 2001)

Astrocyte conditioned media alone can promote neuronal synapse formation, suggesting the importance of secreted molecules (Christopherson et al., 2005a; Chung et al., 2015). Indeed, a number of astrocyte-secreted proteins, including thrombospondin, hevin, glypican 4, glypican 6, and the signaling molecule TGF-β1, are secreted by astrocytes and promote formation of excitatory synapses (Allen et al., 2012; Christopherson et al., 2005a; Diniz, Almeida, Tortelli, Vargas Lopes, et al., 2012; Eroglu et al., 2009; Singh et al., 2016; J. Xu, Xiao, & Xia, 2010). These and many other astrocyte-secreted proteins are often present in extracellular vesicles (EVs) (Carayon et al., 2011; Keerthikumar et al., 2015; J.-E. Lee, Moon, Lee, & Baek, 2015; Webber, Steadman, Mason, Tabi, & Clayton, 2010), suggesting that astrocyte-secreted EVs may participate in synaptogenesis.

EVs, including small and large EVs derived from endosomes or the plasma membrane, mediate cell-cell communication by transporting protein, lipid, and nucleic acid cargoes (Maas, Breakefield, & Weaver, 2017a). Astrocyte-derived EVs are critical regulators of neuroprotection (Adolf et al., 2019; Hira et al., 2018; Pascua-Maestro et al., 2019; S. Wang et al., 2011) and

neurodegeneration (Varcianna et al., 2019; G. Wang et al., 2012). In addition, small EVs (SEVs) isolated from ATP-treated astrocytes increase neurite length, dendrite number, and dendritic complexity (Chaudhuri et al., 2018); however, the underlying mechanism and the relationship to synapse formation is unknown.

In this study, we tested whether astrocyte-derived SEVs regulate neuronal dendritic spine and synapse formation. Treatment of cultured primary cortical neurons with astrocyte-derived SEVs, but not SEVs from neurons or C6 glioma cells, led to a significant increase in dendritic spines and synapses, at both early and late developmental stages. Quantitative proteomic analysis of SEVs identified fibulin-2 as a likely synaptogenic cargo enriched in astrocyte SEVs. Addition of recombinant human fibulin-2 to primary neurons induced spine and synapse formation to a similar extent as astrocyte-derived SEVs. Conversely, fibulin-2 knockdown astrocyte SEVs had a reduced ability to induce synaptogenesis. Investigation of the molecular mechanism indicated that the effects of astrocyte-derived SEVs and fibulin-2 are likely through receptor-mediated activation of transforming growth factor β (TGF-β) signaling.

Materials and Methods

Primary neuron and astrocyte cultures and cell lines

Primary rat cortical neurons were isolated from the brains of embryos from 19 day pregnant Sprague Dawley rats. Cortices from both cerebral hemispheres of the E19 rat embryo brains were chopped into small pieces, incubated in 0.05% Trypsin at 37° C for 15 min and washed three times with Hank's Balanced Salt Solution (HBSS) without calcium and magnesium. After the final wash, cells were triturated with a sterile glass pipet and plated on coverslips in dishes at the desired

density. Neurons were plated either on 18 or 25mm glass coverslips at low density (300,000 in 60mm culture dishes) for fixed cell analysis or at high density (2.6 million in 100mm culture dishes) for exosome isolation, both coated with 50 μg/ml poly-D-lysine. After 4 h, neurons plated at low density on coverslips were transferred to 60mm dishes containing > 80% confluent primary astrocytes, using wax dots to separate the coverslips from the dish surface. The DNA synthesis inhibitor Cytosine Arabinoside (Ara-C) was added on day *in vitro* (*DIV*) 2 to a final concentration of 5 μM to inhibit glia growth.

Primary astrocytes were obtained from postnatal P1-P2 day rats. Both cerebral hemispheres were dissected from each P1-P2 rat and meninges were removed. Collected tissues were chopped into fine pieces and incubated in 0.25% Trypsin, 0.1% DNase I at 37° C for 15 min with occasional swirling. The supernatant containing dissociated cells was passed through a 70 mm nylon mesh cell strainer into to a 50ml conical tube containing horse serum to make final concentration of 10% horse serum and centrifuged at 200xg for 6 min to pellet the cells. The supernatant was carefully removed and cells were resuspended in Minimum Essential Medium containing 0.6% glucose, 10% horse serum, 1% Penicillin-Streptomycin and plated in T75 flasks at a concentration of 5-10 x 10^6 cells per flask. After 24 h, flasks were tapped from the side to detach any microglia and the media was replaced. Thereafter, the media was replaced twice a week until the cells reached 100% confluence. All animal procedures were performed in compliance with IACUC approved protocol M1800027-00 at Vanderbilt University. The C6 glioma cell line was kindly provided by Dr. James G. Patton at Vanderbilt University. C6 glioma cells were cultured in F-12K media (ThermoFisher) supplemented with 10% Horse serum, 2.5% Fetal bovine serum and 1% Penicillin-Streptomycin.

SEV isolation and characterization

For neuronal exosomes, day *in vitro* (*DIV*) 9 cortical neurons cultured at high density (2.6 million in 100 mm culture dishes) were washed three times with HBSS. After the final wash, HBSS was replaced with 4 mL Neurobasal media per 100 mm dish. Neurobasal media does not contain serum but contains growth factors. Neurobasal conditioned media was collected after 4 h incubation. For astrocyte SEVs, primary astrocytes grown to 90%–100% confluency were washed three times with HBSS and then conditioned with neurobasal media for 24 hr. For C6 Glioma cells, 8 million cells were plated per T225 flask and cultured for 48 h in F-12K media containing 10% horse serum and 2.5% FBS to reach 80% confluence. After that, cells were washed three times with prewarmed 1x PBS and cultured in serum free F-12K media for 48 hr. Conditioned media from all cell types was collected and processed for differential ultracentrifugation. Briefly, conditioned media was centrifuged sequentially at 300xg for 10 min, 2000xg for 25 min in a tabletop centrifuge, and 10,000xg for 30min in a Type 45 Ti ultracentrifuge rotor (Beckman) to remove live cells, cell debris and microvesicles (MVs), respectively. The supernatant from the 10,000xg spin was centrifuged at 100,000xg for 18 hr in a Type 45 Ti rotor to obtain SEVs. The 100,000xg SEV-containing pellets were resuspended in 3 mL sterile cold PBS and repelleted at 100,000xg for 4 hr in a TLA110 rotor. SEVs were analyzed for size and number by nanoparticle tracking (ZetaView, ParticleMetrix) and for common SEV markers by western blotting.

Transmission Electron Microscopy

Purified SEVs reconstituted in 20 mM HEPES buffer were added on glow-discharged formvar carbon film-coated grids in 10 mL volume for 1 min at room temperature. Subsequently,

grids were stained with 2% uranyl acetate for 30 s and were allowed to air dry. Grids were imaged using a Philips/FEI T-12 transmission electron microscope at 21000x magnification.

iTRAQ sample preparation and Proteomics

iTRAQ proteomics analysis was performed on purified neuronal, astrocyte or C6 glioma SEVs. To prepare samples, SEVs were washed three times with 1x PBS to remove any soluble protein contaminants. SEV samples in PBS at equal protein concentration were lysed 1:1 with 2X lysis buffer (200 mM TEAB, 600 mM NaCl, 4% NP-40, 1% Sodium Deoxycholate) and incubated in a cold sonicating water bath (Bioruptor) for 15 min. The samples were then centrifuged at 21,100xg for 30 min at 4° C and the supernatants containing soluble protein were carefully collected for iTRAQ proteomics analysis.

Protein samples were precipitated with ice-cold acetone overnight at -20° C. Following precipitation, samples were centrifuged at 18,000x*g* at 4C, and precipitates were washed with cold acetone, dried, and reconstituted in 8M urea in 250 mM TEAB (pH 8.0). Samples were reduced with TCEP, alkylated with MMTS, diluted with TEAB to obtain a final solution containing 2M urea, and digested with sequencing-grade trypsin overnight. To facilitate quantitative analysis, peptides were labeled with iTRAQ reagents according to the manufacturer's instructions (SCIEX). Labeling reagent was reconstituted in ethanol such that each protein sample was labeled at a final concentration of 90% ethanol, and labeling was performed for 2 hours. The resulting peptides were the desalted by a modified Stage-tip method (Jimenez et al., 2019). Peptides were reconstituted and analyzed using a MudPIT LC MS/MS method (Jimenez et al., 2019). Following each salt pulse delivered by the autosampler, peptides were gradient-eluted from the reverse analytical column at a flow rate of 350nL/min. Mobile phase solvents consisted of 0.1% formic acid, 99.9% water

(solvent A) and 0.1% formic acid, 99.9% acetonitrile (solvent B). For the peptides from the first 11 SCX fractions, the reverse phase gradient consisted of 2%– 50% B in 83 min, 50% B for 2 minutes, and a 10 min equilibration at 2% B. For the last 2 SCX-eluted peptide fractions, the peptides were eluted from the reverse phase analytical column using a gradient of 2%–98% B in 83 min, followed by 98% B for 2 minutes, and a 10 min equilibration at 2% B. Peptides were introduced via nano-electrospray into a Q Exactive Plus mass spectrometer (Thermo Scientific). The Q Exactive Plus was operated in the data-dependent mode acquiring HCD MS/MS scans (R = 17,500) after each MS1 scan on the 15 most abundant ions using an MS2 target of 1 x 10^5 ions. The HCD-normalized collision energy was set to 30, dynamic exclusion was set to 30 s, and peptide match and isotope exclusion were enabled. Mass spectra were processed using the Spectrum Mill software package (version B.04.00) (Agilent Technologies) with similar parameters as described in Jimenez et al., (2019). and were searched against a database containing the *Rattus norvegicus* subset of the UniprotKB protein database (https://www.uniprot.org). Search parameters included: trypsin enzyme specificity, ± 20 ppm (HCD) product mass tolerance, and fixed modifications including MMTS alkylation of cysteines and iTRAQ labeling of lysines and peptide N-termini. Oxidation of methionine was allowed as a variable modification. Autovalidation was performed such that the maximum target-decoy-based false-discovery rate (FDR) was set to 1.0%. To obtain iTRAQ protein ratios, the median was calculated for all peptides assigned to each protein.

For statistical analysis of iTRAQ protein ratios, log2 protein ratios were fit to a normal distribution using non-linear (least-squares) regression. The calculated mean derived from the Gaussian fit was used to normalize individual log2 ratios for each quantified protein. The normalized log2 ratios were then fit to a normal distribution, and the mean and standard deviation

values derived from the Gaussian fit of the normalized ratios were used to calculate *p* values using Z score statistics. Subsequently, p values were corrected for multiple comparisons by the Benjamini-Hochberg (BH) method. Proteins with a BH FDR p < 0.05 were defined as significantly changed. Proteins that were identified as Uncharacterized proteins were searched through panther and UniProt databses manually by entering the accession number. Proteins with normalized fold change of > 2 in ADSEVs compared to CNSEVs or C6SEVs were identified. PANTHER (www.pantherdb.org) was used to identify protein classes of the 33 proteins enriched in ADSEVs compared to both CNSEVs and C6SEVs.

Western Blot Analysis

To prepare cell lysates, cells were washed rapidly once with 1x HBSS and then lysed using 10 mM Tris pH 7.4, 1% SDS. Protein concentrations of total cell lysates were measured using the Pierce BCA assay. For SEVs, a MicroBCA Protein Assay Kit (Pierce) was used to determine protein concentration. Samples loaded by equal protein concentration were resolved on 8% SDS-PAGE gels and transferred to nitrocellulose membranes. Ponceau S stain was used to confirm proper protein transfer onto membranes, before washing 3 times with 1X TBS buffer and blocking in 5% milk in 1X TBST. Primary antibodies were diluted in 5% milk (TSG101 1:1000, Flotillin-1 1:1000, GM130 1:1000, Alix 1:1000, Hsp70 1:1000, Fibulin-2 1:2000, Smad2 1:5000) or 5% BSA (pSmad2 1:5000) and HRP-conjugated secondary antibodies were diluted 1:10,000 in 5% milk in TBST before developing with ECL reagent and imaging with an Amersham 680 imager. ImageStudioLite (LI-COR version 5.2.5) was used for densitometry analysis.

Dot blot assay

Astrocyte-derived SEVs at different concentrations in 10 mL final volume were dotted on nitrocellulose membranes and allowed to air dry for 1 h at room temperature. Membranes were then blocked with 5% milk in TBS in the absence (TBS) or presence of 0.1% (v/v) Tween-20 (TBST) for 1 h at room temperature. Subsequently, membranes were incubated with primary antibodies against fibulin-2 or Alix and then HRP conjugated secondary antibodies in 5% milk with TBS or TBST followed by imaging with Amersham 680 imager.

Treatment of primary neurons

Primary neurons on glass coverslips at low density (300,000 in 60 mm culture dishes) were co-cultured with astrocytes in 60 mm dishes. To find a concentration range of SEVs to test, we estimated the SEV secretion rate for neurons, astrocytes, and C6 cells to be ~8 SEVs/cell/h based on the total concentration of purified SEVs measured by NTA divided by the number of cells and the conditioning time. We estimated that ~400 EVs/cell would be the approximate number secreted over 48 h and tested a concentration range above and below that amount (200, 1000, and 2000 SEVs/neuron) for experiments. For experiments in Figures 17 and 18, neurons in co-cultures with astrocytes were treated with increasing doses of SEVs. For all other experiments, neurons were transferred to 12-well plates on *DIV* 5 or *DIV* 10 with 1 mL conditioned media per well from the home dish and treated for 24 h (*DIV*5-*DIV*6) or 48 h (*DIV*10-*DIV*12). Neurons were then fixed and stained with phalloidin or anti-SV2 antibody on *DIV*6 (early stage) or *DIV*12 (late stage) to examine spines and synapses. For analysis of phosphorylated Smad2, neurons plated in poly-D-lysine coated 12-well plates at high density (500,000 per well) were treated on *DIV*10, first with

10 μm SB4315242 or diluent for 5 min and then with 10 ng/ml TGF-β1, 2 μg/ ml recombinant human fibulin-2, or purified SEVs from cortical neurons, astrocytes or C6 cells for 1 h.

Transfection of primary astrocytes

Astrocytes were transfected in 6-well plates with SMARTpool siRNAs (Dharmacon) against fibulin-2 or non-targeted control using X-tremeGENE™ siRNA transfection reagent (Millipore Sigma) according to the manufacturer's instructions. Briefly, astrocytes were grown at ~80%–90% confluency in 6-well plates. Before transfection, media was changed to antibiotic-free glia culture media. For transfection of each well, 2.5 μL of 100 μM siRNAs was diluted in 125 μL of serum free MEM in one tube and 25 μL of transfection reagent was added to 100 μL of serum free MEM in another tube. The resulting mixture from both tubes was combined immediately, incubated at room temperature for 20 min and added dropwise to the cells. 48 h post transfection, the cells were washed three times with HBSS and conditioned with neurobasal media for 24 h. Conditioned media was subjected to differential ultracentrifugation for isolation of purified SEVs.

Immunocytochemistry

Neurons at room temperature were fixed in 4% paraformaldehyde in PBS for 15 mins, for SV2 staining, or 3 mins followed by 10 min incubation with ice cold methanol for PSD95 staining. Neurons were then permeabilized with 0.2% Triton X-100 in PBS for 3 min, then incubated for 1 h with 20% goat serum to block non-specific antibody binding at room temperature. Alexa Fluor 488 phalloidin, anti-PSD95 and anti-SV2 antibody were diluted at 1:1000 in 5% goat serum and incubated overnight with the neurons at 4° C before washing and incubating with 1:1000 anti-mouse Alexa Fluor 647 antibody for 45 mins at room temperature. Coverslips were washed in

PBS, then rinsed in deionized distilled water before mounting on glass slides with Aqua-Poly/Mount.

FM4-64 labeling

A fixable analog of FM4-64FX (Invitrogen) was diluted to 5 μg/ml working solution in high K$^+$ solution (72mM NaCl, 50mM KCl, 1mM NaH$_2$PO$_4$, 26mM NaHCO$_3$, 1.8mM CaCl$_2$, 0.8mM MgSO$_4$, 11mM glucose and 20mM HEPES, pH-7.35). Day 12 neurons were incubated with FM4-64FX for 1 min at room temperature and washed three times using HBSS without magnesium or calcium. Neurons were then fixed with 4% PFA for 15 min and stained with phalloidin before mounting on glass slides for imaging.

Dynasore treatment and transferrin internalization assay

Day 10 neurons were incubated at 37° C with 100 μM Dynasore in neurobasal media for 30 mins. Neurons were then incubated with fluorescent transferrin (Molecular Probes) in neurobasal media with or without 100 μM Dynasore at final concentration of 25 μg/ml for 2 mins at room temperature followed by 30 min incubation at 37° C. Next, neurons were washed three times with neurobasal media with or without 100 μM Dynasore followed by fixing with 4% PFA for 15 min and staining with phalloidin.

Microscopy and image analysis

For most experiments, neurons were imaged on a Nikon A1R HD confocal microscope equipped with an Apo TIRF 60x/1.49 NA oil immersion lens. Images were acquired using NIS-Elements software. For some experiments (Figures 17A and 22A), neurons were imaged using

MetaMorph software on a Quorum Wave-FX Yokogava CSU-X1 spinning disk confocal system with a Nikon Eclipse Ti microscope equipped with an Apo TIRF 60x/1.49 NA oil immersion lens. To examine dendritic spine and synapse density, 12 to 15 images of primary or secondary dendrites were acquired for each experiment for a total of 36-45 images from three independent experiments. Images were analyzed manually for dendritic spine and synapse density using either MetaMorph or NIS-Elements software to trace dendrite length. The scale slider in MetaMorph or the histogram scale in NIS-Elements was used to reduce background and improve signal to aid in visualization of SV2 co-localization in phalloidin/SV2 overlay. Any scale changes were made equally across the whole image. Dendritic spines were defined as phalloidin-positive protrusions co-localized with the presynaptic marker SV2 while synapses were defined as SV2 puncta co-localized to both dendritic protrusions and dendritic shafts. For all images shown in figures, Fiji (ImageJ Version 2.0) was used to adjust the brightness and contrast display levels across the whole image for visualization purposes and all images were cropped to the same size (40 mm x 15 mm) in Fiji.

Table 1: Key Resources Table

REAGENT or RESOURCE	SOURCE	IDENTIFIER
Antibodies		
Mouse monoclonal anti-SV2	Developmental Studies Hybridoma Bank, University of Iowa, Iowa City, IA	Cat# SV2, RRID:AB_2315387
Mouse monoclonal anti-PSD95	Millipore Sigma	Cat# MAB1598, RRID:AB_94278
Alexa Fluor 647 Goat Anti-mouse IgG	Molecular Probes	Cat# A-21236, RRID:AB_141725
Rabbit polyclonal anti-TSG101	Abcam	Cat# ab30871, RRID:AB_2208084
Mouse monoclonal anti-Flotillin-1	BD Biosciences	Cat# 610820, RRID:AB_398139
Mouse monoclonal anti-Hsp70	Santa Cruz Biotechnology	Cat# sc-24, RRID:AB_627760
Mouse monoclonal anti-Alix	Cell Signaling	Cat# 2171, RRID:AB_2299455
Mouse monoclonal anti-GM130	BD Biosciences	Cat# 610822, RRID:AB_398141
Rabbit polyclonal anti-α2M	Abcam	Cat# ab58703 RRID:AB_879541
Rabbit monoclonal anti-Vimentin	Cell Signaling	Cat# 5741 RRID:AB_10695459
Rabbit polyclonal anti-Connexin 43	Cell Signaling	Cat# 3512 RRID:AB_2294590
Rabbit polyclonal anti-Integrin a6	Cell Signaling	Cat# 3750 RRID:AB_2249263
HRP conjugated goat anti-mouse IgG	Promega	Cat# W4021, RRID:AB_430834
HRP conjugated goat anti-rabbit IgG	Promega	Cat# W4011, RRID:AB_430833
Rabbit polyclonal anti-Fibulin-2	GeneTex	Cat# GTX105108, RRID:AB_2036908
Rabbit polyclonal anti-GFAP	Bioss	Cat# bs-0199R RRID: AB_10859014
Rabbit monoclonal anti-Phospho-Smad2	Cell Signaling	Cat# 3108, RRID:AB_490941
Rabbit monoclonal anti-Smad2	Cell Signaling	Cat# 5339, RRID:AB_10626777
Mouse monoclonal anti-TGF-β 1,2,3	R&D Systems	Cat# MAB1835 RRID:AB_1672402
Normal mouse IgG$_1$	Santa Cruz Biotechnology	Cat# sc-3877 RRID:AB_737222
Chemicals, Peptides, and Recombinant Proteins		
Neurobasal^{TM} Medium	Gibco	Cat# 21103-049
B-27 Supplement (50x), serum free	Gibco	Cat# 17504-044
Minimum Essential Medium	Corning	Cat# 10-010-CV
Ham's F-12K (Kaighn's) Medium	Gibco	Cat# 21-127-022
DNase I	Sigma-Aldrich	Cat# DN25-100MG
HBSS (10x), no calcium, no magnesium, no phenol red	Gibco	Cat# 14-185-052
Horse Serum	Gibco	Cat# 16-050-122

Trypsin (2.5%), no phenol red	Gibco	Cat# 15-090-046
Poly-D-lysin hydrobromide	Sigma-Aldrich	Cat# P7886-50MG
Alexa Fluor^{TM} 488 Phalloidin	Molecular Probes	Cat# A12379
Aqua-Poly/Mount	Polysciences Inc	Cat# 18606
Recombinant Human Fibulin 2 Protein	R&D Systems	Cat# 9559-FB-050
Recombinant Human TGF-β1 Protein	R&D Systems	Cat# 240-B-002
SB 431542 hydrate	Sigma-Aldrich	Cat# S4317-5MG
Dynamin Inhibitor I, Dynasore	Sigma-Aldrich	Cat# 32441-10MG
FM4-64FX	Invitrogen	Cat# F34653
Transferrin, AF 546 Conjugate	Thermo Scientific	Cat# T23364
Complete Tablets, Mini Protease Inhibitor Cocktail Tablets	Roche	Cat# 04-693-124-001
PhosSTOP Phosphatase Inhibitor Cocktail Tablets	Roche	Cat# 04-906-837-001
Pierce^{TM} ECL Western Blotting Substrate	Thermo Scientific	Cat# 32106
Supersignal^{TM} West Femto Maxium Sensitivity Substrate	Thermo Scientific	Cat# 34095
X-tremeGENE^{TM} siRNA transfection reagent	Millipore Sigma	Cat# 4476093001
Experimental Models: Cell Lines		
Rat: C6 glioma cell line	Kindly provided by Dr. James G. Patton, Vanderbilt University, USA	N/A
Experimental Models: Organisms/Strains		
Rat: SAS SD-Rat Female Timed Preg-Day 18	Charles River Laboratories	Strain: 24104855
Oligonucleotides		
Non-targeting siRNAs pool UGGUUUACAUGUCGACUAA, UGGUUUACAUGUUGUGUGA, UGGUUUACAUGUUUUCUGA, UGGUUUACAUGUUUUCCUA	Dharmacon	Cat# D-001810-10-20
Rat Fbln2 siRNAs -SMARTpool CGGCAGGUGUGUCGCGUUA, CAAUGAGUGCACAUCGUUA, CCAAUAGCCUGCCGGGAGA, AUGAUCAAAUAGCACGAAA	Dharmacon	Cat# L-095315-02-0050
Software and Algorithms		
Prism 8	GraphPad Prism	RRID:SCR_002798
MetaMorph	MetaMorph Microscopy Automation and Image Analysis Software	RRID:SCR_002368
NIS-Elements	Nikon	RRID:SCR_014329
Fiji	Fiji	RRID:SCR_002285
ImageStudioLite version 5.2.5	LiCOR	RRID:SCR_013715
BioRender	BioRender	https://biorender.com
Other		
Falcon® Cell strainer 70μm Nylon	Corning	Cat# 352350

Quantification and Statistical analysis

GraphPad Prism version 8 was used to analyze and plot all data. The Mann-Whitney test was used to calculate the *p-value* between each set of conditions. The data for dendritic spine and synapse densities from three independent experiments were combined and plotted as box and whiskers plots, where the bar indicates the median with interquartile range and all data points are shown. Image-StudioLite (LI-COR version 5.2.5) was used for densitometry analysis of western blots. The relative density of bands was measured as the signal from the same area for each band, with background correction. For graphs, pSmad2 levels were normalized to total Smad2 levels. The adjusted density was then calculated by normalizing all treatment conditions to control. A Z-test was performed to statistically compare each condition with control.

Results

<u>Astrocyte-derived SEVs promote dendritic spine and synapse formation:</u>

To study the role of astrocyte-derived EVs in development of dendritic spines and synapses, we isolated SEVs by differential ultracentrifugation from the conditioned media of primary astrocytes that were isolated from newborn rat pups. For comparison, we used SEVs isolated from day *in vitro* 9 primary cortical neurons or from an immortalized cell line, C6 glioma, which is a glial cancer cell line with astrocytic characteristics (De Vries & Boullerne, 2010). Serum-free conditioned media was serially centrifuged at 300xg for 10min, 2,000xg for 25min, 10,000xg for 30 min, and 100,000xg for 18 h to pellet dead cells, cell debris, large EVs, and small EVs, respectively. Notably, very few large EVs were present in 10,000 x g fraction, so we were not able to analyze their effects on neurons. Due to the limited number of SEVs obtained from primary cultures, we were unable to further purify the SEVs by density gradient centrifugation.

Purified SEVs were in the expected size range (30–150 nm), as measured by nanoparticle tracking analysis (Figure 16A). Western blot analysis showed that purified SEVs were positive for common SEV markers Alix, flotillin-1, and Hsp70 and negative for the Golgi marker, GM130 (Figures 16B–16D), suggesting minimal contamination with cell debris (Théry et al., 2018). Negative stained purified SEVs observed by transmission electron microscopy showed the expected morphology (Figure 16E).

To study the role of SEVs on spine and synapse formation, primary cortical neurons were isolated from day 19 rat embryos and cultured for 10 days before treatment with increasing doses of purified SEVs isolated from primary astrocytes, primary cortical neurons, or C6 cells. Day 10 after birth is a developmental time point when neurons begin to form spines and synapses and are susceptible to modulation by secreted synaptogenic factors (Michele Papa et al., 1995; Wegner et al., 2008). After 48 h (day *in vitro* 12), neurons were fixed and immunostained for the synaptic marker SV2, along with the actin stain phalloidin for visualization of spines and synapses. Treatment with astrocyte-derived SEVs led to a dose-dependent increase in the number of dendritic spines and synapses, (Figures 17A–17C). By contrast, treatment of neurons with neuronal SEVs had no effect on synapse density and slightly reduced the number of dendritic spines (Figures 17A–17C). Surprisingly, treatment of neurons with C6 glioma SEVs had no effect on spine or synapse density, despite the glial origin of this cell line (Figures 17D–17F).

We also examined whether any of the SEV preparations could affect dendritic spine formation at an earlier stage of development, day *in vitro* 5–6, when neuronal dendrites are in the process of forming actin-rich filopodia. Although many fewer dendritic spines were formed at this early developmental stage, the results were similar. Thus, astrocyte SEVs—but not the other two SEV preparations—induced neuronal dendritic spine and synapse formation (Figures 18A–18D).
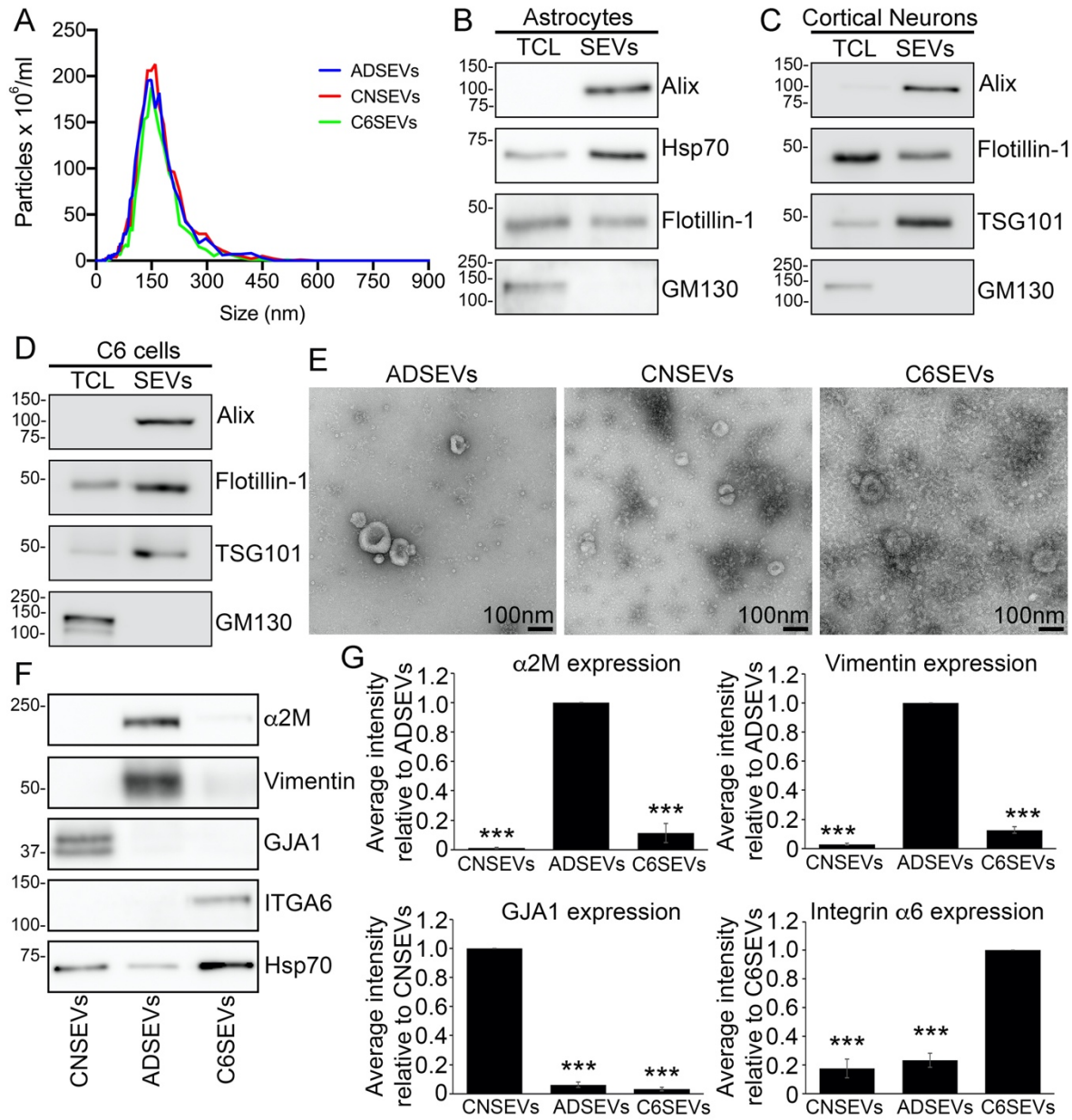
Figure 16: SEV characterization and iTRAQ validation. (A) Representative particle size traces from nanoparticle tracking analysis of SEVs isolated from primary astrocytes (ADSEVs), cortical neurons (CNSEVs) and C6 glioma cells (C6SEVs). (B, C and D) Representative Western blots showing the presence of SEV markers Alix, Flotillin-1, TSG101 or HSP70 and absence of the Golgi marker GM130 in ADSEVs, CNSEVs and C6SEVs. TCL and SEVs loaded at equal protein concentration. TCL, total cell lysate. (E) TEM images of negative stained ADSEVs, CNSEVs and C6SEVs. Scale bar, 100nm. (F) Western blot of CNSEVs, ADSEVs and C6SEVs stained for alpha-2-macroglobulin (α2M), vimentin, gap junction alpha-1 (GJA1), integrin alpha-6 (ITGA6) and Hsp70. (G) Quantification of α2M, vimentin, GJA1 and ITGA6 expression from 3 independent experiments. Data represented as mean±SEM. ***$p < 0.001$.
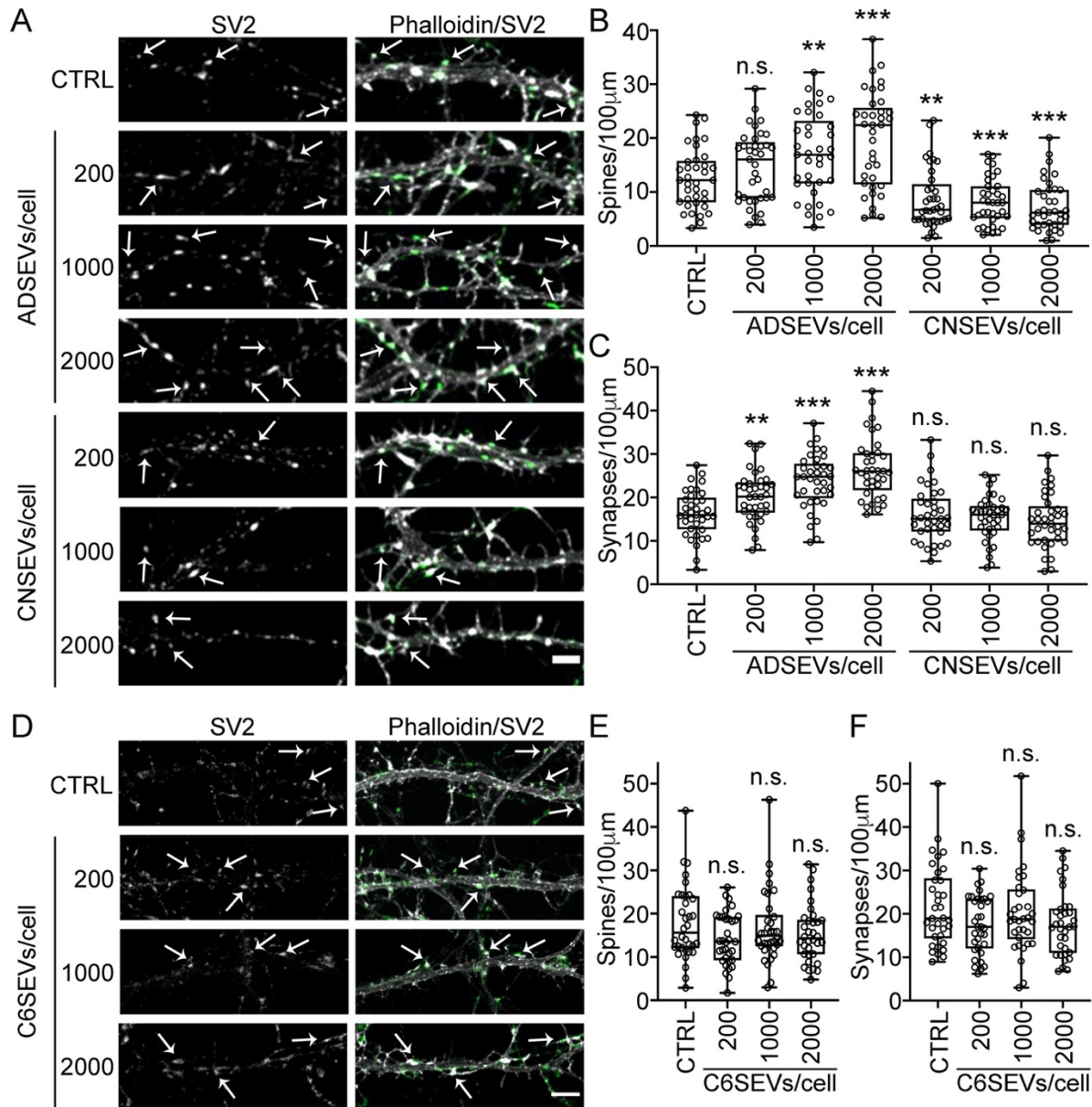
Figure 17. Astrocyte-derived SEVs promote dendritic spine and synapse formation. (A and D) Representative fluorescence images of dendrites in day 12 neurons treated for 48 h with 0 (control), 200, 1,000, or 2,000 astrocyte-derived (ADSEVs), cortical neuron-derived (CNSEVs), or C6 glioma-derived (C6SEVs) SEVs /neuron. Images in (A) and (D) are adjusted for brightness and contrast and cropped to same size using Fiji for better visualization of SV2 colocalization on dendritic spines. Left panel: SV2 only. Right panel: overlay of phalloidin (grayscale) and SV2 (green). Example dendritic spines are indicated with arrows. Scale bars, 5 μm. (B, C, E, and F) Quantification of spine and synapse density from images. n=36 primary or secondary dendrites from 3 independent experiments. Data represented as box and whiskers plots with all data points shown, bar indicating the median, and the box showing interquartile range. **p < 0.01, ***p < 0.001; n.s., not significant.

71
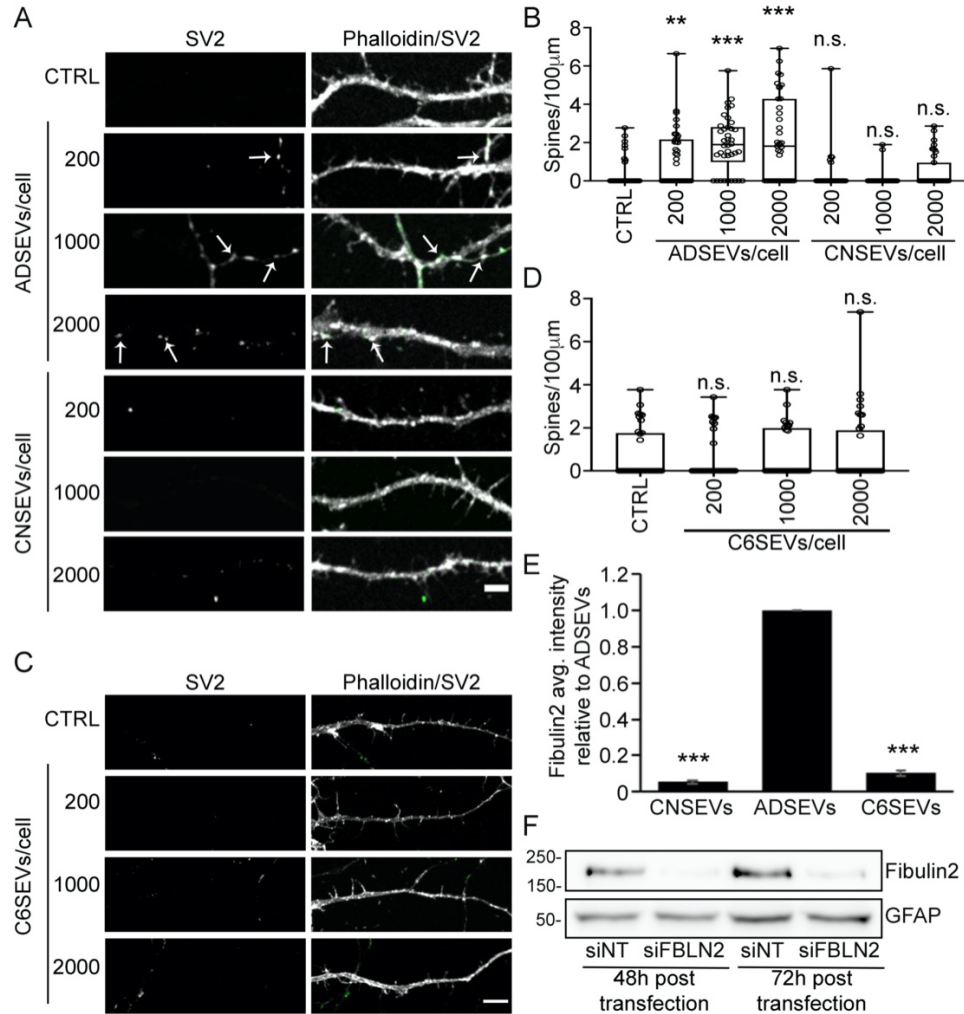
Figure 18: Characterization of astrocyte-derived SEVs for dendritic spine formation at an early developmental stage and fibulin-2 levels. (A) Representative SV2 and Phalloidin/SV2 overlay immunofluorescence images of neuronal dendrites at day 6 in control neurons or neurons treated with 200, 1000 or 2000 ADSEVs or CNSEVs/neuron. (B) Quantification of dendritic spine density from images. n=36 primary or secondary dendrites from 3 independent experiments. (C) Representative SV2 and Phalloidin/SV2 overlay immunofluorescence images of neuronal dendrites at day 6 in control neurons or neurons treated with 200, 1000 or 2000 C6SEVs/neuron. (D) Quantification of dendritic spine density from images. n=36 primary or secondary dendrites from 3 independent experiments. (E) Quantification of fibulin-2 in CNSEVs, ADSEVs and C6SEVs from 3 independent experiments. Data represented as mean±SEM. ***$p<0.001$. (F) Western blot of siNT and siFBLN2 astrocyte total cell lysates at 48 h and 72 h post transfection stained for fibulin-2 and GFAP loading control. For better visualization of SV2 colocalization on dendritic spines, images in A and C were adjusted for brightness and contrast and cropped to same size. Left panel: SV2 only. Right panel: Overlay of phalloidin (gray-scale) and SV2 (green). Some example dendritic spines are indicated with arrows. Data represented as box and whiskers plots with all data points shown, bar indicating the median, and the box showing interquartile range. Scale bar, 5 μm. **$p<0.01$, ***$p<0.001$, n.s. – not significant.

SEVs isolated from primary astrocytes are enriched with proteins distinct from cortical neuron- and C6-derived SEVs:

To identify synaptogenic cargoes of astrocyte-derived SEVs, we performed isobaric tags for relative and absolute quantitation (iTRAQ) proteomic analysis on SEVs isolated from primary astrocytes, cortical neurons, and C6 glioma cells. Because only astrocyte SEVs induce synapse formation, we looked for proteins that were enriched in astrocyte-derived SEVs compared to the other two sets of SEVs. Analysis of the data revealed that proteins enriched in SEVs are reflective of their cells of origin. For instance, cortical neuron SEVs were enriched with neuron- specific proteins, including neural cell adhesion molecule 1, neural cell adhesion molecule L1, synaptic vesicle glycoprotein 2a, and neuromodulin, whereas astrocyte specific proteins such as glial fibrillary acidic protein and ceruloplasmin were abundant in astrocyte-derived SEVs. We also confirmed several proteins previously identified on neuronal SEVs (Faure ́ et al., 2006), including beta tubulin, Hsc70, guanine nucleotide-binding protein G, and 14-3-3 proteins. Several proteins identified as >2-fold enriched in astrocyte, neuronal, or C6 SEVs by iTRAQ proteomics were further validated by western blot analysis and found to be highly enriched in the predicted EV sets (Figures 16F and 61G). In total, 1,237 proteins were identified in the iTRAQ analysis and 97 and 63 proteins had a respective fold change of >2 in astrocyte-derived SEVs compared to neuron SEVs and C6 SEVs. Among these, 33 proteins were >2-fold higher in astrocyte-derived SEVs compared to both neuron and C6 SEVs (Figure 19A; Table 2). Further analysis of these 33 proteins using PANTHER revealed enrichment in protein classes commonly found in EVs, including cell adhesion molecules, extracellular matrix (ECM) proteins, cytoskeletal proteins, and signaling molecules (Jimenez et al., 2019) (Figure 19B). Because astrocyte and C6 glioma SEVs are of similar glial origin and had many proteins present at similar levels in the proteomics dataset, we

were able to use Benjamini-Hochberg statistics (Gobert et al., 2019; Mishra et al., 2018; Voss et al., 2015) to identify significantly enriched proteins in astrocyte-derived SEVs compared to C6 SEVs (see methods). Based on this analysis, 12 out of the 33 proteins were significantly enriched in astrocyte- derived SEVs compared to C6 SEVs (Figure 19C). We prioritized these 12 proteins as top candidates to promote synapse formation.

Fibulin-2 is a synaptogenic cargo present in astrocyte SEVs:

ECM proteins and TGF-β signaling are known to regulate synapse formation and plasticity (Barros, Franco, & Müller, 2011; Diniz, Almeida, Tortelli, Vargas Lopes, et al., 2012; Levy, Omar, & Koleske, 2014; Song & Dityatev, 2018). In our proteomics analysis, we identified the ECM protein, fibulin-2, as significantly enriched in astrocyte SEVs compared to C6 (>6- fold) and neuronal (>5-fold) SEVs (Figure 19C). Fibulin-2 has also been shown to promote TGF-β activation (Khan et al., 2016a) and to regulate TGF-β1-induced differentiation of adult neural stem cells into neurons (Radice et al., 2015a). Based on these studies, we investigated whether fibulin-2 might account for the activity of astrocyte SEVs in promoting spine and synapse density.

Western blot analysis confirmed that fibulin-2 is present in astrocyte cell lysates and SEVs but is undetectable in cell lysates and SEVs from cortical neurons or C6 glioma cells (Figures 20A and 18E). To study its role in synapse formation, recombinant human fibulin-2 was either coated on coverslips before plating neurons or added into the media of cortical neurons on day 10 at 0.5 or 2 µg/mL concentrations. After 48 h, the neurons were analyzed for dendritic spines and synapses (Figure 20B). For all conditions, except for 0.5 µg/mL fibulin-2 coating, there was a significant increase in spine and synapse density (Figures 20C and 20D). Because 2 µg/mL of fibulin-2 added to the media was the most effective condition, we used it for subsequent experiments.

Table 2: Proteins with > 2-fold change in ADSEVs compared to both C6SEVs and CNSEVs

Protein Name	Fold change compared to	
	C6-SEVs	CN-SEVs
Collagen alpha-1(I) chain*	8.65	8.50
Alpha-2-macroglobulin*	8.57	9.03
Microfibril-associated glycoprotein 4-like*	7.76	12.04
Fibulin 2*	6.64	5.29
Protein S100-A6*	6.03	13.53
Epoxide hydrolase 1*	5.86	4.29
Atrial natriuretic peptide receptor 3*	5.80	5.00
Low-density lipoprotein receptor-related protein 2*	5.77	4.04
Tubulin tyrosine ligase-like 12*	5.51	6.25
Annexin A3*	5.37	3.97
Complement C3*	5.09	7.49
Coiled-coil domain-containing 150*	5.08	5.96
Pyruvate dehydrogenase phosphatase regulatory subunit	4.55	3.91
Vimentin	4.54	2.96
LSM4 homolog, U6 small nuclear RNA and mRNA degradation-associated	4.53	7.59
Metalloendopeptidase	4.41	5.51
Collagen alpha-1(III) chain	4.36	4.13
Adipocyte enhancer-binding protein 1	4.33	4.35
Receptor expression-enhancing protein 5	4.23	2.12
Glycogen [starch] synthase, muscle	4.05	4.12
Cell migration-inducing hyaluronan-binding protein	3.77	3.50
Family with sequence similarity 171, member A2	3.66	2.54
Aa1018	3.59	4.70
Cystathionine beta-synthase	3.55	4.55
Chromodomain helicase DNA-binding protein 1-like	2.91	26.10
Alpha-1-macroglobulin	2.82	9.70
Citrate synthase, mitochondrial	2.63	2.69
Creatine kinase S-type, mitochondrial	2.60	2.35
WD repeat-containing protein 1	2.50	2.15
Intercellular adhesion molecule 1	2.49	2.66
Maltase-glucoamylase	2.31	5.30
Cleavage and polyadenylation-specific factor 1	2.19	5.74
Cerebellar degeneration-related protein 2-like	2.11	5.01

*Significantly higher in ADSEVs compared to C6SEVs.

Proteins with a Benjamini-Hochberg (BH) FDR p<0.05 were defined as significantly changed.

Protein Class
- Transporter
- Hydrolase
- Oxidoreductase
- Cell adhesion molecule
- Lyase
- Enzyme modulator
- Transporter
- Nucleic acid binding
- Receptor
- Defence/immunity protein
- Calcium-binding protein
- Isomerase
- Cytoskeletal protein
- Signaling molecule
- Extracellular matrix protein

Protein name	Fold change compared to	
	C6-SEVs	CN-SEVs
Collagen alpha-1(I) chain	8.65	8.50
Alpha-2-macroglobulin	8.57	9.03
Microfibril-associated glycoprotein 4-like	7.76	12.04
Fibulin 2	6.64	5.29
Protein S100-A6	6.03	13.53
Epoxide hydrolase 1	5.86	4.29
Atrial natriuretic peptide receptor 3	5.80	5.00
Low-density lipoprotein receptor-related protein 2	5.77	4.04
Tubulin tyrosine ligase-like 12	5.51	6.25
Annexin A3	5.37	3.97
Complement C3	5.09	7.49
Coiled-coil domain-containing 150	5.08	5.96

Figure 19. Identification of enriched astrocyte SEV proteins using quantitative comparative proteomics. (A) Venn diagram of proteins enriched in ADSEVs compared to CNSEVs and C6SEVs identified by iTRAQ proteomics analysis. n = 1. (B) Classification of 33 proteins from the overlap in (A) represented as the pie chart based on protein class. (C) List of 12 proteins significantly higher in ADSEVs compared to C6SEVs out of the 33 enriched proteins.
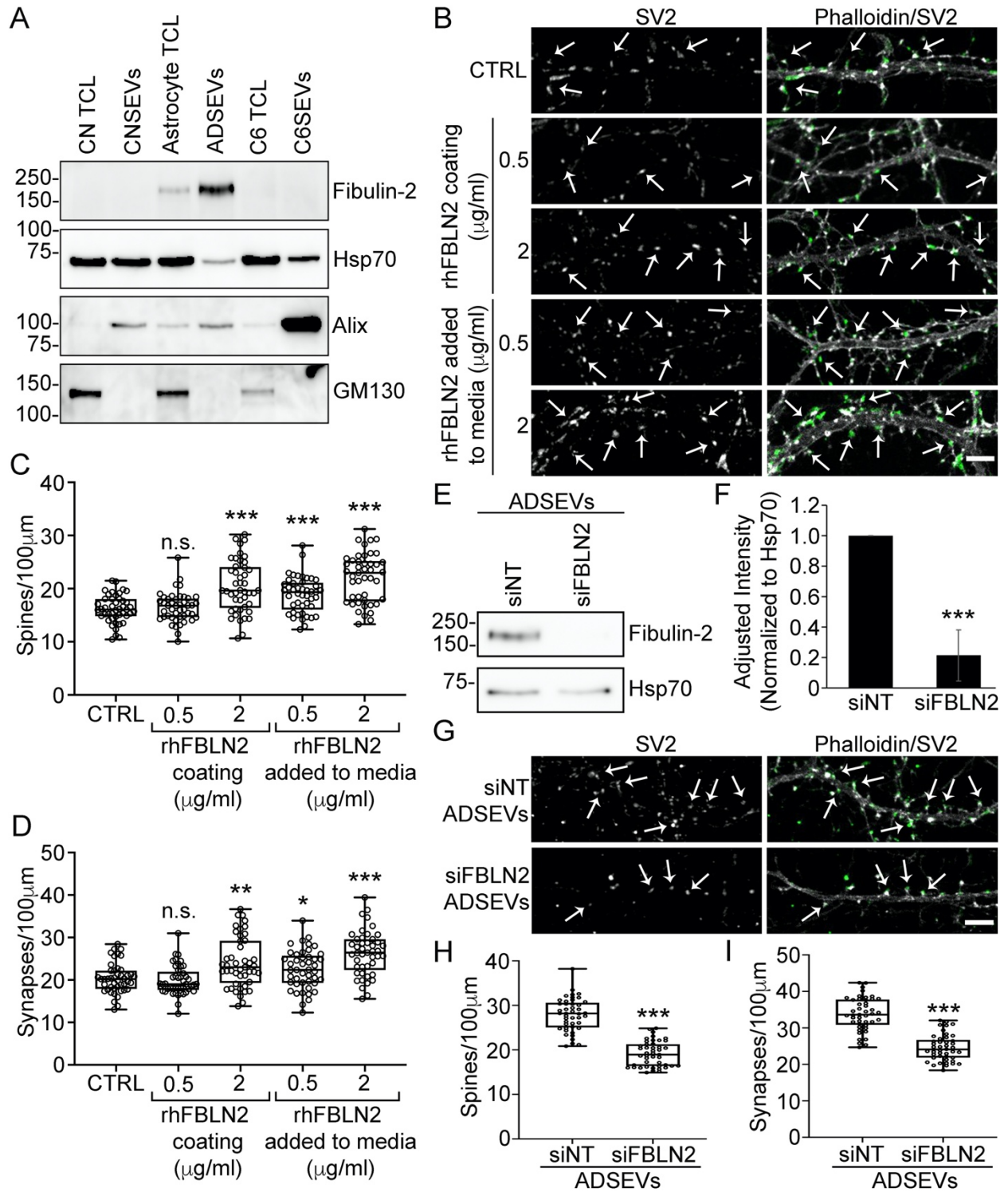
Figure 20. Fibulin-2 is a synaptogenic cargo present in astrocyte SEVs. (A) Western blot of equal protein (10 μg) of cortical neurons, astrocytes and C6 total cell lysates (TCLs) and SEVs stained for fibulin-2, the SEV markers Hsp70 and Alix, or the Golgi marker GM130. n = 3 (quantification in Figure 18E). (B) Representative images from day 12 cortical neurons plated on coverslips coated with poly-D-Lysine (control) in the presence or absence of soluble recombinant human fibulin-2 (rhFBLN2) added to media or plated on coverslips coated with rhFBLN2 for 48 h. Scale bar, 5 μm. (C and D) Quantification of spines and synapses from images. n = 45 primary or secondary dendrites from 3 independent experiments. (E) Representative western blot of control (siNT) and fibulin-2 knockdown (siFBLN2) ADSEVs stained for fibulin-2 and SEV marker Hsp70. (F) Quantification of fibulin-2 levels in siNT and siFBLN2 ADSEVs. n = 3. Data are normalized to Hsp70 levels and represented as mean ± SEM. (G) Representative images of day 12 neuronal dendrites treated for 48 h with 2,000 siNT/siFBLN2 ADSEVs per neuron. Images in (B) and (G) are adjusted for brightness and contrast and cropped to same size using Fiji for better visualization of SV2 colocalization on dendritic spines. Left panel: SV2 only. Right panel: overlay of phalloidin in grayscale and SV2 in green. Example dendritic spines are indicated with arrows. Scale bar, 5 μm. (H and I) Quantification of spine and synapse density from images. n = 45 primary or secondary dendrites from 3 independent experiments. Data represented as box and whiskers plots with all data points shown, bar indicating the median, and the box showing interquartile range. *p < 0.05, **p < 0.01, ***p < 0.001; n.s., not significant.

To test the function of EV-carried fibulin-2 in synaptogenesis, astrocytes were transiently transfected with small interfering RNA (siRNA) against fibulin-2 or non-targeting control. Fibulin- 2 knockdown was confirmed by western blot analysis in cell lysates at the times of conditioning and collection of conditioned media, 48 and 72 h post-transfection, respectively (Figure 18F), and in purified SEVs (Figures 20E and 20F). Consistent with fibulin-2 being a key synaptogenic EV cargo, treatment of neurons with fibulin-2-knockdown astrocyte-derived SEVs induced significantly fewer spines and synapses than control SEVs (Figures 20G–20I).

Astrocyte-derived SEVs and fibulin-2 activate TGF-β signaling to increase spine and synapse formation:

We hypothesized that fibulin-2 carried by SEVs induces TGF-β signaling. Notably, whereas TGF-β1, TGF-β2, and TGF-β3 were present in our proteomics data, they were not enriched in SEVs derived from astrocytes compared to C6 cells, suggesting that any differences would be due to accessory factors. To determine whether astrocyte SEVs or fibulin-2 can induce TGF-β signaling, cortical neurons were treated with SEVs purified from astrocytes, cortical neurons, or C6 cells, 2 μg/mL recombinant fibulin-2, or 10 ng/mL TGF-β1 as a positive control. As an additional control, treatments were performed in the presence or absence of the TGF-β signaling inhibitor, SB431542 (SB). After 1 h, cell lysates were analyzed by western blot for levels of phosphorylated (pSmad2) and total Smad2. Consistent with our hypothesis, neurons treated with TGF-β1, fibulin-2, or astrocyte SEVs had significantly increased pSmad2 levels compared to untreated control neurons (Figures 21A and 21B). pSmad2 levels were unchanged by treatment with neuronal or C6 SEVs. Smad2 phosphorylation was inhibited in all conditions in which 10 μM SB was added.
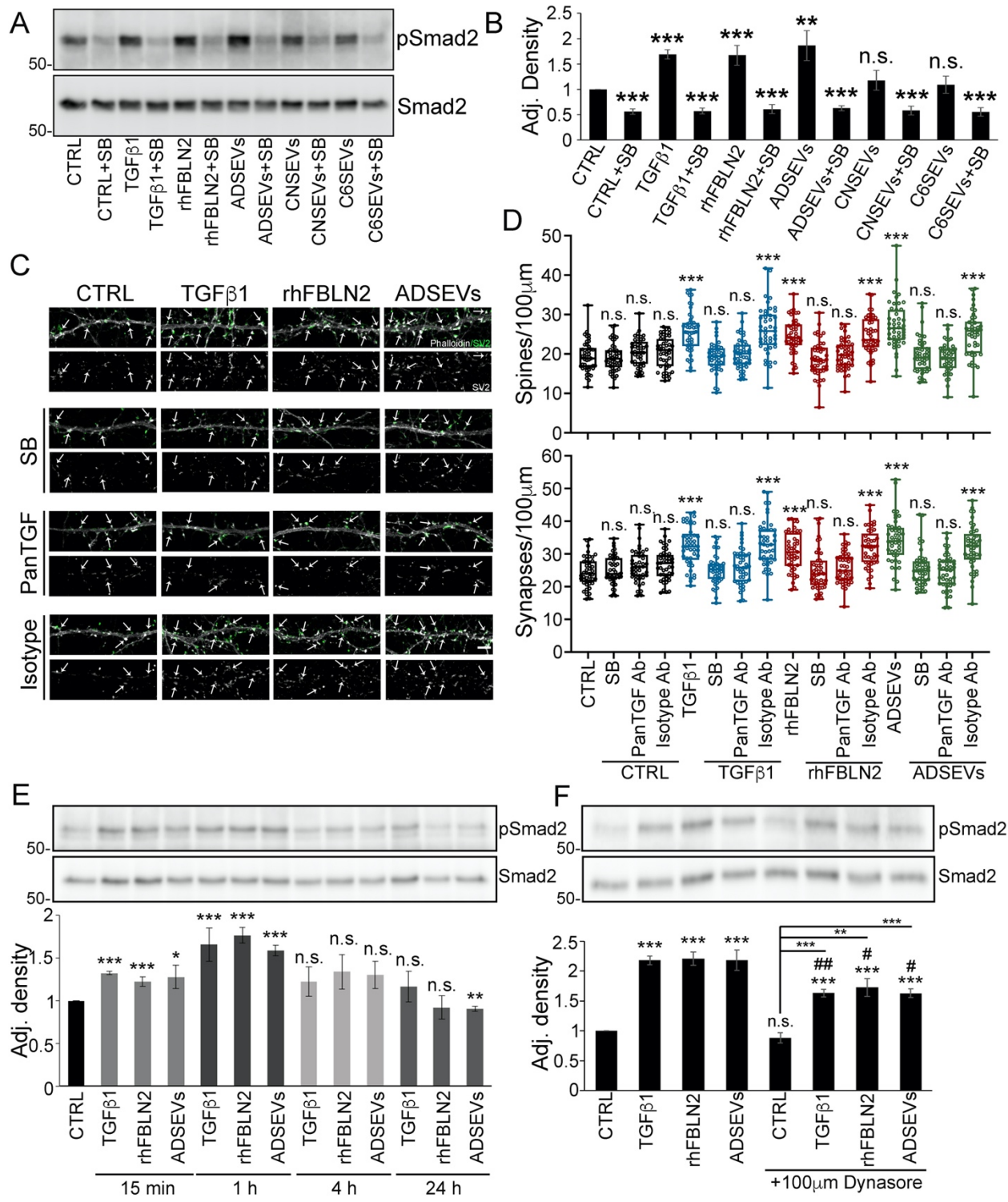
Figure 21. Astrocyte-derived SEVs and fibulin-2 activate TGF-β signaling to increase spine and synapse formation. (A and B) Cortical neurons were treated with 10 ng/mL TGF-β1, 2 μg/mL rhFBLN2, or 2,000 SEVs/cell, as indicated, for 1 h in the absence or presence of 10 μM SB431542 (SB) before lysis and western blot analysis for phospho-Smad2 and total Smad2. (A) Representative western blots. (B) Quantification of absolute density of pSmad2 levels compared to total Smad2 levels. n = 3. Data represented as mean ± SEM. (C) Representative images of day 12 neurons treated with 10 ng/mL TGF-β1, 2 μg/mL rhFBLN2, or ADSEVs in the absence or presence of 2.5 μM SB, 10 μg/mL pan-TGFβ-neutralizing antibody or mouse IgG1 isotype control antibody. Images are adjusted for brightness and contrast and cropped to same size using Fiji for better visualization of SV2 colocalization on dendritic spines. SV2 only in grayscale. Overlay of phalloidin in grayscale and SV2 in green. Example dendritic spines are indicated with arrows. Scale bar, 5 μm. (D) Quantification of spines and synapses from images. n = 45 primary or secondary dendrites from 3 independent experiments. Data represented as box and whiskers plots with all data points shown, bar indicating the median, and the box showing interquartile range. (E) Representative western blot images and quantification of pSmad2 levels compared to total Smad2 levels for cortical neurons treated with 10 ng/ml TGF-β1, 2 μg/ml recombinant human fibulin-2 or 2000 ADSEVs/cell for 15 min, 1 h, 4 h, and 24 h (n = 3). Data represented as mean ± SEM. (F) Representative western blot images and quantification of pSmad2 levels compared to total Smad2 levels for cortical neurons treated with 10 ng/mL TGF-β1, 2 μg/mL recombinant human fibulin-2, or 2,000 ADSEVs/cell in the absence or presence of 100 μM Dynasore (n = 4). Data represented as mean ± SEM # indicates comparison between same condition in the absence or presence of Dynasore. #/*p < 0.05, ##/**p < 0.01, ***p < 0.001; n.s., not significant.
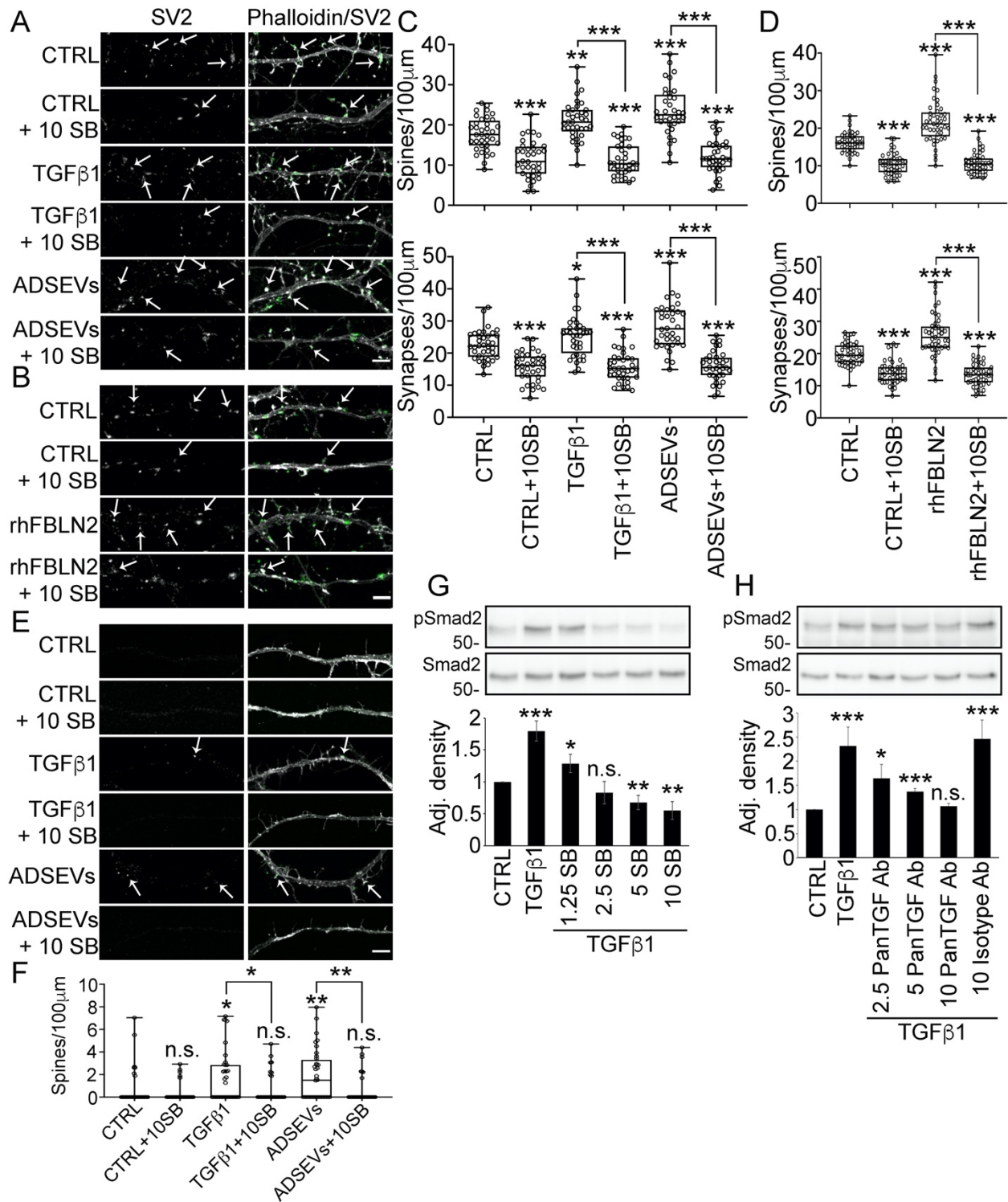
Figure 22: ADSEVs and fibulin-2 promote dendritic spine and synapse formation dependent on TGF-β signaling. (A and B) Representative SV2 and Phalloidin/SV2 overlay immunofluorescence images of day 12 cortical neurons treated with 10 ng/ml TGF-β1 or 2000 ADSEVs/cell (A) or 2 µg/ml rhFBLN2 (B) in the absence or presence of 10 µM SB431542 (SB). (C and D) Quantification of spine and synapse density from images of day 12 cortical neurons treated with 10 ng/ml TGF-β1, or 2000 ADSEVs/cell (C) or with soluble recombinant human fibulin-2 (D) in the absence or presence of 10 µM SB. n=45 primary or secondary dendrites from three independent experiments. (E) Representative SV2 and Phalloidin/SV2 overlay immunofluorescence images of day 6 cortical neurons treated with 10 ng/ml TGF-β1 and 2000 ADSEVs/cell in the absence or presence of 10 µM SB. (F) Quantification of dendritic spine density from images. n=45 primary or secondary dendrites from 3 independent experiments. All images are adjusted for brightness and contrast and cropped to same size for better visualization of SV2 colocalization on dendritic spines. Left panel: SV2 only. Right panel: Overlay of phalloidin (gray-scale) and SV2 (green). Some example dendritic spines are indicated with arrows. Scale bar, 5 µm. Data represented as box and whiskers plots with all data points shown, bar indicating the median, and the box showing interquartile range. (G) Western blot analysis of pSmad2 and Smad2 in day 10 cortical neurons after treatment of 10 ng/ml TGF-β1 for 1 h in the absence or presence of 1.25, 2.5, 5 or 10 µM SB. Representative western blot (top) and quantification of absolute density of pSmad2 compared to total Smad2 (bottom). n=3. Data represented as mean ± SEM. (H) Western blot analysis of pSmad2 and Smad2 in day 10 cortical neurons after treatment of 10 ng/ml TGF-β1 for 1 h in the absence or presence of 2.5, 5 or 10 µg/ml pan-TGFβ-neutralizing antibody or 10 µg/ml isotype control antibody. Representative western blot (top) and quantification of absolute density of pSmad2 compared to total Smad2 (bottom). n=3. Data represented as mean ± SEM. *p<0.05, **p<0.01, ***p<0.001, n.s. – not significant.
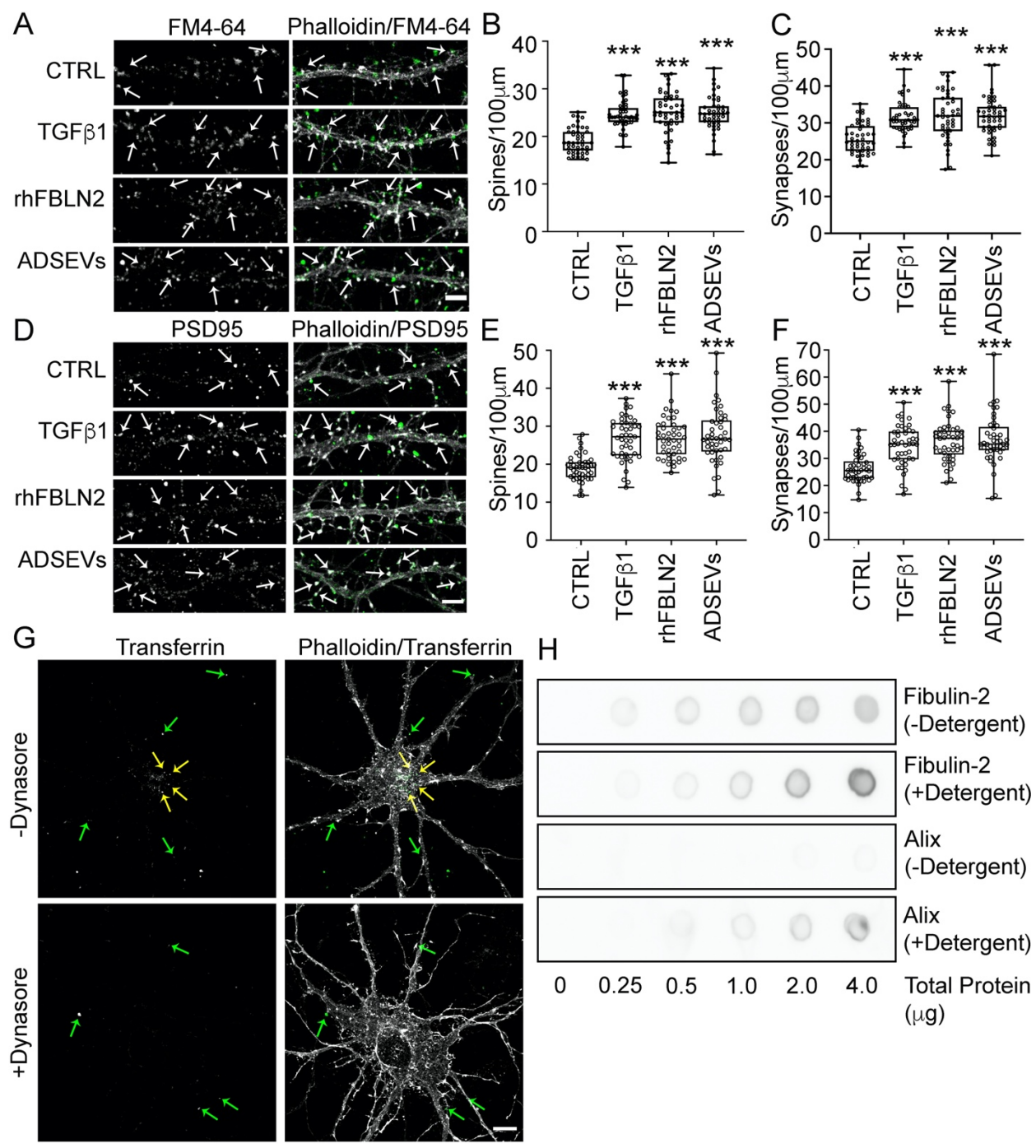
Figure 23: Fibulin-2 promotes formation of active synapses and is present on the outside of ADSEVs. (A) Representative FM4-64 (grayscale) and Phalloidin (gray)/FM4-64 (green) overlay images of day 12 neurons treated with 10 ng/ml TGF-β1, 2 μg/ml rhFBLN2 or 2000 ADSEVs/cell. (B and C) Quantification of spine and synapse density from images in A. n=45 primary or secondary dendrites from three independent experiments. (D) Representative PSD95 (grayscale) and Phalloidin (gray)/PSD95 (green) overlay images of day 12 neurons treated with 10 ng/ml TGF-β1, 2 μg/ml rhFBLN2 or 2000 ADSEVs/cell. (E and F) Quantification of spine and synapse density from images in D. n=45 primary or secondary dendrites from three independent experiments. (G) Representative Transferrin (grayscale) and Phalloidin (gray)/Transferrin (green) overlay images of Transferrin internalization in the absence or presence of 100 μM Dynasore. n=12 images from 3 independent experiments. Yellow arrows show internalized transferrin. Green arrows show transferrin at the surface of or outside of the neuron. Scale bar, 10 μm. (H) Dot blot assay of astrocyte-derived SEVs at 0, 0.25, 0.5, 1, 2 and 4 μg concentrations stained for fibulin-2 or Alix in the absence or presence of 0.1% (v/v) Tween-20 detergent in 1x TBS. Representative of three independent experiments. All images are adjusted for brightness and contrast and cropped to same size. For images in A and D, Left panel: FM4-64/PSD95 only. Right panel: Overlay of phalloidin (gray-scale) and FM4-64/PSD95 (green). Some example dendritic spines are indicated with arrows. Data are represented as box and whiskers plots with all data points shown, bar indicating the median, and the box showing interquartile range. Scale bar 5 μm. ***p<0.001.

To test whether TGF-β signaling is important for the synaptogenic effects of astrocyte SEVs and fibulin-2, day *in vitro* 10 cortical neurons were treated with astrocyte SEVs, 2 µg/mL recombinant fibulin-2, or 10 ng/mL TGF-β1 for 48 h in the presence or absence of 10 µM SB. Analysis of SV2 immunostaining in the cortical neurons revealed that TGF-β signaling inhibition indeed blocks the phenotypic effects of astrocyte SEVs and fibulin-2 (Figures 22A–22D). Furthermore, recombinant TGF-β mimicked the synaptogenic effect of astrocyte SEVs and fibulin-2. Similar effects of astrocyte SEVs and TGF-β were likewise observed for early stage day *in vitro* 6 neurons (Figures 22E and 22F, fibulin-2 was not tested).

In the baseline control condition, pSmad2 and synaptogenesis were significantly reduced by 10 µM SB. Therefore, lower concentrations of SB were tested to identify concentrations that only inhibit TGF-β1-induced Smad2 phosphorylation (Figure 22G). In addition, we used a second method to inhibit TGF-β signaling, with a pan-TGFβ-neutralizing antibody (Figure 22H). We identified 2.5 µM SB or 10 µg/mL pan-TGFβ-neutralizing antibody to be optimal concentrations to inhibit TGFβ1-induced Smad2 phosphorylation (Figures 22G and 22H). Using these conditions, we found that neuronal dendritic spines and synapses induced by TGF-β1, fibulin-2, or astrocyte SEVs were inhibited by 2.5 µM SB or 10 µg/mL pan-TGFβ-neutralizing antibody (Figures 20C and 20D). Dendritic spine and synapse density were also examined using PSD95, a postsynaptic marker, and uptake of the lipophilic dye FM4-64, a marker for synaptic activity. As with SV2 and phalloidin staining, treatment of cortical neurons with TGF-β1, fibulin-2, and astrocyte SEVs induced an increase in spines and synapses positive for PSD95 and FM4-64 (Figures 23A–23F).

Activation of TGF-β signaling in cortical neurons by astrocyte-derived SEVs could be receptor-mediated or require SEV internalization. To help distinguish these possibilities, neurons

were treated with TGF-β1, fibulin-2, or astrocyte SEVs to measure Smad2 phosphorylation at different time points. For all treatments, pSmad2 levels increased at 15 min and 1 h, after which it declined (Figure 21E). To further explore the mechanism, pSmad2 levels were measured in neurons treated with TGF-β1, fibulin-2, or astrocyte SEVs for 1 h in the absence or presence of the endocytosis inhibitor, Dynasore. Dynasore treatment had a small but significant inhibitory effect on TGF-β1, fibulin-2, or astrocyte SEV-induced pSmad2 levels. These data suggest that endocytosis enhances but is not necessary for the induction of TGF-β signaling by astrocyte SEVs and fibulin-2. The ability of Dynasore to inhibit endocytosis in our system was confirmed by observing internalization of fluorescent transferrin by neurons (Figure 23G). The rapid activation of TGF-β signaling by astrocyte SEVs and fibulin-2 (Figure 21E), together with the small effect of Dynasore, suggest that the signaling is likely to be primarily receptor-mediated at the cell surface. To activate extracellular TGF-β, fibulin-2 should be present on the outside of astrocyte SEVs. Indeed, using a dot-blot assay in which EVs are permeabilized with 0.1% Tween to reveal internal cargoes (C. P. Lai et al., 2015; McKenzie et al., 2016; Sung & Weaver, 2017), we detect the cytoplasmic protein Alix mainly in the presence of detergent. However, fibulin-2 was detected with equivalent intensity in the absence or presence of detergent, indicating its localization to the outside of SEVs (Figure 23H).

Discussion

Secreted factors from astrocytes are critical for neuronal development and function. We found that astrocyte-derived SEVs promote spine and synapse formation in primary cultured neurons. Using a quantitative proteomic approach, we identified fibulin-2 as strongly enriched in astrocyte SEVs compared to neuronal and C6 glioma SEVs. Follow-up experiments revealed that recombinant fibulin-2 promotes and that fibulin-2 knock-down SEVs are deficient in inducing

synaptogenesis. Both astrocyte SEV- and fibulin-2-dependent spine and synapse formation depend on TGF-β signaling. The rapid induction of TGF-β signaling by SEVs and fibulin-2, the presence of fibulin-2 on the outside of SEVs, and the relative insensitivity to endocytosis inhibition suggest a model in which fibulin-2 carried by astrocyte SEVs augments TGF-β signaling at the cell surface of neurons.

Astrocyte EVs can regulate neurite length and dendritic complexity (Chaudhuri et al., 2018; Luarte et al., 2020; You et al., 2020). Although treatment of the astrocytes with IL-1β was shown to diminish the neurite-inducing activity of the secreted EVs, via EV-carried miRNAs, no mechanism was investigated for the positive effects of astrocyte EVs on neuronal outgrowth. In our study, we specifically focused on whether astrocyte SEVs induce synapse formation, using SV2, PSD95, and FM-464 staining as readouts. Because increased dendritic complexity typically accompanies synapse formation, it seems possible that fibulin-2 carried by SEVs may drive some of the positive effects of astrocyte SEVs on neuronal dendritic specialization. If so, the downregulation of such activities by SEV-carried miRNAs speaks to the molecular complexity of SEVs secreted by cells and the multiple modes by which SEVs alter the phenotypes of recipient cells.

Although fibulin-2 is an ECM molecule, many of its biologic effects appear related to regulation of TGF-β activity. Fibulin-2 has been shown to be essential for TGF-β-mediated cardiac hypertrophy and fibrosis and to promote TGF-β-signaling (Khan et al., 2016a; Hangxiang Zhang et al., 2014). In one of these studies, addition of recombinant fibulin-2 to fibulin-2 knockout cells was able to partially rescue Smad2 phosphorylation, suggesting that fibulin-2 may directly activate TGF-β signaling (Khan et al., 2016a). Apart from cardiac fibroblasts, fibulin-2 is also required for TGF-β1 to increase neurogenesis in adult neural stem cells (Radice et al., 2015a).

TGF-β1 is a synaptogenic factor secreted by astrocytes that increases excitatory synapse formation (Diniz et al., 2012; Diniz et al., 2014) and protects neurons against spine and synapse loss induced by amyloid beta oligomers (Diniz et al., 2017). Consistent with our finding that TGF-β1 signaling is important for astrocyte SEV-mediated spine and synapse formation, mice deficient for TGF-β1 in the CNS display a significant reduction in dendritic spine density in pyramidal cells of hippocampal slices prepared from 21-day-old mice (Koeglsperger et al., 2013). By contrast, in a mouse model of depression, increased fibulin-2 and TGF-β1 expression were associated with decreased dendritic spines and knockdown of fibulin-led to a partial rescue in dendritic spine density (Tang, Yang, Liu, Wang, & Wang, 2019). Further study will be required to understand why fibulin-2 and/or TGF-β signaling has divergent effects on dendritic specializations in adult disease versus in developing neurons.

TGF-β1 is released from cells as a latent complex and requires activation to exert its functions. Both active and inactive forms of TGF-β1 are present in EVs (Shelke et al., 2019a; Webber et al., 2010). Inactive TGF-β1 present in EVs can be activated and can induce prolonged signaling in recipient cell endosomes (Shelke et al., 2019a). However, astrocyte SEVs did not induce prolonged TGF-β signaling in neurons. Furthermore, astrocyte SEV-induced TGF-β signaling was only slightly diminished by inhibition of endocytosis, suggesting that most of the EV-induced TGF-β signaling occurred at the cell surface. In our proteomics data, we identified multiple TGF-β isoforms and latent TGF-β binding proteins present in astrocyte SEVs; however, none of these proteins were enriched in astrocyte SEVs compared to C6 EVs. We also did not detect the ECM protein thrombospondin-1 that can activate TGF-β1 by direct interaction with the latent complex (Murphy-Ullrich & Poczatek, n.d.; Yu et al., 2008). The molecular mechanism by which fibulin-2 activates TGF-β signaling remains unknown; however it has been postulated that

fibulin-2 may either release active TGF-β1 from the latent complex by facilitating cleavage or increase TGF-β bioavailability by competing with a latent TGF-β binding protein for fibrillin-1 binding (Costanza, Umelo, Bellier, Castronovo, & Turtoi, 2017; Ono et al., 2009). Our data suggest that EVs are an important platform for this process.

For our proteomics analysis, we used a statistical comparison between astrocyte and C6 SEV cargo proteins to narrow our potential candidates to twelve proteins. Of these twelve proteins, none were previously shown to directly regulate synaptogenesis. However, fibulin-2 had been reported to promote TGF-β1 signaling, which has known function in synaptogenesis (Diniz et al., 2012, 2014). Furthermore, fibulin-2 expressed by astrocytes is known to be important for neurogenesis and CNS repair (Radice et al., 2015a; Schaeffer, Tannahill, Cioni, Rowlands, & Keynes, 2018a). Therefore, we followed up on fibulin-2 as our top candidate. Because we did not perform replicate proteomics experiments, more experiments would be required to make firm conclusions about large-scale differences between the SEV samples. However, we note that we were able to easily validate differences in the levels of selected cargoes by western blot analysis and also successfully identified fibulin-2 as a key synaptogenic cargo.

Another limitation of our study is that it was all carried out *in vitro*, albeit with primary cultures. In the brain, EV secretion from multiple cell types may lead to complex regulation of signaling pathways involved in spine and synapse formation. Fibulin-2 has been shown to regulate spinal nerve outgrowth in a chick embryo model and to be expressed at higher levels in reactive astrocytes at the lesion site in a CNS injury mouse model, suggesting functions in CNS repair and plasticity (Schaeffer et al., 2018a). However, the *in vivo* functions of fibulin-2 and astrocyte SEVs in synapse formation during neuronal development remain to be demonstrated.
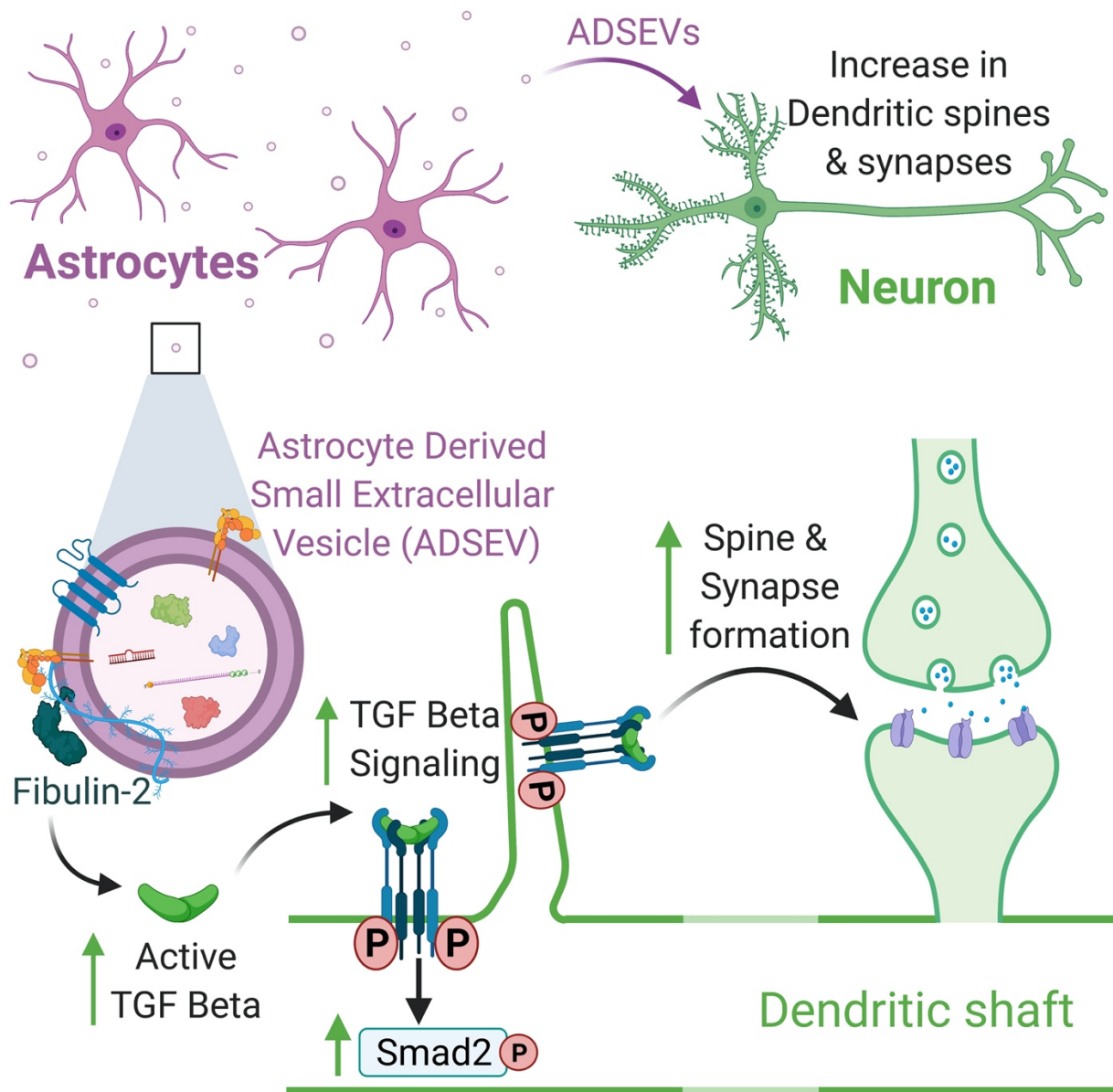
Figure 24: Model for ADSEVs mediated activation of TGF-β signaling via fibulin-2. Fibulin-2 present on the outside of ADSEVs induce TGF-β signaling which in turn lead to increased spine and synapse formation.

We also did not investigate what pathways may regulate secretion of fibulin-2-carrying EVs from astrocytes. Although IL-1β treatment of astrocytes is known to alter EV biogenesis and dendritic complexity, whether it affects the number of fibulin-2-carrying EVs released from astrocytes is currently unknown (Chaudhuri et al., 2018; Dickens et al., 2017).

Fibulin-2 can bind to other ECM proteins, including fibronectin, fibrillin-1, and some heparin sulfate proteoglycans (Sasaki, Göhring, Pan, Chu, & Timpl, 1995; Timpl, Sasaki, Kostka, & Chu, 2003), which were also present on astrocyte SEVs according to our iTRAQ proteomics data. Therefore, it is conceivable that fibulin-2 may be associated with many of its known binding partners on SEVs. Because adhesion molecules may target SEVs to specific sites, it is also possible that ECM associated with SEVs may serve multiple purposes, including binding recipient cells and delivery of signaling molecules.

In summary, we identified a distinct role of primary astrocyte-derived SEVs in the development of dendritic spines and synapses via activation of TGF-β signaling. Our proteomics analysis identified fibulin-2 as a key astrocyte SEV cargo that promotes TGF-β signaling and drives synaptogenesis (Figure 24).

CHAPTER IV

CONCLUSIONS AND FUTURE DIRECTIONS

Conclusions

Neurons communicate with each other at synapses via transmission of chemical and electrical signals from presynaptic axon terminals to postsynaptic sites. Dendritic spines evolving from filopodia play an important role in the regulation of synaptic transmission and therefore in higher brain functions such as learning and memory. Many studies have identified intracellular factors that regulate formation of filopodia, spines and synapses. However, not much is known about extracellular regulators of these structures. EVs secreted from cells are being increasingly recognized for their function in cellular communication.

In this project, I examined the effects of neuron-derived and astrocyte-derived SEVs on filopodia, spine and synapse formation. To study this, I used primary cultures of rat hippocampal and cortical neurons that are well characterized for the formation of filopodia and their subsequent maturation into spines and synapses. I found that neuron-derived SEVs of endocytic origin promote dendritic filopodia formation. The MVB marker Rab27b preferentially localized to the tips and bases of dendritic filopodia and spines suggesting targeted release of exosomes near actin-rich dendritic protrusions. THSD7A was identified as the functional cargo of neuronal exosomes responsible for inducing filopodia. However, the molecular mechanism of its function is still under investigation. I also discovered that astrocyte-derived SEVs induce spine and synapse formation. In ADSEVs, the ECM protein, fibulin-2, was found to enhance synaptogenesis by activating TGF-β signaling. More studies are required to understand how fibulin-2 functions in TGF-β activation.

Future Directions

Function of exosomal THSD7A in promoting filopodia formation:

Using quantitative proteomics, first in cancer cell exosomes and then in neuronal exosomes, I identified THSD7A as a candidate exosomal cargo potentially involved in filopodia formation. Previous studies had proposed a function for the soluble form of THSD7A in filopodia formation in HUVEC cells (Kuo et al., 2011). The full length THSD7A is ~260 kDa while the soluble form is ~210 kDa. In Western blot analyses, I found that neuronal exosomes and cell lysates display one band above ~250 kD, suggesting full length THSD7A, and another band below ~250 kDa, presumably the soluble form of THSD7A. Also, the peptide identified in our iTRAQ proteomics analysis (accession #F1MA97) matched with the transmembrane region of THSD7A. Therefore, THSD7A in neuronal exosomes is most likely present in both soluble and full-length forms that are actively sorted during exosome biogenesis. Furthermore, I found that transfection of THSD7A expression vectors in primary neurons significantly increased filopodia density. However, the molecular mechanism of the function of THSD7A is unclear.

There are several possible mechanisms by which THSD7A could regulate filopodia. One possible mechanism is that THSD7A stabilizes filopodia by interacting with cell adhesion molecules. The extracellular region of THSD7A contains an integrin binding RGD domain (Kuo et al., 2011). It is possible that THSD7A interacts with integrins to stabilize filopodia. In one study, THSD7A was found to co-localize with the αVβ3 integrin and paxillin at the leading edge of migrating HUVEC cells (C. H. Wang et al., 2010). Another study also reported THSD7A localization to filopodia with enhanced adhesion of glomerular epithelial cells expressing THSD7A (Herwig et al., 2019). In agreement with these studies, my finding shows that, also in primary neurons, THSD7A localizes to the tips of filopodia. Whether integrin interactions with

exosomal THSD7A enhances filopodia formation/stability remains to be seen. This could be tested by observing co-localization of THSD7A and integrins by immunostaining and confocal microscopy. Additionally, the RGD domain of THSD7A could be mutated to disrupt its interaction with integrins. Expression of THSD7A with mutated RGD domains could be examined for localization and changes in filopodia density. If THSD7A with mutant RGDs fails to localize at the tips of filopodia and also does not enhance filopodia density, it would suggest its function through interaction with integrins.

Another possibility is that THSD7A activates signaling pathways involved in filopodia formation. THSD7A has at least 10 thrombospondin type -1 repeats (TSR) (Kuo et al., 2011). Since Thrombospondin-1 is known to activate TGF-β by association of TSRs with latent TGF-β complexes (X. Xu et al., 2018), it can be postulated that THSD7A releases active TGF-β from latent complexes to activate TGF-β signaling. Canonical and non-canonical TGF-β signaling pathways are known to induce filopodia formation (Oh, Knelson, Blobe, & Mythreye, 2013; Sun et al., 2011). However, my preliminary data indicate that neuronal exosomes are unable to activate TGF-β signaling, as indicated by Smad2 phosphorylation (data not shown). Therefore, it is unlikely that exosomal THSD7A induces filopodia formation through TGF-β signaling pathway.

Since filopodia formation is frequently regulated by actin regulatory protein-mediated cytoskeletal rearrangements downstream of Cdc42 activation, it is possible that THSD7A regulates filopodia formation through activation of Cdc42. One way to test this hypothesis is to measure the GTP-bound active form of Cdc42 by pull down in cell lysates of neurons treated with exosomes or recombinant THSD7A compared to untreated control neurons. Alternatively, function of neuronal exosomes or recombinant THSD7A could be assessed in the absence or presence of selective inhibitor of Cdc42, ML141 (Surviladze et al., 2010). Additionally, a dominant negative

form of Cdc42 has been shown to reduce filopodia in primary neurons (Gauthier-Campbell, Bredt, Murphy, & El-Din El-Husseini, 2004). Therefore, filopodia density in neurons expressing a dominant negative form of Cdc42 treated with neuronal exosomes or recombinant THSD7A could also be assessed. If THSD7A induced filopodia formation requires Cdc42 activation, then exosome or recombinant THSD7A treatments should fail to rescue filopodia defects in cells expressing this dominant negative Cdc42.

Cdc42 activation is mediated by GEFs in response to upstream signals such as growth factors, cytokines and integrins (Soniya Sinha & Yang, 2008). Adhesion of NIH 3T3 fibroblasts plated on fibronectin or β1-integrin antibody coated coverslip leads to activation of Cdc42 assayed by stimulation of PAK, a downstream effector of Cdc42. Also, expression of dominant negative Cdc42 in these fibroblasts leads to significant reduction in spreading (Price, Leng, Schwartz, & Bokoch, 1998). These results suggest that activation of PAK downstream of Cdc42 is mediated by integrin-dependent adhesion. Additionally, integrin-linked kinase, a signaling protein downstream of ECM-integrin interaction, activates Cdc42 in epithelial cells via Rac/Cdc42-specific GEF α-PIX (Filipenko, Attwell, Roskelley, & Dedhar, 2005). Therefore, it is also possible that THSD7A interaction with integrin could mediate activation of Cdc42 for filopodia formation. To test this, Cdc42 activation can be assessed in cells expressing THSD7A or RGD mutant THSD7A.

Activation of TGF-β signaling mediated by ADSEV associated fibulin-2:

Astrocytes are known to promote spine and synapse formation via interactions with cell surface molecules and also by secreting growth factors (Allen, 2014a; Chung et al., 2015). Primary neurons grown in co-culture with astrocytes form more synapses compared to cultures grown in the absence of astrocytes (Jones et al., 2012). I found that astrocyte-secreted SEVs carry functional

cargo that induce spine and synapse formation in a dose dependent manner. Most studies investigating the function of astrocyte secreted factors are performed using astrocyte conditioned media. Therefore, it is possible that many of the synaptogenic proteins are secreted in association with EVs.

Using comparative proteomics analysis, I identified protein profiles of SEVs isolated from astrocytes, cortical neurons and C6 cells. I found enrichment of cell type specific proteins in SEVs. Specifically, CNSEVs showed high expression of ion channel receptor subunits and components of the SNARE machinery (Table 3). I found that several proteins were expressed at high levels in ADSEVs compared to CNSEVs and C6SEVs (Table 2). Among these proteins, there was no obvious candidate previously known to regulate synaptogenesis. It is possible that proteins that were higher in ADSEVs may not have been well studied for their function in synapse formation or they may indirectly regulate synaptogenesis.

I found various active and latent forms of TGF-β, TGF-β1, 2, 3 and LTBP-1, -3, -4, in all three types of SEVs (Table 4). TGF-β signaling is known to induce excitatory synapse formation (Diniz, Almeida, Tortelli, Lopes, et al., 2012b). However, I found that CNSEVs and C6SEVs had no effect on spine and synapse density despite the presence of TGF-βs suggesting the role of additional factors regulating indirect activation of TGF-β signaling. Among proteins significantly enriched in ADSEVs compared to C6SEVs, fibulin-2 has a known function in activation of TGF-β signaling. In cardiac fibroblasts, addition of recombinant fibulin-2 alone was able to induce TGF-β signaling (Khan et al., 2016b). Additionally, other studies have also reported high expression of fibulin-2 in astrocytes examined by immunostaining (Radice et al., 2015b; Schaeffer, Tannahill, Cioni, Rowlands, & Keynes, 2018b). I found that fibulin-2 is highly expressed in ADSEVs and promotes spine and synapse formation.

Table 3: Ion channel receptor subunits and SNARE proteins in CNSEVs compared to ADSEVs and C6SEVs

Protein Name	Fold change compared to	
	ADSEVs	C6SEVs
Ion channel receptor subunits		
Sodium channel, voltage-gated, type VIII, alpha subunit	11.71	8.18
Sodium/potassium-transporting ATPase subunit beta-1	9.14	5.69
Sodium/potassium-transporting ATPase subunit beta-2	2.62	5.20
Sodium/potassium-transporting ATPase subunit alpha-2	1.99	3.33
Sodium/potassium-transporting ATPase subunit alpha-1	1.76	1.85
Sodium/potassium-transporting ATPase subunit beta-3	0.88	1.02
Voltage-dependent calcium channel subunit alpha-2/delta-1	1.72	2.57
SNARE proteins		
Synaptobrevin homolog YKT6	1.42	2.44
Syntaxin-1A	3.52	6.12
Syntaxin-1B	3.47	12.27
Syntaxin-12	3.26	3.06
Syntaxin-7	1.52	2.37
Synaptosomal-associated protein 25	1.01	2.75
Synaptotagmin-11	2.22	4.16
Synaptotagmin-5	1.59	2.83
Synaptotagmin-1	1.57	2.24

Table 4: Active and latent forms of TGB-βs in ADSEVs compared to CNSEVs and C6SEVs

Protein Name	Fold change compared to	
	CNSEVs	C6SEVs
Transforming growth factor beta-1	1.65	0.48
Transforming growth factor, beta 2, isoform CRA_a	2.32	0.70
Transforming growth factor beta-3	2.02	1.17
Latent-transforming growth factor beta-binding protein 1	1.35	0.44
Latent-transforming growth factor beta-binding protein 3	1.95	0.65
Latent-transforming growth factor beta-binding protein 4	2.00	1.13

The mechanism by which fibulin-2 activates TGF-β is unknown. One model is that fibulin-2 increases bioavailability and activation of TGF-β by competing for binding to other ECM molecules (Tsuda, 2018). For instance, the fibulin-2 binding site on fibrillin-1 is in close proximity to the binding site for LTBPs (Ono et al., 2009). Similarly, fibronectin is also a known binding partner of fibulin-2 that also interacts with LTBPs (Dallas et al., 2005; T. C. Pan et al., 1993). Therefore, fibulin-2 may regulate bioavailability of latent TGF-β complex by competitively binding to ECM molecules. Alternatively, fibulin-2 could directly interact with latent TGF-β complex (Khan et al., 2016b). Conformational changes of latent TGF-β complex mediated by fibulin-2 could release active TGF-β.

There are at least two possible scenarios for how fibulin-2 may access latent TGF-β complexes. iTRAQ analysis showed the presence of latent TGF-βs in ADSEVs and therefore one possibility is that there is a heterogenous population of SEVs secreted from astrocytes carrying fibulin-2 and latent TGF-β complex. Balanced secretion of fibulin-2 and latent TGF-β complex containing ADSEVs may dictate the level of active TGF-β for signaling. Another possibility is that fibulin-2 bind to latent TGF-β complexes already present in the extracellular environment, secreted by neurons and astrocytes, and change their confirmation to allow release of active TGF-β. It is likely that coordinated neuron-astrocyte communication leads to regulated release of latent TGF-β complexes into the extracellular space depending on physiological and pathological state. It will be intriguing to determine whether SEVs from fibulin-2 knockdown astrocytes have any differences in active and latent forms of TGF-β. To test this, TGF-β ELISAs can be used on purified SEVs to identify total and active TGF-β levels in the presence or absence of mild acid treatment, respectively. It is also possible that fibulin-2 could release TGF-β from other

complexes, such as binding to alpha-2-macroglobulin (Feige, Negoescu, Keramidas, Souchelnitskiy, & Chambaz, 1996; Stouffer, LaMarre, Gonias, & Owens, 1993), which was also present in ADSEVs by our proteomics analysis (Table 2).

Recently, it was reported that mast cell exosomes carry active and latent TGF-β that induces Smad phosphorylation in MSCs from endosomes in a prolonged manner compared to free TGF-β1 (Shelke et al., 2019c). The mast cell exosomes also exhibited greater function in MSC migration compared to treatment with TGF-β1 (Shelke et al., 2019c). By contrast, I found that ADSEVs and fibulin-2 activated TGF-β signaling to almost the same extent at different time points, and that the signaling occurred by 15 min, with a peak of 1 hour. Furthermore, treatment of neurons with the endocytosis inhibitor, Dynasore, only minimally reduced Smad2 phosphorylation induced by TGF-β1, fibulin-2 or ADSEVs treatment. Those data suggest that fibulin-2 primarily functions in the extracellular space.

Using a dot-blot analysis, I found that fibulin-2 is localized on the outside of SEVs. Whether fibulin-2 is actively sorted or binds to ADSEVs after secretion still remains to be determined. However, the lack of a membrane linkage suggests that fibulin-2 may associate with other EV-carried binding proteins. Several studies have identified the presence of fibulin-2 in proteomics analysis of EVs from different cell types (Chan et al., 2015; Chavez-Muñoz, Kilani, & Ghahary, 2009; Skogberg et al., 2013). However, none of these studies examined its localization on EVs. One possibility is that fibulin-2 binds to other ECM molecules such as fibronectin, that are commonly found on EVs (Bin et al., 2016; Chanda et al., 2019; Sung et al., 2015). Indeed, I found several fibulin-2-binding proteins including fibronectin, fibrillin-1 and nidogen-1 (Tsuda, 2018) to be present in ADSEVs by our proteomics analysis. A future direction could be to identify critical proteins that mediate binding of fibulin-2 to SEVs.

Our findings suggest that actin-rich dendritic filopodia and spines are potential sites of MVB docking and exosome release as most of the GFP-Rab27b localization was observed near these dendritic protrusions. Several other studies have also identified association between actin-rich plasma membrane protrusions, invadopodia, and exosome release (Beghein et al., 2018; D. Hoshino et al., 2013). A previous study from our lab has shown that cortactin, an actin regulating protein, controls exosome secretion in cancer cells by stabilizing branched actin (Seema Sinha et al., 2016). Recently, SH3 and NTA domains of Cortactin were found to be important for EV release as single-domain antibodies significantly reduced EV secretion. Additionally, the actin-bundling protein Fascin-1 was also identified to regulate EV release (Beghein et al., 2018). Therefore, mounting evidence suggests a clear link between actin structures and exosome release. Targeted delivery of MVBs to actin structures at the plasma membrane could provide a way to transport required growth factors and signaling molecules to create microenvironment suitable for filopodia formation/stability. In future, live imaging experiments using pH sensitive fluorescent probes to visualize exosome secretion will help us better understand sites of exosome release.

It would also be interesting to investigate molecular partners of Rab27b required at the plasma membrane that help facilitate docking and fusion of MVBs for exosome release in neurons. Only few studies have examined functions of Rab interacting proteins in exosome release. Previously, Rab27 effector proteins, Slp4 and Slac2, have been shown to regulate exosome secretion in HeLa cells (Ostrowski et al., 2010). Recently, a Rab binding protein, Munc13-4, was also shown to regulate Ca^{+2} triggered exosome release in Rab11 dependent pathway (Messenger et al., 2018). However, more studies are required to identify molecular machinery that regulate MVB docking and exosome release. Rab27b is required for MVB docking and also synaptic

vesicle docking at presynaptic site. Additionally, synaptic vesicles release at presynaptic terminal and exosome release are known to be triggered by changes in Ca^{+2} levels (Lachenal et al., 2011; N. J. Pavlos et al., 2010). Therefore, MVB docking and fusion may also involve similar proteins that regulate SV docking and fusion. In fact, all core components of SNARE complex, syntaxin, synaptobrevin and SNAP-25, were found in CNSEVs, mostly at high levels compared to ADSEVs and C6SEVs. However, role of SNARE proteins in exosome release is less well studied. SNARE proteins VAMP7 and YKT6 are required for exosome release in erythroleukemia cells and lung cancer cells, respectively (Fader, Sánchez, Mestre, & Colombo, 2009; Ruiz-Martinez et al., 2016). Also, synaptotagmin-7, a SNARE binding protein, is known to affect exosome release in cancer cells (D. Hoshino et al., 2013; Sung et al., 2015). In neurons, synaptotagmin-7 is mainly involved in synaptic vesicle fusion and neurotransmitter release. It is possible that various synaptotagmin isoforms that are differentially expressed at axons and dendrites (Dean et al., 2012) may have function in MVB fusion. Co-localization of specific synaptotagmin isoforms with exosome markers can be observed to identify synaptotagmin involved in MVB fusion. Next, knockdown of specific synaptotagmin isoform can be performed to examine changes in exosome secretion and dendritic filopodia formation.

Developmental stage specific functions of CNSEVs and ADSEVs:

I identified a function of neuronal exosomes at a specific developmental time point, *DIV*6. Although, other studies have shown exosome secretion from developing neurons (*DIV*9) and mature neurons (*DIV*15), no direct comparison was made to analyze changes in secretion rates and cargo composition (Chivet et al., 2014; Lachenal et al., 2011). In a recent study, researchers analyzed the proteome of primary hippocampal neurons at different developmental stages, *DIV*1,

*DIV*5 and *DIV*14 (Frese et al., 2017). Significant differences in protein profiles were observed with consistent decrease in expression of proteins related to cell cycle, DNA replication and RNA metabolism and a steady increase in proteins related to ion transport, neurotransmitter release and synaptic proteins. Similarly, proteome analysis of cortical synaptic membrane from postnatal mice showed significant differences in proteins at different developmental stages (Gonzalez-Lozano et al., 2016). These studies demonstrate that protein expression changes dramatically in neurons throughout development. Therefore, it is possible that the functional cargo and the number of exosomes secreted at different developmental stages also differ based on their functional requirement.

Neuronal exosomes are likely to have stage specific functions during development. Early in development they may be required for axon guidance and filopodia formation. Whereas, at later stages when synaptic contacts are made, they may regulate synaptic activity. EVs secreted by primary neurons are capable of inducing ephrinB1 reverse signaling to regulate axon repulsion at *DIV*3 (Gong, Körner, Gaitanos, & Klein, 2016). More recently, Synaptobrevin-2 containing EVs secreted by mature primary neurons (*DIV*14) were shown to regulate neurotransmission by incorporating EV associated Synaptobrevin-2 into synaptic vesicles (Vilcaes, Chanaday, & Kavalali, 2021). Comparison of cargo changes in exosomes isolated at different developmental stages, together with mechanistic analyses of the roles of those cargoes, will be required to further understand developmental stage specific functions of neuronal exosomes.

Similarly, I studied the function of astrocyte-derived SEVs at a developmental stage where neurons actively form spines and synapses, *DIV*12. It is possible that during different developmental stages, ADSEVs may have different functions. In the developing brain, similar to primary cultures, synapses are formed in excess at early stages of development and later

unnecessary synapses are selectively removed during the phase of synaptic pruning. Although astrocytes mainly provide factors for synapse formation, stability and maturation, some studies have also suggested their function in synapse elimination (Chung et al., 2013). A recent study showed that astrocytes eliminate excitatory synapses through the phagocytic receptor MEGF10 in adult mouse hippocampus (J. H. Lee et al., 2020). It is possible that astrocyte derived SEVs are involved in this communication with neurons to identify unnecessary synapses for elimination. Future studies focused on developmental stage specific functions of ADSEVs will provide a better understanding of their diverse roles during neuronal development by analyzing cargo changes and functional effects of ADSEVs at different developmental stages.

In summary, my work shows that neuronal exosomes induce filopodia through THSD7A via a yet unidentified molecular mechanism. In addition, I found that astrocyte-derived SEVs enhance spine and synapse formation through fibulin-2 via activation of TGF-β signaling. These are the first reported studies to identify specific cargoes and functions of neuron-derived and astrocyte-derived SEVs in regulating filopodia, spine and synapse formation. ECM molecules play a critical role in regulating filopodia and spine formation. Interestingly, both THSD7A and fibulin-2 are ECM molecules themselves, but are carried by and mediate their functions in the context of EVs. In the future, improved understanding of how these and other ECM cargoes are targeted to EVs and mediate their functions may lead to a greater general understanding of how EVs communicate along with development of novel applications for diagnosis and treatment of neurological disorders.

REFERENCES:

Adolf, A., Rohrbeck, A., Münster-Wandowski, A., Johansson, M., Kuhn, H.-G., Kopp, M. A., … Höltje, M. (2019). Release of astroglial vimentin by extracellular vesicles: Modulation of binding and internalization of C3 transferase in astrocytes and neurons. *Glia*, *67*(4), 703–717. https://doi.org/10.1002/glia.23566

Aguilar, B. J., Zhu, Y., & Lu, Q. (2017). Rho GTPases as therapeutic targets in Alzheimer's disease. *Alzheimer's Research & Therapy*, *9*(1), 97. https://doi.org/10.1186/s13195-017-0320-4

Akers, J. C., Gonda, D., Kim, R., Carter, B. S., & Chen, C. C. (2013). Biogenesis of extracellular vesicles (EV): Exosomes, microvesicles, retrovirus-like vesicles, and apoptotic bodies. *Journal of Neuro-Oncology*, *113*(1), 1–11. https://doi.org/10.1007/s11060-013-1084-8

Allen, N. J. (2014a). Astrocyte Regulation of Synaptic Behavior. *Annual Review of Cell and Developmental Biology*. https://doi.org/10.1146/annurev-cellbio-100913-013053

Allen, N. J. (2014b). Synaptic plasticity: Astrocytes wrap it up. *Current Biology : CB*, *24*(15), R697-9. https://doi.org/10.1016/j.cub.2014.06.030

Allen, N. J., Bennett, M. L., Foo, L. C., Wang, G. X., Chakraborty, C., Smith, S. J., & Barres, B. A. (2012). Astrocyte glypicans 4 and 6 promote formation of excitatory synapses via GluA1 AMPA receptors. *Nature*, *486*(7403), 410–414. https://doi.org/10.1038/nature11059

Allenson, K., Castillo, J., San Lucas, F. A., Scelo, G., Kim, D. U., Bernard, V., … Alvarez, H. (2017). High prevalence of mutant KRAS in circulating exosome-derived DNA from early-stage pancreatic cancer patients. *Annals of Oncology*, *28*(4), 741–747. https://doi.org/10.1093/annonc/mdx004

Alvarez-Erviti, L., Seow, Y., Yin, H., Betts, C., Lakhal, S., & Wood, M. J. A. (2011). Delivery

of siRNA to the mouse brain by systemic injection of targeted exosomes. *Nature Biotechnology*. https://doi.org/10.1038/nbt.1807

Andreu, Z., & Yáñez-Mó, M. (2014). Tetraspanins in extracellular vesicle formation and function. *Frontiers in Immunology*, *5*(SEP). https://doi.org/10.3389/fimmu.2014.00442

Antonucci, F., Turola, E., Riganti, L., Caleo, M., Gabrielli, M., Perrotta, C., … Verderio, C. (2012). Microvesicles released from microglia stimulate synaptic activity via enhanced sphingolipid metabolism. *EMBO Journal*, *31*(5), 1231–1240. https://doi.org/10.1038/emboj.2011.489

Aoto, J., Ting, P., Maghsoodi, B., Xu, N., Henkemeyer, M., & Chen, L. (2007). Postsynaptic ephrinB3 promotes shaft glutamatergic synapse formation. *Journal of Neuroscience*, *27*(28), 7508–7519. https://doi.org/10.1523/JNEUROSCI.0705-07.2007

Arias-Hervert, E. R., Xu, N., Njus, M., Murphy, G. G., Hou, Y., Williams, J. A., … Stuenkel, E. L. (2020). Actions of Rab27B-GTPase on mammalian central excitatory synaptic transmission. *Physiological Reports*, *8*(9), 1–15. https://doi.org/10.14814/phy2.14428

Azmi, A. S., Bao, B., & Sarkar, F. H. (2013). Exosomes in cancer development, metastasis, and drug resistance: a comprehensive review. *Cancer and Metastasis Reviews*, *32*(3–4), 623–642. https://doi.org/10.1007/s10555-013-9441-9

Bache, K. G., Brech, A., Mehlum, A., & Stenmark, H. (2003). Hrs regulates multivesicular body formation via ESCRT recruitment to endosomes. *Journal of Cell Biology*. https://doi.org/10.1083/jcb.200302131

Banker, G. A. (1980). Trophic interactions between astroglial cells and hippocampal neurons in culture. *Science*, *209*(4458), 809–810. https://doi.org/10.1126/science.7403847

Barros, C. S., Franco, S. J., & Müller, U. (2011). Extracellular matrix: functions in the nervous

system. *Cold Spring Harbor Perspectives in Biology*, *3*(1), a005108.

https://doi.org/10.1101/cshperspect.a005108

Barzik, M., McClain, L. M., Gupton, S. L., & Gertler, F. B. (2014). Ena/VASP regulates mDia2-

initiated filopodial length, dynamics, and function. *Molecular Biology of the Cell*.

https://doi.org/10.1091/mbc.E14-02-0712

Beghein, E., Devriese, D., Van Hoey, E., & Gettemans, J. (2018). Cortactin and fascin-1 regulate

extracellular vesicle release by controlling endosomal trafficking or invadopodia formation

and function. *Scientific Reports*, *8*(1), 1–16. https://doi.org/10.1038/s41598-018-33868-z

Bin, B.-H., Kim, D.-K., Kim, N.-H., Choi, E.-J., Bhin, J., Kim, S. T., … Cho, E.-G. (2016).

Fibronectin-Containing Extracellular Vesicles Protect Melanocytes against Ultraviolet

Radiation-Induced Cytotoxicity. *Journal of Investigative Dermatology*, *136*(5), 957–966.

https://doi.org/10.1016/j.jid.2015.08.001

Bliss, T.V.P. & Collingridge, G. L. (1993). A synaptic model of memory: LTP in the

hippocampus. *Nature*, *361*, 31–39.

Breitenfeld, T., Jurasic, M. J., & Breitenfeld, D. (2014). Hippocrates: The forefather of

neurology. *Neurological Sciences*, *35*(9), 1349–1352. https://doi.org/10.1007/s10072-014-

1869-3

Budnik, V., Ruiz-Cañada, C., & Wendler, F. (2016a). Extracellular vesicles round off

communication in the nervous system. *Nature Reviews. Neuroscience*, *17*(3), 160–172.

https://doi.org/10.1038/nrn.2015.29

Budnik, V., Ruiz-Cañada, C., & Wendler, F. (2016b). Extracellular vesicles round off

communication in the nervous system. *Nature Reviews Neuroscience*, *17*(3), 160–172.

https://doi.org/10.1038/nrn.2015.29

Buzás, E. I., Tóth, E., Sódar, B. W., & Szabó-Taylor, K. (2018). Molecular interactions at the
surface of extracellular vesicles. *Seminars in Immunopathology*, *40*(5), 453–464.
https://doi.org/10.1007/s00281-018-0682-0

Calabrese, B., Wilson, M. S., & Halpain, S. (2006). Development and regulation of dendritic
spine synapses. *Physiology*, *21*(1), 38–47. https://doi.org/10.1152/physiol.00042.2005

Carayon, K., Chaoui, K., Ronzier, E., Lazar, I., Bertrand-Michel, J., Roques, V., … Joly, E.
(2011). Proteolipidic composition of exosomes changes during reticulocyte maturation. *The
Journal of Biological Chemistry*, *286*(39), 34426–34439.
https://doi.org/10.1074/jbc.M111.257444

Caroni, P., Donato, F., & Muller, D. (2012). Structural plasticity upon learning: Regulation and
functions. *Nature Reviews Neuroscience*, *13*(7), 478–490. https://doi.org/10.1038/nrn3258

Chan, Y. K., Zhang, H., Liu, P., Tsao, S. W., Lung, M. L., Mak, N. K., … Yue, P. Y. K. (2015).
Proteomic analysis of exosomes from nasopharyngeal carcinoma cell identifies intercellular
transfer of angiogenic proteins. *International Journal of Cancer*, *137*(8), 1830–1841.
https://doi.org/10.1002/ijc.29562

Chanda, D., Otoupalova, E., Hough, K. P., Locy, M. L., Bernard, K., Deshane, J. S., …
Thannickal, V. J. (2019). Fibronectin on the Surface of Extracellular Vesicles Mediates
Fibroblast Invasion. *American Journal of Respiratory Cell and Molecular Biology*, *60*(3),
279–288. https://doi.org/10.1165/rcmb.2018-0062OC

Chargaff, E., & West, R. (1946). The biological significance of the thromboplastic protein of
blood. *The Journal of Biological Chemistry*, *166*(1), 189–197.
https://doi.org/10.1016/s0021-9258(17)34997-9

Chaudhuri, A. D., Dastgheyb, R. M., Yoo, S. W., Trout, A., Talbot, C. C., Hao, H., … Haughey,

N. J. (2018). TNFα and IL-1β modify the miRNA cargo of astrocyte shed extracellular vesicles to regulate neurotrophic signaling in neurons article. *Cell Death and Disease*, *9*(3). https://doi.org/10.1038/s41419-018-0369-4

Chavez-Muñoz, C., Kilani, R. T., & Ghahary, A. (2009). Profile of exosomes related proteins released by differentiated and undifferentiated human keratinocytes. *Journal of Cellular Physiology*, *221*(1), 221–231. https://doi.org/10.1002/jcp.21847

Chen, C. C., Lu, J., & Zuo, Y. (2014). Spatiotemporal dynamics of dendritic spines in the living brain. *Frontiers in Neuroanatomy*, *8*(MAY), 1–7. https://doi.org/10.3389/fnana.2014.00028

Cheng, L., Doecke, J. D., Sharples, R. A., Villemagne, V. L., Fowler, C. J., Rembach, A., … Hill, A. F. (2015). Prognostic serum miRNA biomarkers associated with Alzheimer's disease shows concordance with neuropsychological and neuroimaging assessment. *Molecular Psychiatry*, *20*(10), 1188–1196. https://doi.org/10.1038/mp.2014.127

Chivet, M., Javalet, C., Laulagnier, K., Blot, B., Hemming, F. J., & Sadoul, R. (2014). Exosomes secreted by cortical neurons upon glutamatergic synapse activation specifically interact with neurons. *Journal of Extracellular Vesicles*. https://doi.org/10.3402/jev.v3.24722

Christopherson, K. S., Ullian, E. M., Stokes, C. C. A., Mullowney, C. E., Hell, J. W., Agah, A., … Barres, B. A. (2005a). Thrombospondins are astrocyte-secreted proteins that promote CNS synaptogenesis. *Cell*, *120*(3), 421–433. https://doi.org/10.1016/j.cell.2004.12.020

Christopherson, K. S., Ullian, E. M., Stokes, C. C. A., Mullowney, C. E., Hell, J. W., Agah, A., … Barres, B. A. (2005b). Thrombospondins are astrocyte-secreted proteins that promote CNS synaptogenesis. *Cell*, *120*(3), 421–433. https://doi.org/10.1016/j.cell.2004.12.020

Chung, W. S., Allen, N. J., & Eroglu, C. (2015). Astrocytes control synapse formation, function, and elimination. *Cold Spring Harbor Perspectives in Biology*.

https://doi.org/10.1101/cshperspect.a020370

Chung, W. S., Clarke, L. E., Wang, G. X., Stafford, B. K., Sher, A., Chakraborty, C., … Barres, B. A. (2013). Astrocytes mediate synapse elimination through MEGF10 and MERTK pathways. *Nature*, *504*(7480), 394–400. https://doi.org/10.1038/nature12776

Citri, A., & Malenka, R. C. (2008). Synaptic plasticity: Multiple forms, functions, and mechanisms. *Neuropsychopharmacology*, *33*(1), 18–41. https://doi.org/10.1038/sj.npp.1301559

Cocucci, E., & Meldolesi, J. (2011). Ectosomes. *Current Biology*, *21*(23), 940–941. https://doi.org/10.1016/j.cub.2011.10.011

Cohen, N. J., & Squire, L. R. (1980). Preserved learning and retention of pattern-analyzing skill in amnesia: dissociation of knowing how and knowing that. *Science (New York, N.Y.)*, *210*(4466), 207–210. https://doi.org/10.1126/science.7414331

Colombo, M., Raposo, G., & Théry, C. (2014a). Biogenesis, secretion, and intercellular interactions of exosomes and other extracellular vesicles. *Annual Review of Cell and Developmental Biology*, *30*, 255–289. https://doi.org/10.1146/annurev-cellbio-101512-122326

Colombo, M., Raposo, G., & Théry, C. (2014b). Biogenesis, Secretion, and Intercellular Interactions of Exosomes and Other Extracellular Vesicles. *Annual Review of Cell and Developmental Biology*. https://doi.org/10.1146/annurev-cellbio-101512-122326

Costa Verdera, H., Gitz-Francois, J. J., Schiffelers, R. M., & Vader, P. (2017). Cellular uptake of extracellular vesicles is mediated by clathrin-independent endocytosis and macropinocytosis. *Journal of Controlled Release*, *266*(September), 100–108. https://doi.org/10.1016/j.jconrel.2017.09.019

Costanza, B., Umelo, I. A., Bellier, J., Castronovo, V., & Turtoi, A. (2017). Stromal Modulators of TGF-β in Cancer. *Journal of Clinical Medicine*, *6*(1). https://doi.org/10.3390/jcm6010007

Cui, W., Allen, N. D., Skynner, M., Gusterson, B., & Clark, A. J. (2001). Inducible ablation of astrocytes shows that these cells are required for neuronal survival in the adult brain. *Glia*, *34*(4), 272–282. https://doi.org/10.1002/glia.1061

Dallas, S. L., Sivakumar, P., Jones, C. J. P., Chen, Q., Peters, D. M., Mosher, D. F., … Kielty, C. M. (2005). Fibronectin regulates latent transforming growth factor-beta (TGF beta) by controlling matrix assembly of latent TGF beta-binding protein-1. *The Journal of Biological Chemistry*, *280*(19), 18871–18880. https://doi.org/10.1074/jbc.M410762200

De Vries, G. H., & Boullerne, A. I. (2010). Glial cell lines: an overview. *Neurochemical Research*, *35*(12), 1978–2000. https://doi.org/10.1007/s11064-010-0318-9

Dean, C., Dunning, F. M., Liu, H., Bomba-Warczak, E., Martens, H., Bharat, V., … Chapman, E. R. (2012). Axonal and dendritic synaptotagmin isoforms revealed by a pHluorin-syt functional screen. *Molecular Biology of the Cell*, *23*(9), 1715–1727. https://doi.org/10.1091/mbc.E11-08-0707

DeFelipe, J. (2006). Brain plasticity and mental processes: Cajal again. *Nature Reviews. Neuroscience*, *7*(10), 811–817. https://doi.org/10.1038/nrn2005

DeKosky, S. T., & Scheff, S. W. (1990). Synapse loss in frontal cortex biopsies in Alzheimer's disease: correlation with cognitive severity. *Annals of Neurology*, *27*(5), 457–464. https://doi.org/10.1002/ana.410270502

Delaney, C. L., Brenner, M., & Messing, A. (1996). Conditional ablation of cerebellar astrocytes in postnatal transgenic mice. *Journal of Neuroscience*, *16*(21), 6908–6918.

https://doi.org/10.1523/jneurosci.16-21-06908.1996

Di Nardo, A., Cicchetti, G., Falet, H., Hartwig, J. H., Stossel, T. P., & Kwiatkowski, D. J. (2005). Arp2/3 complex-deficient mouse fibroblasts are viable and have normal leading-edge actin structure and function. *Proceedings of the National Academy of Sciences of the United States of America*, *102*(45), 16263–16268. https://doi.org/10.1073/pnas.0508228102

Dickens, A. M., Tovar-Y-Romo, L. B., Yoo, S.-W., Trout, A. L., Bae, M., Kanmogne, M., … Haughey, N. J. (2017). Astrocyte-shed extracellular vesicles regulate the peripheral leukocyte response to inflammatory brain lesions. *Science Signaling*, *10*(473). https://doi.org/10.1126/scisignal.aai7696

Diniz, L. P., Almeida, J. C., Tortelli, V., Lopes, C. V., Setti-Perdigão, P., Stipursky, J., … Gomes, F. C. A. (2012a). Astrocyte-induced synaptogenesis is mediated by transforming growth factor β signaling through modulation of d-serine levels in cerebral cortex neurons. *Journal of Biological Chemistry*. https://doi.org/10.1074/jbc.M112.380824

Diniz, L. P., Almeida, J. C., Tortelli, V., Lopes, C. V., Setti-Perdigão, P., Stipursky, J., … Gomes, F. C. A. (2012b). Astrocyte-induced synaptogenesis is mediated by transforming growth factor β signaling through modulation of d-serine levels in cerebral cortex neurons. *Journal of Biological Chemistry*, *287*(49), 41432–41445. https://doi.org/10.1074/jbc.M112.380824

Diniz, L. P., Almeida, J. C., Tortelli, V., Vargas Lopes, C., Setti-Perdigão, P., Stipursky, J., … Gomes, F. C. A. (2012). Astrocyte-induced synaptogenesis is mediated by transforming growth factor β signaling through modulation of D-serine levels in cerebral cortex neurons. *The Journal of Biological Chemistry*, *287*(49), 41432–41445. https://doi.org/10.1074/jbc.M112.380824

Diniz, L. P., Tortelli, V., Matias, I., Morgado, J., Bérgamo Araujo, A. P., Melo, H. M., …

    Gomes, F. C. A. (2017). Astrocyte Transforming Growth Factor Beta 1 Protects Synapses

    against Aβ Oligomers in Alzheimer's Disease Model. *The Journal of Neuroscience : The*

    Official Journal of the Society for Neuroscience, *37*(28), 6797–6809.

    https://doi.org/10.1523/JNEUROSCI.3351-16.2017

Doyle, L. M., & Wang, M. Z. (2019). Overview of Extracellular Vesicles, Their Origin,

    Composition, Purpose, and Methods for Exosome Isolation and Analysis. *Cells*, *8*(7), 41–

    68. https://doi.org/10.3390/cells8070727

Ebrahimi, S., & Okabe, S. (2014). Structural dynamics of dendritic spines: Molecular

    composition, geometry and functional regulation. *Biochimica et Biophysica Acta -*

    Biomembranes. https://doi.org/10.1016/j.bbamem.2014.06.002

Eroglu, C., Allen, N. J., Susman, M. W., O'Rourke, N. A., Park, C. Y., Ozkan, E., … Barres, B.

    A. (2009). Gabapentin receptor alpha2delta-1 is a neuronal thrombospondin receptor

    responsible for excitatory CNS synaptogenesis. *Cell*, *139*(2), 380–392.

    https://doi.org/10.1016/j.cell.2009.09.025

Ethell, I. M., & Pasquale, E. B. (2005). Molecular mechanisms of dendritic spine development

    and remodeling. *Progress in Neurobiology*, *75*(3), 161–205.

    https://doi.org/10.1016/j.pneurobio.2005.02.003

Evans, J. C., Robinson, C. M., Shi, M., & Webb, D. J. (2015). The guanine nucleotide exchange

    factor (GEF) Asef2 promotes dendritic spine formation via Rac activation and Spinophilin-

    dependent targeting. *Journal of Biological Chemistry*, *290*(16), 10295–10308.

    https://doi.org/10.1074/jbc.M114.605543

Fader, C. M., Sánchez, D. G., Mestre, M. B., & Colombo, M. I. (2009). TI-VAMP/VAMP7 and

VAMP3/cellubrevin: two v-SNARE proteins involved in specific steps of the autophagy/multivesicular body pathways. *Biochimica et Biophysica Acta*, *1793*(12), 1901–1916. https://doi.org/10.1016/j.bbamcr.2009.09.011

Fauré, J., Lachenal, G., Court, M., Hirrlinger, J., Chatellard-Causse, C., Blot, B., … Sadoul, R. (2006). Exosomes are released by cultured cortical neurones. *Molecular and Cellular Neuroscience*, *31*(4), 642–648. https://doi.org/10.1016/j.mcn.2005.12.003

Feige, J. J., Negoescu, A., Keramidas, M., Souchelnitskiy, S., & Chambaz, E. M. (1996). Alpha 2-macroglobulin: a binding protein for transforming growth factor-beta and various cytokines. *Hormone Research*, *45*(3–5), 227–232. https://doi.org/10.1159/000184793

Feng, D., Zhao, W. L., Ye, Y. Y., Bai, X. C., Liu, R. Q., Chang, L. F., … Sui, S. F. (2010). Cellular internalization of exosomes occurs through phagocytosis. *Traffic*, *11*(5), 675–687. https://doi.org/10.1111/j.1600-0854.2010.01041.x

Feng, Z., & Ko, C. P. (2008). Schwann cells promote synaptogenesis at the neuromuscular junction via transforming growth factor-β1. *Journal of Neuroscience*, *28*(39), 9599–9609. https://doi.org/10.1523/JNEUROSCI.2589-08.2008

Fidler, I. J. (2003). The pathogenesis of cancer metastasis: the "seed and soil" hypothesis revisited. *Nature Reviews. Cancer*, *3*(6), 453–458. https://doi.org/10.1038/nrc1098

Filipenko, N. R., Attwell, S., Roskelley, C., & Dedhar, S. (2005). Integrin-linked kinase activity regulates Rac- and Cdc42-mediated actin cytoskeleton reorganization via alpha-PIX. *Oncogene*, *24*(38), 5837–5849. https://doi.org/10.1038/sj.onc.1208737

Fischer, M., Kaech, S., Wagner, U., Brinkhaus, H., & Matus, A. (2000). Glutamate receptors regulate actin-based plasticity in dendritic spines. *Nature Neuroscience*, *3*(9), 887–894. https://doi.org/10.1038/78791

Fitzner, D., Schnaars, M., Van Rossum, D., Krishnamoorthy, G., Dibaj, P., Bakhti, M., …

Simons, M. (2011). Selective transfer of exosomes from oligodendrocytes to microglia by

macropinocytosis. *Journal of Cell Science*, *124*(3), 447–458.

https://doi.org/10.1242/jcs.074088

French, K. C., Antonyak, M. A., & Cerione, R. A. (2017). Extracellular vesicle docking at the

cellular port: Extracellular vesicle binding and uptake. *Seminars in Cell and Developmental

Biology*, *67*, 48–55. https://doi.org/10.1016/j.semcdb.2017.01.002

Frese, C. K., Mikhaylova, M., Stucchi, R., Gautier, V., Liu, Q., Mohammed, S., … Hoogenraad,

C. C. (2017). Quantitative Map of Proteome Dynamics during Neuronal Differentiation.

Cell Reports, *18*(6), 1527–1542. https://doi.org/10.1016/j.celrep.2017.01.025

Fröhlich, D., & Kuo, W. D. (2014). Multifaceted effects of oligodendroglial exosomes on

neurons. Retrieved from https://www.researchgate.net/profile/Eva-Maria_Kraemer-

Albers/publication/264809938_Multifaceted_effects_of_oligodendroglial_exosomes_on_ne

urons_impact_on_neuronal_firing_rate_signal_transduction_and_gene_regulation/links/552

ad6390cf2e089a3aa10bd.pdf

Frühbeis, C., Fröhlich, D., Kuo, W. P., Amphornrat, J., Thilemann, S., Saab, A. S., … Krämer-

Albers, E. M. (2013a). Neurotransmitter-Triggered Transfer of Exosomes Mediates

Oligodendrocyte-Neuron Communication. *PLoS Biology*.

https://doi.org/10.1371/journal.pbio.1001604

Frühbeis, C., Fröhlich, D., Kuo, W. P., Amphornrat, J., Thilemann, S., Saab, A. S., … Krämer-

Albers, E. M. (2013b). Neurotransmitter-Triggered Transfer of Exosomes Mediates

Oligodendrocyte-Neuron Communication. *PLoS Biology*, *11*(7).

https://doi.org/10.1371/journal.pbio.1001604

Gabrielli, M., Battista, N., Riganti, L., Prada, I., Antonucci, F., Cantone, L., … Verderio, C. (2015). Active endocannabinoids are secreted on the surface of microglial microvesicles. *SpringerPlus*, *4*(2), 1–32. https://doi.org/10.1186/2193-1801-4-S1-L29

Gallo, G. (2013). *Mechanisms Underlying the Initiation and Dynamics of Neuronal Filopodia. From Neurite Formation to Synaptogenesis. International Review of Cell and Molecular Biology* (Vol. 301). Elsevier. https://doi.org/10.1016/B978-0-12-407704-1.00003-8

Gauthier-Campbell, C., Bredt, D. S., Murphy, T. H., & El-Din El-Husseini, A. (2004). Regulation of Dendritic Branching and Filopodia Formation in Hippocampal Neurons by Specific Acylated Protein Motifs □ D□ V. *Molecular Biology of the Cell*, *15*, 2205–2217. https://doi.org/10.1091/mbc.E03

Gobert, A. P., Latour, Y. L., Asim, M., Finley, J. L., Verriere, T. G., Barry, D. P., … Wilson, K. T. (2019). Bacterial Pathogens Hijack the Innate Immune Response by Activation of the Reverse Transsulfuration Pathway. *MBio*, *10*(5). https://doi.org/10.1128/mBio.02174-19

Gong, J., Körner, R., Gaitanos, L., & Klein, R. (2016). Exosomes mediate cell contact-independent ephrin-Eph signaling during axon guidance. *The Journal of Cell Biology*, *214*(1), 35–44. https://doi.org/10.1083/jcb.201601085

Gonzalez-Lozano, M. A., Klemmer, P., Gebuis, T., Hassan, C., Van Nierop, P., Van Kesteren, R. E., … Li, K. W. (2016). Dynamics of the mouse brain cortical synaptic proteome during postnatal brain development. *Scientific Reports*, *6*, 1–15. https://doi.org/10.1038/srep35456

Gross, N., Kropp, J., & Khatib, H. (2017). MicroRNA signaling in embryo development. *Biology*, *6*(3). https://doi.org/10.3390/biology6030034

Halassa, M. M., Fellin, T., Takano, H., Dong, J.-H., & Haydon, P. G. (2007). Synaptic Islands Defined by the Territory of a Single Astrocyte. *Journal of Neuroscience*.

https://doi.org/10.1523/JNEUROSCI.1419-07.2007

Harding, C., Heuser, J., & Stahl, P. (n.d.). Receptor-mediated Endocytosis of Transferrin and of the Transferrin Receptor in Rat Reticulocytes Recycling.

Harding, C. V., Heuser, J. E., & Stahl, P. D. (2013). Exosomes: Looking back three decades and into the future. *Journal of Cell Biology*, *200*(4), 367–371. https://doi.org/10.1083/jcb.201212113

Hartmann, M., Brigadski, T., Erdmann, K. S., Holtmann, B., Sendtner, M., Narz, F., & Leßmann, V. (2004). Truncated TrkB receptor-induced outgrowth of dendritic filopodia involves the p75 neurotrophin receptor. *Journal of Cell Science*, *117*(24), 5803–5814. https://doi.org/10.1242/jcs.01511

Heckman, C. A., & Plummer, H. K. (2013). Filopodia as sensors. *Cellular Signalling*, *25*(11), 2298–2311. https://doi.org/10.1016/j.cellsig.2013.07.006

Heimsath, E. G., Yim, Y. I., Mustapha, M., Hammer, J. A., & Cheney, R. E. (2017). Myosin-X knockout is semi-lethal and demonstrates that myosin-X functions in neural tube closure, pigmentation, hyaloid vasculature regression, and filopodia formation. *Scientific Reports*, *7*(1), 1–17. https://doi.org/10.1038/s41598-017-17638-x

Hering, H., & Sheng, M. (2003). Activity-Dependent Redistribution and Essential Role of Cortactin in Dendritic Spine Morphogenesis. *Journal of Neuroscience*, *23*(37), 11759–11769. https://doi.org/10.1523/jneurosci.23-37-11759.2003

Herwig, J., Skuza, S., Sachs, W., Sachs, M., Failla, A. V., Rune, G., … Meyer-Schwesinger, C. (2019). Thrombospondin type 1 domain–containing 7A localizes to the slit diaphragm and stabilizes membrane dynamics of fully differentiated podocytes. *Journal of the American Society of Nephrology*, *30*(5), 824–839. https://doi.org/10.1681/ASN.2018090941

Hill, J. J., Hashimoto, T., & Lewis, D. A. (2006). Molecular mechanisms contributing to

    dendritic spine alterations in the prefrontal cortex of subjects with schizophrenia. *Molecular*

    Psychiatry, *11*(6), 557–566. https://doi.org/10.1038/sj.mp.4001792

Hira, K., Ueno, Y., Tanaka, R., Miyamoto, N., Yamashiro, K., Inaba, T., … Hattori, N. (2018).

    Astrocyte-Derived Exosomes Treated With a Semaphorin 3A Inhibitor Enhance Stroke

    Recovery via Prostaglandin D2 Synthase. *Stroke*, *49*(10), 2483–2494.

    https://doi.org/10.1161/STROKEAHA.118.021272

Holtmaat, A., & Svoboda, K. (2009). Experience-dependent structural synaptic plasticity in the

    mammalian brain. *Nature Reviews. Neuroscience*, *10*(9), 647–658.

    https://doi.org/10.1038/nrn2699

Hoshino, A., Costa-Silva, B., Shen, T. L., Rodrigues, G., Hashimoto, A., Tesic Mark, M., …

    Lyden, D. (2015). Tumour exosome integrins determine organotropic metastasis. *Nature*,

    527(7578), 329–335. https://doi.org/10.1038/nature15756

Hoshino, D., Kirkbride, K., Costello, K., Clark, E., Sinha, S., Grega-Larson, N., … Weaver, A.

    (2013). Exosome secretion is enhanced by invadopodia and drives invasive behavior. *Cell*

    Reports. https://doi.org/10.1016/j.celrep.2013.10.050

Hsu, C., Morohashi, Y., Yoshimura, S. I., Manrique-Hoyos, N., Jung, S. Y., Lauterbach, M. A.,

    … Simons, M. (2010). Regulation of exosome secretion by Rab35 and its GTPase-

    activating proteins TBC1D10A-C. *Journal of Cell Biology*, *189*(2), 223–232.

    https://doi.org/10.1083/jcb.200911018

Hu, M., Hong, L., Liu, C., Hong, S., He, S., Zhou, M., … Chen, Q. (2019). Electrical stimulation

    enhances neuronal cell activity mediated by Schwann cell derived exosomes. *Scientific*

    Reports, (February), 1–12. https://doi.org/10.1038/s41598-019-41007-5

Hutsler, J. J., & Zhang, H. (2010). Increased dendritic spine densities on cortical projection

    neurons in autism spectrum disorders. *Brain Research*.

    https://doi.org/10.1016/j.brainres.2009.09.120

Ibáñez, F., Montesinos, J., Ureña-Peralta, J. R., Guerri, C., & Pascual, M. (2019). TLR4

    participates in the transmission of ethanol-induced neuroinflammation via astrocyte-derived

    extracellular vesicles. *Journal of Neuroinflammation*, *16*(1), 1–14.

    https://doi.org/10.1186/s12974-019-1529-x

Irie, F., & Yamaguchi, Y. (2002). EphB receptors regulate dendritic spine development via

    intersectin, Cdc42 and N-WASP. *Nature Neuroscience*, *5*(11), 1117–1118.

    https://doi.org/10.1038/nn964

Irwin, S. A., Patel, B., Idupulapati, M., Harris, J. B., Crisostomo, R. A., Larsen, B. P., …

    Greenough, W. T. (2001). Abnormal dendritic spine characteristics in the temporal and

    visual cortices of patients with fragile-X syndrome: A quantitative examination. *American*

    Journal of Medical Genetics. https://doi.org/10.1002/1096-8628(20010115)98:2<161::AID-

    AJMG1025>3.0.CO;2-B

Jaiswal, R., Breitsprecher, D., Collins, A., Corrêa, I. R., Xu, M. Q., & Goode, B. L. (2013). The

    formin daam1 and fascin directly collaborate to promote filopodia formation. *Current*

    Biology, *23*(14), 1373–1379. https://doi.org/10.1016/j.cub.2013.06.013

Jan, Y.-N. (2001). Dendrites. *Genes & Development*, *15*(20), 2627–2641.

    https://doi.org/10.1101/gad.916501

Jimenez, L., Yu, H., McKenzie, A. J., Franklin, J. L., Patton, J. G., Liu, Q., & Weaver, A. M.

    (2019). Quantitative Proteomic Analysis of Small and Large Extracellular Vesicles (EVs)

    Reveals Enrichment of Adhesion Proteins in Small EVs. *Journal of Proteome Research*,

18(3), 947–959. https://doi.org/10.1021/acs.jproteome.8b00647

Johnstone, R. M., Adam, M., Hammond, J. R., Orr, L., & Turbide, C. (1987). Vesicle formation

during reticulocyte maturation. Association of plasma membrane activities with released

vesicles (exosomes). *Journal of Biological Chemistry*, *262*(19), 9412–9420.

https://doi.org/10.1016/s0021-9258(18)48095-7

Jones, E. V., Cook, D., & Murai, K. K. (2012). A neuron-astrocyte co-culture system to

investigate astrocyte-secreted factors in mouse neuronal development. *Methods in

Molecular Biology*, *814*, 341–352. https://doi.org/10.1007/978-1-61779-452-0_22

Kaech, S., & Banker, G. (2006). Culturing hippocampal neurons. *Nature Protocols*, *1*(5), 2406–

2415. https://doi.org/10.1254/fpj.119.163

Kayser, M. S., Nolt, M. J., & Dalva, M. B. (2008). EphB Receptors Couple Dendritic Filopodia

Motility to Synapse Formation. *Neuron*, *59*(1), 56–69.

https://doi.org/10.1016/j.neuron.2008.05.007

Keerthikumar, S., Gangoda, L., Liem, M., Fonseka, P., Atukorala, I., Ozcitti, C., … Mathivanan,

S. (2015). Proteogenomic analysis reveals exosomes are more oncogenic than ectosomes.

Oncotarget, *6*(17), 15375–15396. https://doi.org/10.18632/oncotarget.3801

Kellner, Y., Gödecke, N., Dierkes, T., Thieme, N., Zagrebelsky, M., & Korte, M. (2014). The

BDNF effects on dendritic spines of mature hippocampal neurons depend on neuronal

activity. *Frontiers in Synaptic Neuroscience*, *6*(MAR), 1–17.

https://doi.org/10.3389/fnsyn.2014.00005

Ketschek, A., & Gallo, G. (2010). Nerve Growth Factor Induces Axonal Filopodia through

Localized Microdomains of Phosphoinositide 3-Kinase Activity That Drive the Formation

of Cytoskeletal Precursors to Filopodia. *Journal of Neuroscience*, *30*(36), 12185–12197.

https://doi.org/10.1523/JNEUROSCI.1740-10.2010

Khan, S. A., Dong, H., Joyce, J., Sasaki, T., Chu, M.-L., & Tsuda, T. (2016a). Fibulin-2 is

essential for angiotensin II-induced myocardial fibrosis mediated by transforming growth

factor (TGF)-β. *Laboratory Investigation; a Journal of Technical Methods and Pathology*,

96(7), 773–783. https://doi.org/10.1038/labinvest.2016.52

Khan, S. A., Dong, H., Joyce, J., Sasaki, T., Chu, M.-L., & Tsuda, T. (2016b). Fibulin-2 is

essential for angiotensin II-induced myocardial fibrosis mediated by transforming growth

factor (TGF)-β. *Laboratory Investigation; a Journal of Technical Methods and Pathology*,

96(7), 773–783. https://doi.org/10.1038/labinvest.2016.52

Koeglsperger, T., Li, S., Brenneis, C., Saulnier, J. L., Mayo, L., Carrier, Y., … Weiner, H. L.

(2013). Impaired glutamate recycling and GluN2B-mediated neuronal calcium overload in

mice lacking TGF-β1 in the CNS. *Glia*, *61*(6), 985–1002. https://doi.org/10.1002/glia.22490

Koles, K., Nunnari, J., Korkut, C., Barria, R., Brewer, C., Li, Y., … Budnik, V. (2012).

Mechanism of evenness interrupted (Evi)-exosome release at synaptic boutons. *Journal of*

Biological Chemistry, *287*(20), 16820–16834. https://doi.org/10.1074/jbc.M112.342667

Korobova, F., & Svitkina, T. (2010). Molecular architecture of synaptic actin cytoskeleton in

hippocampal neurons reveals a mechanism of dendritic spine morphogenesis. *Molecular*

Biology of the Cell, *21*(1), 165–176. https://doi.org/10.1091/mbc.e09-07-0596

Krueger, D. D., Tuffy, L. P., Papadopoulos, T., & Brose, N. (2012). The role of neurexins and

neuroligins in the formation, maturation, and function of vertebrate synapses. *Current*

Opinion in Neurobiology, *22*(3), 412–422. https://doi.org/10.1016/j.conb.2012.02.012

Kucukdereli, H., Allen, N. J., Lee, A. T., Feng, A., Ozlu, M. I., Conatser, L. M., … Eroglu, C.

(2011). Control of excitatory CNS synaptogenesis by astrocyte-secreted proteins hevin and

SPARC. *Proceedings of the National Academy of Sciences of the United States of America*, *108*(32). https://doi.org/10.1073/pnas.1104977108

Kulkarni, V. A., & Firestein, B. L. (2012). The dendritic tree and brain disorders. *Molecular and Cellular Neuroscience*. https://doi.org/10.1016/j.mcn.2012.03.005

Kuo, M. W., Wang, C. H., Wu, H. C., Chang, S. J., & Chuang, Y. J. (2011). Soluble THSD7A is an N-glycoprotein that promotes endothelial cell migration and tube formation in angiogenesis. *PLoS ONE*, *6*(12). https://doi.org/10.1371/journal.pone.0029000

Kurian, N. K., & Modi, D. (2019). Extracellular vesicle mediated embryo-endometrial cross talk during implantation and in pregnancy. *Journal of Assisted Reproduction and Genetics*, *36*(2), 189–198. https://doi.org/10.1007/s10815-018-1343-x

Kyykallio, H., Oikari, S., Álvez, M. B., Dodd, C. J. G., Capra, J., & Rilla, K. (2020). The density and length of filopodia associate with the activity of hyaluronan synthesis in tumor cells. *Cancers*, *12*(7), 1–14. https://doi.org/10.3390/cancers12071908

Lachenal, G., Pernet-Gallay, K., Chivet, M., Hemming, F. J., Belly, A., Bodon, G., … Sadoul, R. (2011). Release of exosomes from differentiated neurons and its regulation by synaptic glutamatergic activity. *Molecular and Cellular Neuroscience*. https://doi.org/10.1016/j.mcn.2010.11.004

Lai, C. P. K., & Breakefield, X. O. (2012). Role of exosomes/microvesicles in the nervous system and use in emerging therapies. *Frontiers in Physiology*. https://doi.org/10.3389/fphys.2012.00228

Lai, C. P., Kim, E. Y., Badr, C. E., Weissleder, R., Mempel, T. R., Tannous, B. A., & Breakefield, X. O. (2015). Visualization and tracking of tumour extracellular vesicle delivery and RNA translation using multiplexed reporters. *Nature Communications*, *6*,

7029. https://doi.org/10.1038/ncomms8029

Lamprecht, R., & LeDoux, J. (2004). Structural plasticity and memory. *Nature Reviews Neuroscience*, *5*(1), 45–54. https://doi.org/10.1038/nrn1301

Larsen, B. R., Assentoft, M., Cotrina, M. L., Hua, S. Z., Nedergaard, M., Kaila, K., … Macaulay, N. (2014). Contributions of the Na+/K+-ATPase, NKCC1, and Kir4.1 to hippocampal K+ clearance and volume responses. *Glia*, *62*(4), 608–622. https://doi.org/10.1002/glia.22629

Lee, J.-E., Moon, P.-G., Lee, I.-K., & Baek, M.-C. (2015). Proteomic Analysis of Extracellular Vesicles Released by Adipocytes of Otsuka Long-Evans Tokushima Fatty (OLETF) Rats. *The Protein Journal*, *34*(3), 220–235. https://doi.org/10.1007/s10930-015-9616-z

Lee, J. H., Kim, J. young, Noh, S., Lee, H., Lee, S. Y., Mun, J. Y., … Chung, W. S. (2020). Astrocytes phagocytose adult hippocampal synapses for circuit homeostasis. *Nature*, *590*(February). https://doi.org/10.1038/s41586-020-03060-3

Lee, S., Zhang, H., & Webb, D. J. (2015). Dendritic spine morphology and dynamics in health and disease. *Cell Health and Cytoskeleton*. https://doi.org/10.2147/CHC.S82214

Lesuisse, C., & Martin, L. J. (2002). Long-term culture of mouse cortical neurons as a model for neuronal development, aging, and death. *Journal of Neurobiology*, *51*(1), 9–23. https://doi.org/10.1002/neu.10037

Levy, A. D., Omar, M. H., & Koleske, A. J. (2014). Extracellular matrix control of dendritic spine and synapse structure and plasticity in adulthood. *Frontiers in Neuroanatomy*, *8*, 116. https://doi.org/10.3389/fnana.2014.00116

Lin, W. H., Hurley, J. T., Raines, A. N., Cheney, R. E., & Webb, D. J. (2013). Myosin X and its motorless isoform differentially modulate dendritic spine development by regulating trafficking and retention of vasodilator-stimulated phosphoprotein. *Journal of Cell Science*,

126(20), 4756–4768. https://doi.org/10.1242/jcs.132969

Lin, W. H., Nebhan, C. A., Anderson, B. R., & Webb, D. J. (2010). Vasodilator-stimulated phosphoprotein (VASP) induces actin assembly in dendritic spines to promote their development and potentiate synaptic strength. *Journal of Biological Chemistry*, *285*(46), 36010–36020. https://doi.org/10.1074/jbc.M110.129841

López-Bayghen, E., & Ortega, A. (2011). Glial glutamate transporters: New actors in brain signaling. *IUBMB Life*, *63*(10), 816–823. https://doi.org/10.1002/iub.536

Lopez-verrilli, A., Picou, F., & Court, F. A. (2013). Schwann Cell-Derived Exosomes Enhance Axonal Regeneration in the Peripheral Nervous System, 1795–1806. https://doi.org/10.1002/glia.22558

Lu, C., & Malenka, R. C. (2012). NMDA Receptor-Dependent Long-Term Potentiation and Long-Term Depression (LTP / LTD), 1–15.

Luarte, A., Henzi, R., Fernández, A., Gaete, D., Cisternas, P., Pizarro, M., … Wyneken, U. (2020). Astrocyte-Derived Small Extracellular Vesicles Regulate Dendritic Complexity through miR-26a-5p Activity. *Cells*, *9*(4). https://doi.org/10.3390/cells9040930

Luo, L., Hensch, T. K., Ackerman, L., Barbel, S., Jan, L. Y., & Jan, Y. N. (1996). Differential effects of the Rac GTPase on Purkinje cell axons and dendritic trunks and spines. *Nature*, *379*(6568), 837–840. https://doi.org/10.1038/379837a0

Ma, L., Rohatgi, R., & Kirschner, M. W. (1998). The Arp2/3 complex mediates actin polymerization induced by the small GTP-binding protein Cdc42. *Proceedings of the National Academy of Sciences of the United States of America*, *95*(26), 15362–15367. https://doi.org/10.1073/pnas.95.26.15362

Maas, S. L. N., Breakefield, X. O., & Weaver, A. M. (2017a). Extracellular Vesicles: Unique

Intercellular Delivery Vehicles. *Trends in Cell Biology*, *27*(3), 172–188.

https://doi.org/10.1016/j.tcb.2016.11.003

Maas, S. L. N., Breakefield, X. O., & Weaver, A. M. (2017b). Extracellular Vesicles: Unique

Intercellular Delivery Vehicles. *Trends in Cell Biology*, *27*(3), 172–188.

https://doi.org/10.1016/j.tcb.2016.11.003

Machtinger, R., Laurent, L. C., & Baccarelli, A. A. (2016). Extracellular vesicles: Roles in

gamete maturation, fertilization and embryo implantation. *Human Reproduction Update*,

22(2), 182–193. https://doi.org/10.1093/humupd/dmv055

Manabe, T., & Nicoll, R. (1994). Long-term potentiation: evidence against an increase in

transmitter release probability in the CA1 region of the hippocampus. *Science*, *265*(5180),

1888–1892. https://doi.org/10.1126/science.7916483

Manabe, T., Wyllie, D. J., Perkel, D. J., & Nicoll, R. A. (1993). Modulation of synaptic

transmission and long-term potentiation: effects on paired pulse facilitation and EPSC

variance in the CA1 region of the hippocampus. *Journal of Neurophysiology*, *70*(4), 1451–

1459. https://doi.org/10.1152/jn.1993.70.4.1451

Marleau, A. M., Chen, C. S., Joyce, J. A., & Tullis, R. H. (2012). Exosome removal as a

therapeutic adjuvant in cancer. *Journal of Translational Medicine*, *10*(1), 1–12.

https://doi.org/10.1186/1479-5876-10-134

Marrs, G. S., Green, S. H., & Dailey, M. E. (2001). Rapid formation and remodeling of

postsynaptic densities in developing dendrites. https://doi.org/10.1038/nn717

Matsumoto-Miyai, K., Sokolowska, E., Zurlinden, A., Gee, C. E., Lüscher, D., Hettwer, S., …

Sonderegger, P. (2009). Coincident Pre- and Postsynaptic Activation Induces Dendritic

Filopodia via Neurotrypsin-Dependent Agrin Cleavage. *Cell*, *136*(6), 1161–1171.

https://doi.org/10.1016/j.cell.2009.02.034

Matsuzaki, M., Honkura, N., Ellis-Davies, G. C. R., & Kasai, H. (2004). Structural basis of long-term potentiation in single dendritic spines. *Nature*, *429*(6993), 761–766. https://doi.org/10.1038/nature02617

Mattila, P. K., & Lappalainen, P. (2008a). Filopodia: molecular architecture and cellular functions. *Nature Reviews Molecular Cell Biology*. https://doi.org/10.1038/nrm2406

Mattila, P. K., & Lappalainen, P. (2008b). Filopodia: Molecular architecture and cellular functions. *Nature Reviews Molecular Cell Biology*, *9*(6), 446–454. https://doi.org/10.1038/nrm2406

Mayford, M., Siegelbaum, S. A., & Kandel, E. R. (2012). Synapses and memory storage. *Cold Spring Harbor Perspectives in Biology*, *4*(6), 1–18. https://doi.org/10.1101/cshperspect.a005751

McKenzie, A. J., Hoshino, D., Hong, N. H., Cha, D. J., Franklin, J. L., Coffey, R. J., … Weaver, A. M. (2016). KRAS-MEK Signaling Controls Ago2 Sorting into Exosomes. *Cell Reports*, *15*(5), 978–987. https://doi.org/10.1016/j.celrep.2016.03.085

Menna, E., Disanza, A., Cagnoli, C., Schenk, U., Gelsomino, G., Frittoli, E., … Matteoli, M. (2009). Eps8 regulates axonal filopodia in hippocampal neurons in response to brain-derived neurotrophic factor (BDNF). *PLoS Biology*, *7*(6). https://doi.org/10.1371/journal.pbio.1000138

Messenger, S. W., Woo, S. S., Sun, Z., & Martin, T. F. J. (2018). A Ca2+-stimulated exosome release pathway in cancer cells is regulated by Munc13-4. *Journal of Cell Biology*, *217*(8), 2877–2890. https://doi.org/10.1083/jcb.201710132

Mishra, S., Wu, S.-Y., Fuller, A. W., Wang, Z., Rose, K. L., Schey, K. L., & Mchaourab, H. S.

(2018). Loss of αB-crystallin function in zebrafish reveals critical roles in the development

of the lens and stress resistance of the heart. *The Journal of Biological Chemistry*, *293*(2),

740–753. https://doi.org/10.1074/jbc.M117.808634

Mittelbrunn, M., Gutiérrez-Vázquez, C., Villarroya-Beltri, C., González, S., Sánchez-Cabo, F.,

González, M. Á., … Sánchez-Madrid, F. (2011). Unidirectional transfer of microRNA-

loaded exosomes from T cells to antigen-presenting cells. *Nature Communications*.

https://doi.org/10.1038/ncomms1285

Mukherjee, C., Kling, T., Russo, B., Miebach, K., Kess, E., Schifferer, M., … Simons, M.

(2020). Oligodendrocytes Provide Antioxidant Defense Function for Neurons by Secreting

Ferritin Heavy Chain. *Cell Metabolism*, *32*(2), 259-272.e10.

https://doi.org/10.1016/j.cmet.2020.05.019

Muralidharan-Chari, V., Clancy, J., Plou, C., Romao, M., Chavrier, P., Raposo, G., & D'Souza-

Schorey, C. (2009). ARF6-Regulated Shedding of Tumor Cell-Derived Plasma Membrane

Microvesicles. *Current Biology*, *19*(22), 1875–1885.

https://doi.org/10.1016/j.cub.2009.09.059

Murphy-Ullrich, J. E., & Poczatek, M. (n.d.). Activation of latent TGF-beta by thrombospondin-

1: mechanisms and physiology. *Cytokine & Growth Factor Reviews*, *11*(1–2), 59–69.

https://doi.org/10.1016/s1359-6101(99)00029-5

Nabhan, J. F., Hu, R., Oh, R. S., Cohen, S. N., & Lu, Q. (2012). Formation and release of

arrestin domain-containing protein 1-mediated microvesicles (ARMMs) at plasma

membrane by recruitment of TSG101 protein. *Proceedings of the National Academy of

Sciences of the United States of America*, *109*(11), 4146–4151.

https://doi.org/10.1073/pnas.1200448109

Nimchinsky, E. A., Sabatini, B. L., & Svoboda, K. (2002). Structure and Function of Dendritic

Spines. *Annual Review of Physiology*.

https://doi.org/10.1146/annurev.physiol.64.081501.160008

Oh, S. Y., Knelson, E. H., Blobe, G. C., & Mythreye, K. (2013). The type III TGFβ receptor

regulates filopodia formation via a Cdc42-mediated IRSp53–N-WASP interaction in

epithelial cells. *Biochemical Journal*, *454*(1), 79–89. https://doi.org/10.1042/BJ20121701

Ono, R. N., Sengle, G., Charbonneau, N. L., Carlberg, V., Bächinger, H. P., Sasaki, T., … Sakai,

L. Y. (2009). Latent transforming growth factor beta-binding proteins and fibulins compete

for fibrillin-1 and exhibit exquisite specificities in binding sites. *The Journal of Biological

Chemistry*, *284*(25), 16872–16881. https://doi.org/10.1074/jbc.M809348200

Ostrowski, M., Carmo, N. B., Krumeich, S., Fanget, I., Raposo, G., Savina, A., … Thery, C.

(2010). Rab27a and Rab27b control different steps of the exosome secretion pathway.

Nature Cell Biology. https://doi.org/10.1038/ncb2000

Pan, B. T., & Johnstone, R. (1984). Selective externalization of the transferrin receptor by sheep

reticulocytes in vitro. Response to ligands and inhibitors of endocytosis. *Journal of

Biological Chemistry*, *259*(15), 9776–9782. https://doi.org/10.1016/s0021-9258(17)42767-0

Pan, T. C., Sasaki, T., Zhang, R. Z., Fässler, R., Timpl, R., & Chu, M. L. (1993). Structure and

expression of fibulin-2, a novel extracellular matrix protein with multiple EGF-like repeats

and consensus motifs for calcium binding. *Journal of Cell Biology*, *123*(5), 1269–1277.

https://doi.org/10.1083/jcb.123.5.1269

Papa, M, Bundman, M. C., Greenberger, V., & Segal, M. (1995). Morphological analysis of

dendritic spine development in primary cultures of hippocampal neurons. *The Journal of

Neuroscience : The Official Journal of the Society for Neuroscience*, *15*(1 Pt 1), 1–11.

Retrieved from http://www.ncbi.nlm.nih.gov/pubmed/7823120

Papa, Michele, Bundman, M. C., Greenberger, V., & Segal, M. (1995). Morphological Analysis of Dendritic Spine Development in Primary Cultures of Hippocampal Neurons. *The Journal of Neuroscience*, *15*(l), 1–11.

Pappas, G. D., & Purpura~, D. P. (1961). Fine Structure of Dendrites in the Superficial Neocorticai Neuropil. *EXPERIMENTAL NEUROLCGY*, *4*, 507–530.

Parolini, I., Federici, C., Raggi, C., Lugini, L., Palleschi, S., De Milito, A., … Fais, S. (2009). Microenvironmental pH is a key factor for exosome traffic in tumor cells. *Journal of Biological Chemistry*. https://doi.org/10.1074/jbc.M109.041152

Pascua-Maestro, R., González, E., Lillo, C., Ganfornina, M. D., Falcón-Pérez, J. M., & Sanchez, D. (2019). Extracellular vesicles secreted by astroglial cells transport apolipoprotein D to neurons and mediate neuronal survival upon oxidative stress. *Frontiers in Cellular Neuroscience*, *12*(January), 1–13. https://doi.org/10.3389/fncel.2018.00526

Pavlos, N. J., Gronborg, M., Riedel, D., Chua, J. J. E., Boyken, J., Kloepper, T. H., … Jahn, R. (2010). Quantitative Analysis of Synaptic Vesicle Rabs Uncovers Distinct Yet Overlapping Roles for Rab3a and Rab27b in Ca2+-Triggered Exocytosis. *Journal of Neuroscience*. https://doi.org/10.1523/JNEUROSCI.0907-10.2010

Pavlos, Nathan J., & Jahn, R. (2011). Distinct yet overlapping roles of Rab GTPases on synaptic vesicles. *Small GTPases*. https://doi.org/10.4161/sgtp.2.2.15201

Pellegrin, S., & Mellor, H. (2005). The Rho family GTPase Rif induces filopodia through mDia2. *Current Biology : CB*, *15*(2), 129–133. https://doi.org/10.1016/j.cub.2005.01.011

Peng, J., Wallar, B. J., Flanders, A., Swiatek, P. J., & Alberts, A. S. (2003). Disruption of the Diaphanous-related formin Drf1 gene encoding mDia1 reveals a role for Drf3 as an effector

for Cdc42. *Current Biology : CB*, *13*(7), 534–545. https://doi.org/10.1016/s0960-9822(03)00170-2

Penzes, P., Cahill, M. E., Jones, K. A., VanLeeuwen, J.-E., & Woolfrey, K. M. (2011). Dendritic spine pathology in neuropsychiatric disorders. *Nature Neuroscience*. https://doi.org/10.1038/nn.2741

Perea, G., Navarrete, M., & Araque, A. (2009). Tripartite synapses: astrocytes process and control synaptic information. *Trends in Neurosciences*. https://doi.org/10.1016/j.tins.2009.05.001

Portera-Cailliau, C., Pan, D. T., & Yuste, R. (2003). Activity-regulated dynamic behavior of early dendritic protrusions: Evidence for different types of dendritic filopodia. *Journal of Neuroscience*, *23*(18), 7129–7142. https://doi.org/10.1523/jneurosci.23-18-07129.2003

Price, L. S., Leng, J., Schwartz, M. A., & Bokoch, G. M. (1998). Activation of Rac and Cdc42 by integrins mediates cell spreading. *Molecular Biology of the Cell*, *9*(7), 1863–1871. https://doi.org/10.1091/mbc.9.7.1863

Radice, P. D., Mathieu, P., Leal, M. C., Farías, M. I., Ferrari, C., Puntel, M., … Pitossi, F. J. (2015a). Fibulin-2 is a key mediator of the pro-neurogenic effect of TGF-beta1 on adult neural stem cells. *Molecular and Cellular Neurosciences*, *67*, 75–83. https://doi.org/10.1016/j.mcn.2015.06.004

Radice, P. D., Mathieu, P., Leal, M. C., Farías, M. I., Ferrari, C., Puntel, M., … Pitossi, F. J. (2015b). Fibulin-2 is a key mediator of the pro-neurogenic effect of TGF-beta1 on adult neural stem cells. *Molecular and Cellular Neuroscience*, *67*, 75–83. https://doi.org/10.1016/j.mcn.2015.06.004

Raiborg, C., Bache, K. G., Gillooly, D. J., Madshus, I. H., Stang, E., & Stenmark, H. (2002). Hrs

sorts ubiquitinated proteins into clathrin-coated microdomains of early endosomes. *Nature Cell Biology*. https://doi.org/10.1038/ncb791

Raisman, G. (1991). Glia, neurons, and plasticity. *Annals of the New York Academy of Sciences*, *633*, 209–213. https://doi.org/10.1111/j.1749-6632.1991.tb15612.x

Rajendran, L., Honsho, M., Zahn, T. R., Keller, P., Geiger, K. D., Verkade, P., & Simons, K. (2006). Alzheimer's disease beta-amyloid peptides are released in association with exosomes. *Proceedings of the National Academy of Sciences*. https://doi.org/10.1073/pnas.0603838103

Raposo, G., Nijman, H. W., Stoorvogel, W., Leijendekker, R., Harding, C., Melief, C. J. M., & Geuze, H. J. (1996). B Lymphocytes Secrete Antigen-presentingVesicles, *183*(March).

Raposo, Graça, & Stoorvogel, W. (2013). Extracellular vesicles: Exosomes, microvesicles, and friends. *Journal of Cell Biology*, *200*(4), 373–383. https://doi.org/10.1083/jcb.201211138

Rohatgi, R., Ma, L., Miki, H., Lopez, M., Kirchhausen, T., Takenawa, T., & Kirschner, M. W. (1999). The interaction between N-WASP and the Arp2/3 complex links Cdc42-dependent signals to actin assembly. *Cell*, *97*(2), 221–231. https://doi.org/10.1016/s0092-8674(00)80732-1

Romorini, S., Piccoli, G., & Sala, C. (2006). Regulation of dendritic spine morphology and synaptic function by scaffolding proteins. *Molecular Mechanisms of Synaptogenesis*, *31*, 261–276. https://doi.org/10.1007/978-0-387-32562-0_19

Ruiz-Martinez, M., Navarro, A., Marrades, R. M., Viñolas, N., Santasusagna, S., Muñoz, C., … Monzo, M. (2016). YKT6 expression, exosome release, and survival in non-small cell lung cancer. *Oncotarget*, *7*(32), 51515–51524. https://doi.org/10.18632/oncotarget.9862

Saman, S., Kim, W. H., Raya, M., Visnick, Y., Miro, S., Saman, S., … Hall, G. F. (2012).

Exosome-associated tau is secreted in tauopathy models and is selectively phosphorylated in cerebrospinal fluid in early Alzheimer disease. *Journal of Biological Chemistry*. https://doi.org/10.1074/jbc.M111.277061

Sasaki, T., Göhring, W., Pan, T. C., Chu, M. L., & Timpl, R. (1995). Binding of mouse and human fibulin-2 to extracellular matrix ligands. *Journal of Molecular Biology*, *254*(5), 892–899. https://doi.org/10.1006/jmbi.1995.0664

Savina, A., Furlán, M., Vidal, M., & Colombo, M. I. (2003). Exosome release is regulated by a calcium-dependent mechanism in K562 cells. *Journal of Biological Chemistry*, *278*(22), 20083–20090. https://doi.org/10.1074/jbc.M301642200

Schaeffer, J., Tannahill, D., Cioni, J.-M., Rowlands, D., & Keynes, R. (2018a). Identification of the extracellular matrix protein Fibulin-2 as a regulator of spinal nerve organization. *Developmental Biology*, *442*(1), 101–114. https://doi.org/10.1016/j.ydbio.2018.06.014

Schaeffer, J., Tannahill, D., Cioni, J. M., Rowlands, D., & Keynes, R. (2018b). Identification of the extracellular matrix protein Fibulin-2 as a regulator of spinal nerve organization. *Developmental Biology*, *442*(1), 101–114. https://doi.org/10.1016/j.ydbio.2018.06.014

SCOVILLE, W. B., & MILNER, B. (1957). Loss of recent memory after bilateral hippocampal lesions. *Journal of Neurology, Neurosurgery, and Psychiatry*, *20*(1), 11–21. https://doi.org/10.1136/jnnp.20.1.11

Sekino, Y., Kojima, N., & Shirao, T. (2007). Role of actin cytoskeleton in dendritic spine morphogenesis. *Neurochemistry International*. https://doi.org/10.1016/j.neuint.2007.04.029

Sheffler-Collins, S. I., & Dalva, M. B. (2012). EphBs: An integral link between synaptic function and synaptopathies. *Trends in Neurosciences*, *35*(5), 293–304. https://doi.org/10.1016/j.tins.2012.03.003

Shelke, G. V., Yin, Y., Jang, S. C., Lässer, C., Wennmalm, S., Hoffmann, H. J., … Lötvall, J. (2019a). Endosomal signalling via exosome surface TGFβ-1. *Journal of Extracellular Vesicles*, *8*(1), 1650458. https://doi.org/10.1080/20013078.2019.1650458

Shelke, G. V., Yin, Y., Jang, S. C., Lässer, C., Wennmalm, S., Hoffmann, H. J., … Lötvall, J. (2019b). Endosomal signalling via exosome surface TGFβ-1. *Journal of Extracellular Vesicles*, *8*(1). https://doi.org/10.1080/20013078.2019.1650458

Shelke, G. V., Yin, Y., Jang, S. C., Lässer, C., Wennmalm, S., Hoffmann, H. J., … Lötvall, J. (2019c). Endosomal signalling via exosome surface TGFβ-1. *Journal of Extracellular Vesicles*, *8*(1), 1–20. https://doi.org/10.1080/20013078.2019.1650458

Shi, M., Majumdar, D., Gao, Y., Brewer, B. M., Goodwin, C. R., McLean, J. A., … Webb, D. J. (2013). Glia co-culture with neurons in microfluidic platforms promotes the formation and stabilization of synaptic contacts. *Lab on a Chip*, *13*(15), 3008–3021. https://doi.org/10.1039/c3lc50249j

Singh, S. K., Stogsdill, J. A., Pulimood, N. S., Dingsdale, H., Kim, Y. H., Pilaz, L.-J., … Eroglu, C. (2016). Astrocytes Assemble Thalamocortical Synapses by Bridging NRX1α and NL1 via Hevin. *Cell*, *164*(1–2), 183–196. https://doi.org/10.1016/j.cell.2015.11.034

Sinha, Seema, Hoshino, D., Hong, N. H., Kirkbride, K. C., Grega-Larson, N. E., Seiki, M., … Weaver, A. M. (2016). Cortactin promotes exosome secretion by controlling branched actin dynamics. *Journal of Cell Biology*, *214*(2), 197–213. https://doi.org/10.1083/jcb.201601025

Sinha, Soniya, & Yang, W. (2008). Cellular signaling for activation of Rho GTPase Cdc42. *Cellular Signalling*, *20*(11), 1927–1934. https://doi.org/10.1016/j.cellsig.2008.05.002

Skog, J., Würdinger, T., van Rijn, S., Meijer, D. H., Gainche, L., Curry, W. T., … Breakefield, X. O. (2008). Glioblastoma microvesicles transport RNA and proteins that promote tumour

growth and provide diagnostic biomarkers. *Nature Cell Biology*, *10*(12), 1470–1476.

https://doi.org/10.1038/ncb1800

Skogberg, G., Gudmundsdottir, J., van der Post, S., Sandström, K., Bruhn, S., Benson, M., … Ekwall, O. (2013). Characterization of Human Thymic Exosomes. *PLoS ONE*, *8*(7), 1–10. https://doi.org/10.1371/journal.pone.0067554

Song, I., & Dityatev, A. (2018). Crosstalk between glia, extracellular matrix and neurons. *Brain Research Bulletin*, *136*, 101–108. https://doi.org/10.1016/j.brainresbull.2017.03.003

Spillane, M., Ketschek, A., Donnelly, C. J., Pacheco, A., Twiss, J. L., & Gallo, G. (2012). Nerve growth factor-induced formation of axonal filopodia and collateral branches involves the intra-axonal synthesis of regulators of the actin-nucleating Arp2/3 complex. *Journal of Neuroscience*, *32*(49), 17671–17689. https://doi.org/10.1523/JNEUROSCI.1079-12.2012

Steffen, A., Faix, J., Resch, G. P., Linkner, J., Wehland, J., Small, J. V., … Stradal, T. E. B. (2006). Filopodia formation in the absence of functional WAVE- and Arp2/3-complexes. *Molecular Biology of the Cell*, *17*(6), 2581–2591. https://doi.org/10.1091/mbc.e05-11-1088

Stouffer, G. A., LaMarre, J., Gonias, S. L., & Owens, G. K. (1993). Activated alpha 2-macroglobulin and transforming growth factor-beta 1 induce a synergistic smooth muscle cell proliferative response. *The Journal of Biological Chemistry*, *268*(24), 18340–18344. Retrieved from http://www.ncbi.nlm.nih.gov/pubmed/7688745

Sun, J., He, H., Xiong, Y., Lu, S., Shen, J., Cheng, A., … Yang, S. (2011). Fascin Protein Is Critical for Transforming Growth Factor β Protein-induced Invasion and Filopodia Formation in Spindle-shaped Tumor Cells. *Journal of Biological Chemistry*, *286*(45), 38865–38875. https://doi.org/10.1074/jbc.M111.270413

Sung, B. H., Ketova, T., Hoshino, D., Zijlstra, A., & Weaver, A. M. (2015). Directional cell

movement through tissues is controlled by exosome secretion. *Nature Communications*. https://doi.org/10.1038/ncomms8164

Sung, B. H., von Lersner, A., Guerrero, J., Krystofiak, E. S., Inman, D., Pelletier, R., … Weaver, A. M. (2020). A live cell reporter of exosome secretion and uptake reveals pathfinding behavior of migrating cells. *Nature Communications*, *11*(1), 1–15. https://doi.org/10.1038/s41467-020-15747-2

Sung, B. H., & Weaver, A. M. (2017). Exosome secretion promotes chemotaxis of cancer cells. *Cell Adhesion & Migration*, *11*(2), 187–195. https://doi.org/10.1080/19336918.2016.1273307

Surviladze, Z., Waller, A., Strouse, J. J., Bologa, C., Ursu, O., Salas, V., … Aubé, J. (2010). *A Potent and Selective Inhibitor of Cdc42 GTPase. Probe Reports from the NIH Molecular Libraries Program*. Retrieved from http://www.ncbi.nlm.nih.gov/pubmed/21433396

Tada, T., & Sheng, M. (2006). Molecular mechanisms of dendritic spine morphogenesis. *Current Opinion in Neurobiology*, *16*(1), 95–101. https://doi.org/10.1016/j.conb.2005.12.001

Tamai, K., Tanaka, N., Nakano, T., Kakazu, E., Kondo, Y., Inoue, J., … Sugamura, K. (2010). Exosome secretion of dendritic cells is regulated by Hrs, an ESCRT-0 protein. *Biochemical and Biophysical Research Communications*. https://doi.org/10.1016/j.bbrc.2010.07.083

Tamai, K., Toyoshima, M., Tanaka, N., Yamamoto, N., Owada, Y., Kiyonari, H., … Sugamura, K. (2008). Loss of Hrs in the Central Nervous System Causes Accumulation of Ubiquitinated Proteins and Neurodegeneration. *The American Journal of Pathology*. https://doi.org/10.2353/ajpath.2008.080684

Tang, C.-Z., Yang, J.-T., Liu, Q.-H., Wang, Y.-R., & Wang, W.-S. (2019). Up-regulated miR-192-5p expression rescues cognitive impairment and restores neural function in mice with

depression via the Fbln2-mediated TGF-β1 signaling pathway. *FASEB Journal : Official Publication of the Federation of American Societies for Experimental Biology*, *33*(1), 606–618. https://doi.org/10.1096/fj.201800210RR

Tashiro, A., Minden, A., & Yuste, R. (2000). Regulation of dendritic spine morphology by the Rho family of small GTPases: Antagonistic roles of Rac and Rho. *Cerebral Cortex*, *10*(10), 927–938. https://doi.org/10.1093/cercor/10.10.927

Taylor, D. D., & Gercel-Taylor, C. (2008). MicroRNA signatures of tumor-derived exosomes as diagnostic biomarkers of ovarian cancer. *Gynecologic Oncology*, *110*(1), 13–21. https://doi.org/10.1016/j.ygyno.2008.04.033

Thakur, B. K., Zhang, H., Becker, A., Matei, I., Huang, Y., Costa-Silva, B., … Lyden, D. (2014). Double-stranded DNA in exosomes: A novel biomarker in cancer detection. *Cell Research*, *24*(6), 766–769. https://doi.org/10.1038/cr.2014.44

Théry, C., Duban, L., Segura, E., Véron, P., Lantz, O., & Amigorena, S. (2002). Indirect activation of naïve CD4+ T cells by dendritic cell–derived exosomes. *Nature Immunology*. https://doi.org/10.1038/ni854

Théry, C., Witwer, K. W., Aikawa, E., Alcaraz, M. J., Anderson, J. D., Andriantsitohaina, R., … Zuba-Surma, E. K. (2018). Minimal information for studies of extracellular vesicles 2018 (MISEV2018): a position statement of the International Society for Extracellular Vesicles and update of the MISEV2014 guidelines. *Journal of Extracellular Vesicles*, *7*(1), 1535750. https://doi.org/10.1080/20013078.2018.1535750

Tian, T., Zhu, Y. L., Zhou, Y. Y., Liang, G. F., Wang, Y. Y., Hu, F. H., & Xiao, Z. D. (2014). Exosome uptake through clathrin-mediated endocytosis and macropinocytosis and mediating miR-21 delivery. *Journal of Biological Chemistry*, *289*(32), 22258–22267.

https://doi.org/10.1074/jbc.M114.588046

Timpl, R., Sasaki, T., Kostka, G., & Chu, M. L. (2003). Fibulins: A versatile family of

extracellular matrix proteins. *Nature Reviews Molecular Cell Biology*, *4*(6), 479–489.

https://doi.org/10.1038/nrm1130

Toni, N., Buchs, P. A., Nikonenko, I., Bron, C. R., & Muller, D. (1999). LTP promotes

formation of multiple spine synapses between a single axon terminal and a dendrite. *Nature*,

402(6760), 421–425. https://doi.org/10.1038/46574

Trajkovic, K., Hsu, C., Chiantia, S., Rajendran, L., Wenzel, D., Wieland, F., … Simons, M.

(2008). Ceramide triggers budding of exosome vesicles into multivesicular endosomes.

Science, *319*(5867), 1244–1247. https://doi.org/10.1126/science.1153124

Tsuda, T. (2018). Extracellular interactions between fibulins and transforming growth factor

(TGF)-β in physiological and pathological conditions. *International Journal of Molecular*

Sciences, *19*(9). https://doi.org/10.3390/ijms19092787

Ullian, E. M., Sapperstein, S. K., Christopherson, K. S., & Barres, B. A. (2001). Control of

synapse number by glia. *Science (New York, N.Y.)*, *291*(5504), 657–661.

https://doi.org/10.1126/science.291.5504.657

Urabe, F., Kosaka, N., Ito, K., Kimura, T., Egawa, S., & Ochiya, T. (2020). Extracellular

vesicles as biomarkers and therapeutic targets for cancer. *American Journal of Physiology -*

Cell Physiology, *318*(1), C29–C39. https://doi.org/10.1152/ajpcell.00280.2019

Urbanelli, L., Magini, A., Buratta, S., Brozzi, A., Sagini, K., Polchi, A., … Emiliani, C. (2013).

Signaling pathways in exosomes biogenesis, secretion and fate. *Genes*.

https://doi.org/10.3390/genes4020152

Valadi, H., Ekström, K., Bossios, A., Sjöstrand, M., Lee, J. J., & Lötvall, J. O. (2007). Exosome-

mediated transfer of mRNAs and microRNAs is a novel mechanism of genetic exchange

between cells. *Nature Cell Biology*, *9*(6), 654–659. https://doi.org/10.1038/ncb1596

van Niel, G., Charrin, S., Simoes, S., Romao, M., Rochin, L., Saftig, P., … Raposo, G. (2011).

The Tetraspanin CD63 Regulates ESCRT-Independent and -Dependent Endosomal Sorting

during Melanogenesis. *Developmental Cell*, *21*(4), 708–721.

https://doi.org/10.1016/j.devcel.2011.08.019

Van Wagenen, S., & Rehder, V. (2001). Regulation of neuronal growth cone filopodia by nitric

oxide depends on soluble guanylyl cyclase. *Journal of Neurobiology*, *46*(3), 206–219.

https://doi.org/10.1002/1097-4695(20010215)46:3<206::AID-NEU1003>3.0.CO;2-S

Varcianna, A., Myszczynska, M. A., Castelli, L. M., O'Neill, B., Kim, Y., Talbot, J., …

Ferraiuolo, L. (2019). Micro-RNAs secreted through astrocyte-derived extracellular vesicles

cause neuronal network degeneration in C9orf72 ALS. *EBioMedicine*, *40*, 626–635.

https://doi.org/10.1016/j.ebiom.2018.11.067

Vilcaes, A. A., Chanaday, N. L., & Kavalali, E. T. (2021). Interneuronal exchange and functional

integration of synaptobrevin via extracellular vesicles. *Neuron*, *109*(6), 971-983.e5.

https://doi.org/10.1016/j.neuron.2021.01.007

Voss, B. J., Loh, J. T., Hill, S., Rose, K. L., McDonald, W. H., & Cover, T. L. (2015). Alteration

of the Helicobacter pylori membrane proteome in response to changes in environmental salt

concentration. *Proteomics. Clinical Applications*, *9*(11–12), 1021–1034.

https://doi.org/10.1002/prca.201400176

Wang, C. H., Su, P. T., Du, X. Y., Kuo, M. W., Lin, C. Y., Yang, C. C., … Chuang, Y. J. (2010).

Thrombospondin type I domain containing 7A (THSD7A) mediates endothelial cell

migration and tube formation. *Journal of Cellular Physiology*, *222*(3), 685–694.

https://doi.org/10.1002/jcp.21990

Wang, G., Dinkins, M., He, Q., Zhu, G., Poirier, C., Campbell, A., … Bieberich, E. (2012).
Astrocytes secrete exosomes enriched with proapoptotic ceramide and prostate apoptosis
response 4 (PAR-4): potential mechanism of apoptosis induction in Alzheimer disease
(AD). *The Journal of Biological Chemistry*, *287*(25), 21384–21395.
https://doi.org/10.1074/jbc.M112.340513

Wang, S., Cesca, F., Loers, G., Schweizer, M., Buck, F., Benfenati, F., … Kleene, R. (2011).
Synapsin I is an oligomannose-carrying glycoprotein, acts as an oligomannose-binding
lectin, and promotes neurite outgrowth and neuronal survival when released via glia-derived
exosomes. *The Journal of Neuroscience : The Official Journal of the Society for
Neuroscience*, *31*(20), 7275–7290. https://doi.org/10.1523/JNEUROSCI.6476-10.2011

Webber, J., Steadman, R., Mason, M. D., Tabi, Z., & Clayton, A. (2010). Cancer exosomes
trigger fibroblast to myofibroblast differentiation. *Cancer Research*, *70*(23), 9621–9630.
https://doi.org/10.1158/0008-5472.CAN-10-1722

Wegner, A. M., Nebhan, C. A., Hu, L., Majumdar, D., Meier, K. M., Weaver, A. M., & Webb,
D. J. (2008). N-wasp and the arp2/3 complex are critical regulators of actin in the
development of dendritic spines and synapses. *The Journal of Biological Chemistry*,
283(23), 15912–15920. https://doi.org/10.1074/jbc.M801555200

Wells, R. B. (2005). Cortical Neurons and Circuits: A Tutorial Introduction.

Wijetunge, L. S., Angibaud, J., Frick, A., Kind, P. C., & Nägerl, U. V. (2014). Stimulated
emission depletion (STED) microscopy reveals nanoscale defects in the developmental
trajectory of dendritic spine morphogenesis in a mouse model of fragile X syndrome. *The
Journal of Neuroscience : The Official Journal of the Society for Neuroscience*, *34*(18),

6405–6412. https://doi.org/10.1523/JNEUROSCI.5302-13.2014

Wolfe, P. (1967). The nature and significance of platelet products in human plasma. *British Journal of Haematology*, *13*, 269–288. https://doi.org/10.3109/03008208909002412

Xiao, T., Zhang, W., Jiao, B., Pan, C.-Z., Liu, X., & Shen, L. (2017). The role of exosomes in the pathogenesis of Alzheimer' disease. *Translational Neurodegeneration*. https://doi.org/10.1186/s40035-017-0072-x

Xu, J., Xiao, N., & Xia, J. (2010). Thrombospondin 1 accelerates synaptogenesis in hippocampal neurons through neuroligin 1. *Nature Neuroscience*, *13*(1), 22–24. https://doi.org/10.1038/nn.2459

Xu, X., Zheng, L., Yuan, Q., Zhen, G., Crane, J. L., Zhou, X., & Cao, X. (2018). Transforming growth factor-β in stem cells and tissue homeostasis. *Bone Research*, *6*(1). https://doi.org/10.1038/s41413-017-0005-4

Yoshihara, Y., De Roo, M., & Muller, D. (2009). Dendritic spine formation and stabilization. *Current Opinion in Neurobiology*, *19*(2), 146–153. https://doi.org/10.1016/j.conb.2009.05.013

You, Y., Borgmann, K., Edara, V. V., Stacy, S., Ghorpade, A., & Ikezu, T. (2020). Activated human astrocyte-derived extracellular vesicles modulate neuronal uptake, differentiation and firing. *Journal of Extracellular Vesicles*, *9*(1), 1706801. https://doi.org/10.1080/20013078.2019.1706801

Yu, K., Ge, J., Summers, J. B., Li, F., Liu, X., Ma, P., … Zhuang, J. (2008). TSP-1 secreted by bone marrow stromal cells contributes to retinal ganglion cell neurite outgrowth and survival. *PloS One*, *3*(6), e2470. https://doi.org/10.1371/journal.pone.0002470

Yuyama, K., & Igarashi, Y. (2016). Physiological and pathological roles of exosomes in the

nervous system. *Biomolecular Concepts*, *7*(1), 53–68. https://doi.org/10.1515/bmc-2015-0033

Zakharenko, S. S., Zablow, L., & Siegelbaum, S. A. (2001). Visualization of changes in presynaptic function during long-term synaptic plasticity. *Nature Neuroscience*, *4*(7), 711–717. https://doi.org/10.1038/89498

Zhang, Haiying, Freitas, D., Kim, H. S., Fabijanic, K., Li, Z., Chen, H., … Lyden, D. (2018). Identification of distinct nanoparticles and subsets of extracellular vesicles by asymmetric flow field-flow fractionation. *Nature Cell Biology*, *20*(3), 332–343. https://doi.org/10.1038/s41556-018-0040-4

Zhang, Haiying, & Lyden, D. (2019). Asymmetric-flow field-flow fractionation technology for exomere and small extracellular vesicle separation and characterization. *Nature Protocols*, *14*(4), 1027–1053. https://doi.org/10.1038/s41596-019-0126-x

Zhang, Hangxiang, Wu, J., Dong, H., Khan, S. A., Chu, M.-L., & Tsuda, T. (2014). Fibulin-2 deficiency attenuates angiotensin II-induced cardiac hypertrophy by reducing transforming growth factor-β signalling. *Clinical Science (London, England : 1979)*, *126*(4), 275–288. https://doi.org/10.1042/CS20120636

Zhang, Huaye, Webb, D. J., Asmussen, H., & Horwitz, A. F. (2003). Synapse formation is regulated by the signaling adaptor GIT1. *Journal of Cell Biology*, *161*(1), 131–142. https://doi.org/10.1083/jcb.200211002

Zhang, Q., Higginbotham, J. N., Jeppesen, D. K., Yang, Y. P., Li, W., McKinley, E. T., … Coffey, R. J. (2019). Transfer of Functional Cargo in Exomeres. *Cell Reports*, *27*(3), 940-954.e6. https://doi.org/10.1016/j.celrep.2019.01.009

Zhou, M., Weber, S. R., Zhao, Y., Chen, H., & Sundstrom, J. M. (2020). *Methods for exosome*

isolation and characterization. *Exosomes*. Elsevier Inc. https://doi.org/10.1016/b978-0-12-816053-4.00002-x

Zhou, Q., Homma, K. J., & Poo, M. (2004). Shrinkage of dendritic spines associated with long-term depression of hippocampal synapses. *Neuron*, *44*(5), 749–757. https://doi.org/10.1016/j.neuron.2004.11.011

Zitvogel, L., Regnault, A., Lozier, A., Wolfers, J., Flament, C., Tenza, D., … Amigorena, S. (1998). Eradication of established murine tumors using a novel cell-free vaccine: Dendritic cell-derived exosomes. *Nature Medicine*, *4*(5), 594–600. https://doi.org/10.1038/nm0598-594

Ziv, N. E., & Smith, S. J. (1996). Evidence for a role of dendritic filopodia in synaptogenesis and spine formation. *Neuron*. https://doi.org/10.1016/S0896-6273(00)80283-4

Zuo, Y., Lin, A., Chang, P., & Gan, W. B. (2005). Development of long-term dendritic spine stability in diverse regions of cerebral cortex. *Neuron*. https://doi.org/10.1016/j.neuron.2005.04.001